

# Thermodynamic Analysis of Dehumidification

by

Bernd Heitele

Project

(Studienarbeit)

in

Chemical Engineering

at the

University of Wisconsin-Madison

1992

# Thermodynamic Analysis of Dehumidifiers

Bernd Heitele and John W. Mitchell  
Solar Energy Laboratory  
University of Wisconsin  
1500 Johnson Drive  
Madison, WI 53706

## Abstract

The effect of desiccant isotherms on the dehumidification process in solar cooling systems has been studied. A thermodynamic analysis of the temperature dependence of isotherms has established several fundamental relations that must be satisfied. These relations are then applied to experimental results and proposed properties of desiccants.

A recent report (SERI / NREL, 1989) stresses the possibility to improve the COP of desiccant cooling systems with new advanced desiccants. Polystyrene sulfonic acid sodium salt (PSSASS) and other desiccants with polymer bases were shown by Czanderna to be the most promising polymers for desiccant cooling applications. The isotherm measurements taken at 17°C, 22.1°C, and 27°C showed an unexpected temperature dependence. A thermodynamic analysis of these data indicates that either the measurements are incorrect since they violate the Second Law of Thermodynamics, or that the differential heat of adsorption has a large negative value. A negative heat of adsorption requires an endothermic reaction between water vapor and desiccant surface, and does not follow the law of physical adsorption.

Theoretical isotherms based on the SERI / NREL results are formulated and evaluated. These change shape from Brunauer Type 1 at 30°C to Type 3 at 70°C. A Brunauer Type 1 moderate is considered as the best shape for adsorption and a Brunauer Type 3 as the best shape for regeneration [Collier, Cale, and Lavan, 1986]. The formulation is based on the Clausius Clapeyron equation and the assumptions that the differential heat of adsorption depends only on the matrix water uptake and that the ratio heat of adsorption to heat of vaporization is independent of temperature.

The desiccant isotherms are implemented in a numerical model developed by McLain-Cross for a dehumidifier. The dehumidifier performance is evaluated in the classical cooling cycles: ventilation cycle, recirculation cycle, and Dunkle cycle. It is found that desiccants which have the proposed extreme changes in shape between the adsorption and the desorption temperature are not beneficial for desiccant cooling applications. None of the desiccants improved the COP of a cooling cycle compared to silica gel. Although a Brunauer Type 1 is the best shape for adsorption and a Type 3 for regeneration, the Clausius Clapeyron equation states that a desiccant isotherm shape

changes with temperature only due to a difference between the differential heat of adsorption and the heat of vaporization. Thus, the proposed desiccant isotherms require heats of adsorption which are in the range of two times the heat of vaporization. This is not desirable for desiccant cooling applications since the process air stream through the dehumidifier is excessively heated.

In summary, thermodynamic relations are established between the isotherm shape and differential heat of adsorption. These provide a criteria against which to judge the validity of experimental measurements. Temperature dependent isotherms for desiccants are found to have adverse effects on the COP for solar cooling systems.

#### References:

Czanderna, A.W. 1990. "Polymers as advanced materials for desiccant applications: Progress Report for 1989." SERI/TP-213-3608. Golden, CO: Solar Energy Research Institute.

Collier, K., T. S. Cale, and Z. Laven, 1986. "Advanced desiccant materials assessment." GRI-86/0181, Final Report, February 1985-May 1986. Chicago: Gas Research Institute.

---

## Acknowledgments

---

I got lucky! It was not as easy for me to come to the US as it might seem.

I got lucky since I applied for this DAAD exchange program. Thanks to Prof. Eigenberger who told me that I might have a chance.

I got lucky since another program did not want me. Otherwise I would be in Tucson and would never get the experience of the Terrace.

I got lucky since I passed the TOEFL Test with six points more than required.

I got lucky since Marissa Wright trained me for the interview in English. It was not necessary - the interview was the first time in German.

I got lucky since another applicant with more chances rejected at the day of the interview.

I got almost lucky since I got only the place of the reserve candidate. It was the first time that this program applied for five DAAD fellowships. Thanks to Professor Zeitz who thought that it is worth to try it regardless of the additional effort.

I got lucky since one guy made a major mistake at another program and lost his DAAD fellowship. Thanks to Professor Zeitz. He saw the opportunity and managed the money transfer from one program to the other. He did the negotiations with the DAAD. Thanks again.

Finally I got so lucky that I reached the US with DAAD support. In the US my good luck was still there.

Thanks to Beckman's barbecue welcome party I got lucky again and chose a project (Studienarbeit) in the Solar Energy Laboratory. It is great to be in this Lab. I enjoyed it.

I got lucky since my advisor John Mitchell helped during my struggle through desiccants and dehumidification. At the beginning when I met John Mitchell the first time I could not even remember the title of my project which I had already chosen. I was so embarrassed. He ignored my language problems and gave me the key references I needed for my research. John gave me always the feeling that I am free in my research. I could develop my own ideas. Thanks John!

Special thanks to Harald Klein when I discovered his program EXCHANGER on the VAX it was a feeling like Christmas and Easter at the same time.

I got lucky since the social aspects of the Solar Energy Laboratory are extraordinary. I will never forget in my life John's thanksgiving turkey. Thanks to all the great guys in the Solar Energy Lab. I never expected that somebody plays 'Schafskopf' in US, but almost the whole Solar Energy Lab plays.

The weekly calls home to Germany helped me a lot even when the news were not always good.

I showed at the beginning that I am a really lucky person.

This is right!

But after all,

I must say

I did it!

---

# Table of Contents

---

Abstract	ii
Acknowledgments	iv
List of Figures	ix
List of Tables	xii
Nomenclature	xiii

## **Chapter 1 Introduction**

1.1 Open Cycle Desiccant Air Conditioners	2
1.1.1 Adiabatic Evaporative Cooler	2
1.1.2 Sensible Heat Exchanger	3
1.1.3 Rotary Dehumidifier	4
1.2 Simple Evaporative Cooler as Air Conditioner	5
1.3 Regenerative Evaporative Cooler	7
1.4 Ventilation Cycle Desiccant Cooling System	9
1.5 Recirculation Cycle	11
1.6 Dunkle Cycle	13
1.7 Thesis Objectives	15

## **Chapter 2 Analysis of SERI/NREL Isotherm Measurements**

2.1 Background	16
2.2 The Polymers PSSA, PSSALS, PSSASS, PSSAKS	17
2.3 The Intention of the SERI Research	18
2.4 The Brunauer Isotherm Classification	18
2.5 The Results of the SERI Isotherm Measurements Compared	19

to Silica Gel	
2.6 General Behavior of Desiccant and Humid Air in a Closed Adiabatic System	22
2.7 Application of the First Law of Thermodynamics on This System	23
2.8 The General Behavior of a Desiccant and Temperature Dependent Adsorption Isotherm Shapes	26
2.9 The Proposed Thermodynamic Cycle and Second Law of Thermodynamics	27
2.10 Conclusions from the Second Law Analysis	29
 <b>Chapter 3 Isotherm Formulations</b>	
3.1 Dubinin - Polanyi Equilibrium for Microporus Adsorbents	31
3.2 The Jurinak - Polynomial Formulation	33
3.3 The Function $G(W_D^*)$	36
3.4 Isotherm Curve Fits for Silica Gel and SERI Isotherm Measurements	37
3.5 Temperature Dependent Isotherms Based on Jurinaks's Model	41
3.6 Conclusions	45
 <b>Chapter 4 The Models of the System Components</b>	
4.1 The Dehumidifier Model	46
4.1.1 The Dehumidifier Matrix Geometry	46
4.1.2 Assumption for the Model	48
4.1.3 The Model Equations	49
4.1.4 The Solution of the Model Equations	52
4.2 Sensible Heat Exchanger Model	56
4.3 The Evaporative Cooler Model	58
4.4 Conclusions	59

<b>Chapter 5 Simulations</b>	
5.1 Simulation Conditions	60
5.2 The Simulation Method	63
5.3 The Performance of the Different Desiccant Cooling Cycles	64
5.3.1 Cycle Performance with Respect to Equipment Size	64
5.3.2 Cycle Performance with Respect to Ambient Conditions	66
5.3.3 Cycle Performance with Respect to Inlet Conditions	68
5.3.4 Performance with Respect to the Regeneration Mass Flow	71
5.3.5 Assessment of the Different Cycles	72
5.4 The Evaluation of the Isotherms Based on the SERI Measurements	73
5.4.1 Variation of the Isotherm Shape with Respect to Equipment Size	74
5.4.2 Isotherm Shape with Respect to Ambient Conditions	76
5.4.3 Isotherm Shape with Respect to the Room Inlet State	77
5.4.4 Assessment of the Simulation Results and Interpretation	78
5.4.5 The Heat of Adsorption and Isotherm Shape	81
5.4.6 Summary of the Performance of the Theoretical Isotherms Based on the SERI/NREL Results	82
5.5 New Cooling Cycles with Staged Dehumidification	83
5.5.1 Simulation Results of the New Cooling Cycles	86
5.5.2 Staged Dehumidification Conclusions	88
<b>Chapter 6 Results and Conclusions</b>	<b>89</b>
<b>Appendix A The Nature of Physical Adsorption</b>	
<b>Appendix B Program Description</b>	
<b>Appendix C Derivatives Calculations</b>	
<b>Bibliography</b>	

---

## List of Figures

---

Figure 1.1	Evaporative Cooler	2
Figure 1.2	Sensible Heat Exchanger	3
Figure 1.3	Rotary Dehumidifier	4
Figure 1.4	Schematic Diagram of an Evaporative Cooler	5
Figure 1.5	Psychometric Diagram of an Evaporative Cooler	6
Figure 1.6	Schematic Diagram of a Regenerative Cooler	7
Figure 1.7	Psychometric Diagram of a Regenerative Cooler	8
Figure 1.8	Schematic Diagram of a Ventilation Cycle	9
Figure 1.9	Psychometric Diagram of Ventilation Cycle	10
Figure 1.10	Schematic Diagram of a Recirculation Cycle	12
Figure 1.11	Psychometric Diagram of Recirculation Cycle	12
Figure 1.12	Schematic Diagram of a Closed Dunkle Cycle	14
Figure 1.13	Psychometric Diagram of a Closed Dunkle Cycle	14
Figure 2.1	Structural Repeating Units for SERI Polymers	17
Figure 2.2	Brunauer Type 1, Type 2, and Linear Isotherms	19
Figure 2.3	Silica Gel Isotherm	20
Figure 2.4	Isotherms Measurement for SPSS Taken by SERI	21
Figure 2.5	Closed Adiabatic System	22
Figure 2.6	The Theoretical Cycle	28
Figure 2.7	The Process Conditions for Process 2 to 3	28
Figure 3.1	SERI R19-52-3 and Fifth Order Polynomial Curve Fit	38
Figure 3.2	The Approximation of the SERI Measurements	39

Figure 3.3	Polynomial Curve Fit and Van Den Bulk Curve Fit at 50°C	41
Figure 3.4	Polynomial Curve Fit and Van Den Bulk Curve Fit at 30°C and 70°C	42
Figure 3.5	SERI R19-52-3 $dh^* = 0.25$	43
Figure 3.6	SERI R19-52-3 $dh^* = 0.6$	43
Figure 3.7	SERI R19-52-3 $dh^* = 1.0$	43
Figure 3.8	SERI R19-52-3 $dh^* = 1.4$	43
Figure 3.9	Artificial Silica Gel $dh^* = 0.25$	43
Figure 3.10	Artificial Silica Gel $dh^* = 0.6$	43
Figure 3.11	Artificial Silica Gel $dh^* = 1.0$	44
Figure 3.12	Artificial Silica Gel $dh^* = 1.4$	44
Figure 3.13	SERI R19-52-3 Variation of $k$ at $dh^* = 1.0$	44
Figure 4.1	Nomenclature and Coordinate System for a Regenerative Dehumidifier	47
Figure 4.2	One Finite Difference Element	53
Figure 4.3	Dehumidifier with Three Inlets	55
Figure 5.1	Equipment Size, Recirculation and Ventilation Cycle, Los Angeles	64
Figure 5.2	Equipment Size, Recirculation and Ventilation Cycle, Miami	65
Figure 5.3	Equipment Size, All Cycles, Chicago Design	66
Figure 5.4	Variation of the Ambient Temperature at Constant Relative Humidity, Ventilation and Recirculation Cycle	67
Figure 5.5	Variation of the Ambient Temperature at Constant Relative Humidity, Open and Closed Dunkle Cycle	68
Figure 5.6	Variation of the Enthalpy Difference, Chicago	69

	Ventilation and Recirculation Cycle	
Figure 5.7	Variation of the Enthalpy Difference, Chicago Open and Closed Dunkle Cycle	70
Figure 5.8	Variation of the Enthalpy Difference at 69% Relative Humidity and 34°C	71
Figure 5.9	Regeneration Mass Flow Variation, Chicago	72
Figure 5.10	COP Silica Gel Isotherm Set, Ventilation Cycle Chicago Design Conditions	74
Figure 5.11	COP of SERI Isotherms, Ventilation Cycle, Chicago	75
Figure 5.12	COP Silica Gel Isotherm Set, Dunkle Cycle, Chicago	76
Figure 5.13	Variation of the Ambient Temperature for Various Isotherm Shapes	77
Figure 5.14	Enthalpy Difference Variation for Different Shapes at Chicago Design	78
Figure 5.15	SERI Approximation, Dehumidifier Outlet State Depending on Rotation Speed, $dh^*=0.25$	81
Figure 5.16	SERI Approximation, Dehumidifier Outlet State Depending on Rotation Speed, $dh^*=1.4$	81
Figure 5.17	Inlet and Outlet Nozzles of a Four Way Dehumidifier	83
Figure 5.18	Open Cycle with Staged Dehumidification and a Four Way Dehumidifier	85
Figure 5.19	Closed Cycle with Staged Dehumidification and a Three Way Dehumidifier	86

---

## List of Tables

---

Table 3.1	SERI Approximation Parameters	39
Table 3.2	Van Den Bulk Parameters for Silica Gel	40
Table 3.3	Jurinak Polynomial Approximation Parameters	40
Table 5.1	Design Data for Commercial Buildings	60
Table 5.2	ASHRAE 1% Design Conditions for Chicago, Los Angeles, and Miami	61
Table 5.3	Room States and Process Air Inlet States	62
Table 5.4	Simulation Inputs	62
Table 5.5	SERI Approximation, Dehumidifier Outlet Temperatures	79
Table 5.6	Simulation Results for the Different Dehumidifiers	87

---

## Nomenclature

---

### English Letter Symbols

---

Symbol	Definition	SI-Units
$a_1$ - $a_5$	scaling parameters Jurinak isotherm formulation	
$A$	adsorption potential	[kJ/kg]
$A_j$	heat and mass transfer area at period $j$	[m <sup>2</sup> ]
$c$	specific heat capacity at constant volume	[kJ/kgC]
$c_p$	specific heat capacity at constant pressure	[kJ/kgC]
$C$	air capacitance rate	[kJ/Cs]
$C^*$	ratio minimum to maximum air capacitance rate	
$D_m$	convective mass transfer coefficient	[kg/m <sup>2</sup> s]
$E_{o1}, E_{o2}$	scaling parameters of Dubinin-Astrakov isotherm	
$dh^*$	scaling parameter Jurinak isotherm formulation	
$h$	specific enthalpy	[kJ/kg]
$h_{VL}$	specific heat of vaporization	[kJ/kg]
$H$	enthalpy	[kJ]
$h^*$	ratio heat of adsorption to heat of vaporization	
$is$	specific entropy production	[kJ/kgC]
$k$	scaling parameter Jurinak isotherm formulation	
$L_{ex}$	exegetic work	[kJ/kg]
$L$	axial flow length	[m]
$Le$	Lewis number	
$m$	mass flow rate	[kg/s]

$M_m$	mass of dry matrix	[kg]
$NTU_t$	number of transfer units for sensible heat transfer	
$NTU_w$	number of transfer units for mass transfer	
$p_S$	saturation pressure	[Pa]
$p_V$	partial pressure of water vapor	[Pa]
$s$	specific entropy	[kJ/kgC]
$R$	gas constant of water vapor	[kJ/kgK]
$t$	temperature	[C]
$T$	thermodynamic temperature	[K]
$T$	time for one rotation of the desiccant wheel	[s]
$u$	specific internal energy	[kJ/kg]
$U$	internal energy	[kJ]
$w$	humidity ratio of moist air	[kg water/kg dry air]
$W_D$	water content of the desiccant	[kg water/ kg dry desiccant]
$W_{max}$	water content at 100% relative humidity	[kg water/ kg dry desiccant]
$W_D^*$	WD/WDmax	
$W_{o1}, W_{o2}$	scaling parameters of Dubinin-Astrakov isotherm	
$x$	axial flow coordinate	[m]
$z$	dimensionless flow coordinate	

### Greek Letter Symbols

Symbol	Definition	SI-Units
$\alpha$	convective heat transfer coefficient	[kJ/m <sup>2</sup> sC]
$\epsilon_t$	heat transfer effectiveness	
$\epsilon_{direct}$	effectiveness of direct counterflow heat exchanger	
$\epsilon_r$	effectiveness of a regenerative heat exchanger	

$\Gamma$	ratio matrix flow rate to air flow rate	
$\theta$	dwel time (time coordinate)	[s]
$\tau$	dimensionless time	

### Subscripts

---

Symbol	Definition
a, air	air state
c	cold stream
d	direct heat exchanger
D	desiccant
eq	air state in equilibrium with desiccant
h	hot stream
i	inlet
j	period 1 or 2 (cold or hot stream)
L	liquid
m	matrix
o	outlet
r	regenerative heat exchanger
s	sorption or saturation
t	sensible heat
w	water
V	vapor



---

# Chapter one

---

## **Introduction**

Desiccant cooling research is currently under review all over the world . Chlorofluorohydrocarbons (CFCs) used in conventional compression refrigeration machines are partially responsible for stratospheric ozone depletion. This negative impact on the environment and prohibition of CFCs enforces the development of new refrigerants with less ozone destroying potential and the improvement of alternative air conditioning methods.

One of the most promising methods without any refrigerant in the cooling machine are the traditional desiccant cooling cycles; refrigerant is the air itself. Besides their principal advantage that they need no working fluid desiccant cooling cycles have the advantage of the possibility to use low temperature heat for operation. The required temperature level is below 90°C which is low enough for the application of solar energy provided by solar collectors.

The classical desiccant cooling cycles show always limits in the ambient conditions which can be handled by the air conditioner. This and the fact that reasonable performance is only possible with heat exchanger effectiveness above 80% and a large dehumidifier (NTU about 10) made a commercial success of desiccant cooling machines compared to compact compression air conditioners impossible.

This study focuses on the dehumidifier and the possible improvement of the classical cooling cycles with new advanced desiccants as well as staged dehumidification. The effect of temperature depended desiccant isotherms is especially investigated.

### 1.1 Open Cycle Desiccant Air Conditioners

Open cycle air conditioners are distinguished from closed cycle air conditioners by the fact that in a closed cycle air conditioner the refrigerant never leaves the boundaries of the machine, whereas in an open cycle the refrigerant crosses the boundaries of the air conditioner.

Open cycle desiccant air conditioners consist of several components. The following sections discuss briefly the main components of a desiccant cooling cycle. In this discussion only overall mass and energy balances are shown to give some feeling for the processes. The dehumidifier and heat exchanger are discussed in Chapter 4 with more detail.

#### 1.1.1 Adiabatic Evaporative Cooler (Adiabatic Humidifier)

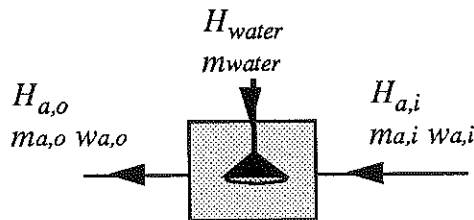


Figure 1.1

The evaporative cooler converts sensible heat into latent heat. Warm and dry air cools down due to the sensible heat consumed by an adiabatic evaporation process. The air is at the outlet of the component wetter and cooler than before. The enthalpy of wet air is a function of temperature and humidity.

Energy Balance:

$$H_{a,i} + H_{water,i} = H_{a,o}$$

Mass Balance:

$$m_{a,i}w_{a,i} + m_{water,i} = m_{a,o}w_{a,o}$$

The maximum temperature decrease is possible up to the wet bulb temperature of the process air at the inlet with the corresponding increase in air humidity. When the air reaches wet bulb temperature at the outlet the air is saturated with water vapor.

### 1.1.2 Sensible Heat Exchanger

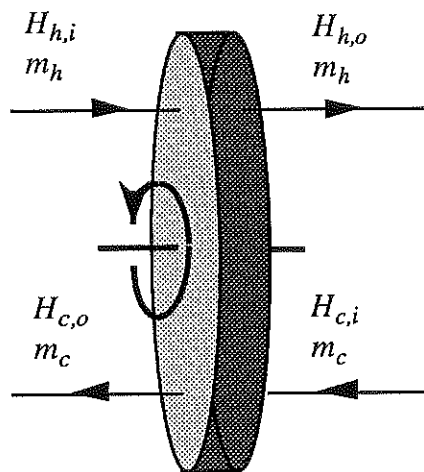


Figure 1.2 Sensible Heat Exchanger

The sensible heat exchanger is a regenerative rotary heat exchanger with no water adsorption ability. The well known relationships for counter current sensible heat exchangers can be applied for the regenerative rotary heat exchanger. Since the humidity of the air streams through the exchanger does not change, the enthalpy difference between inlets and outlets is only a function of temperature.

Enthalpy Balance:

$$H_{c,i} - H_{c,o} + H_{h,i} - H_{h,o} = 0$$

or  $(\dot{m} cp)_c(T_{c,o} - T_{c,i}) = -(\dot{m} cp)_h(T_{h,o} - T_{h,i})$

Effectiveness Model:

$$\text{heat exchanger effectiveness} = \frac{(\dot{m}c_p)_h(T_{h,i} - T_{h,o})}{(\dot{m}c_p)_{\min}(T_{h,i} - T_{c,i})} = \frac{(\dot{m}c_p)_c(T_{c,o} - T_{c,i})}{(\dot{m}c_p)_{\min}(T_{h,i} - T_{c,i})}$$

Equal heat capacity streams result in equal temperature differences between inlet and outlet of the 'cold' and the 'hot' stream.

### 1.1.3 The Rotary Dehumidifier

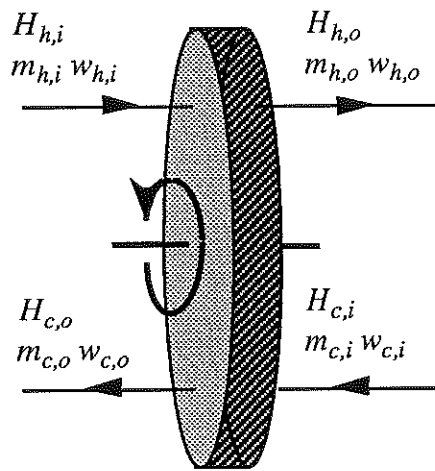


Figure 1.3. Rotary Dehumidifier

In a rotary dehumidifier heat and mass exchange occur at the same time. The energy and mass balances are coupled due to the fact that the enthalpy is a function of humidity and temperature.

Enthalpy Balance:

$$H_{c,i} - H_{c,o} + H_{h,i} - H_{h,o} = 0$$

Moisture Balance:

$$m_c(w_{c,i} - w_{c,o}) + m_h(w_{h,i} - w_{h,o}) = 0$$

An easy way to visualize the processes involved in a dehumidifier is the method to associate adsorption with condensation and desorption with evaporation of water at partial water vapor pressures below saturation pressure. This way to look at it makes it easy to understand the temperature increase of the process stream as water is adsorbed (condensed) and the temperature decrease of the regeneration stream as water is desorbed (evaporated).

### 1.2 Simple Evaporative Cooler as Air Conditioner

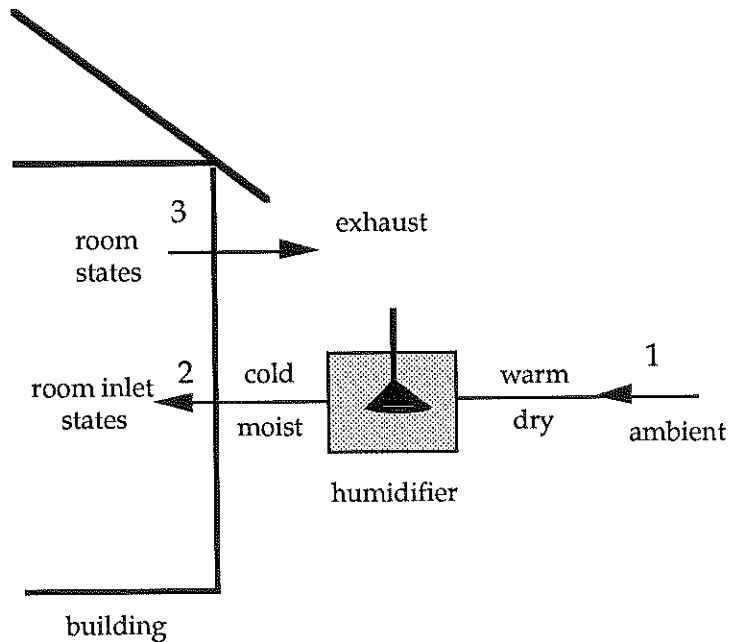
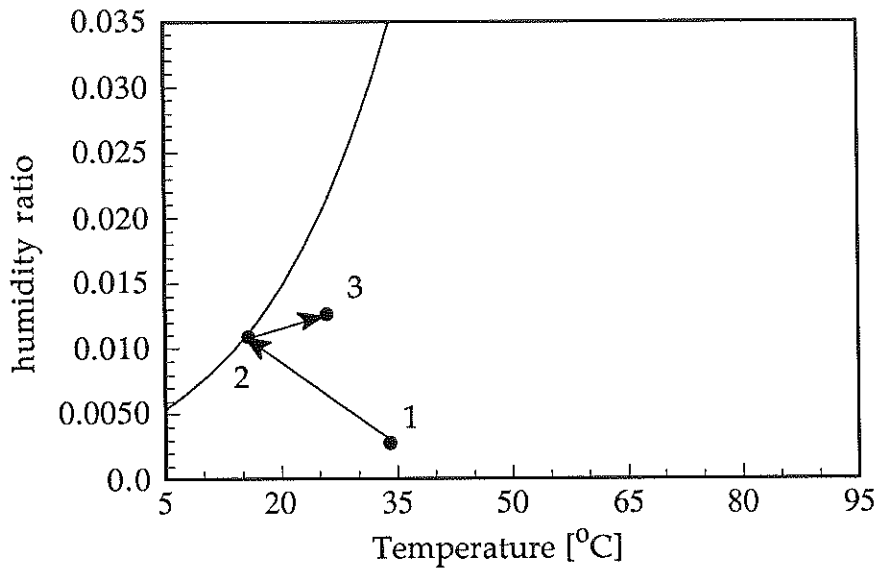


Figure 1.4. Evaporative Cooler



*Figure 1.6. Psychrometric Diagram of a Evaporative Cooler*

Evaporative coolers work with satisfying results only in temperate climates. The wet bulb temperature of the ambient must be less than the desired room wet bulb temperature. This is only true for very dry and not too hot climates. Some places in the US, for example in Arizona or New Mexico, can meet the cooling requirements 95% of the year with evaporative coolers. These cooling devices convert simply sensible heat into latent heat. Evaporative coolers are commonplace in the commercial market and are used extensively for residential cooling in these climates. In more humid climates, evaporative and indirect evaporative coolers are used in conjunction with conventional vapor compression machines.

### 1.3 Regenerative Evaporative Coolers

The cooling machine consists now of two evaporative coolers and one sensible heat exchanger. The process air stream is cooled by a sensible regenerative rotary heat exchanger from ambient temperature (state 1) to a temperature around or below room temperature (state 2). The temperature is further decreased by an adiabatic humidifier to the desired room inlet states. The exhaust air stream is saturated by a second humidifier. This air stream is the heat sink for the sensible heat exchanger. This configuration works at higher ambient humidity and temperatures than the simple evaporative cooler, since the sensible heat exchanger cools the process stream down without an increase in humidity and higher latent heat. Figure 1.6 shows a regenerative evaporative cooler.

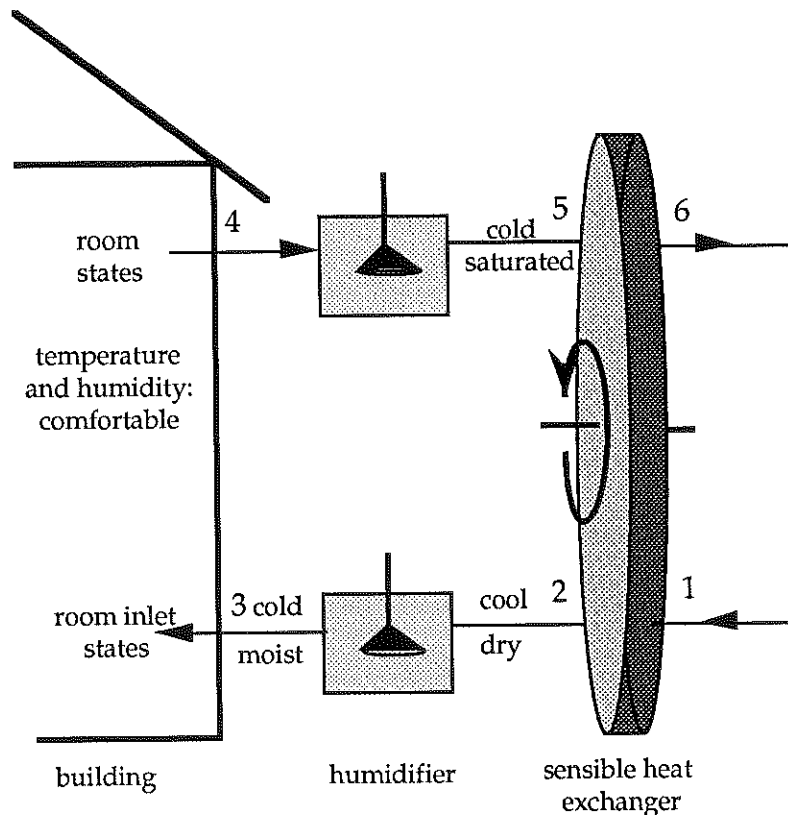
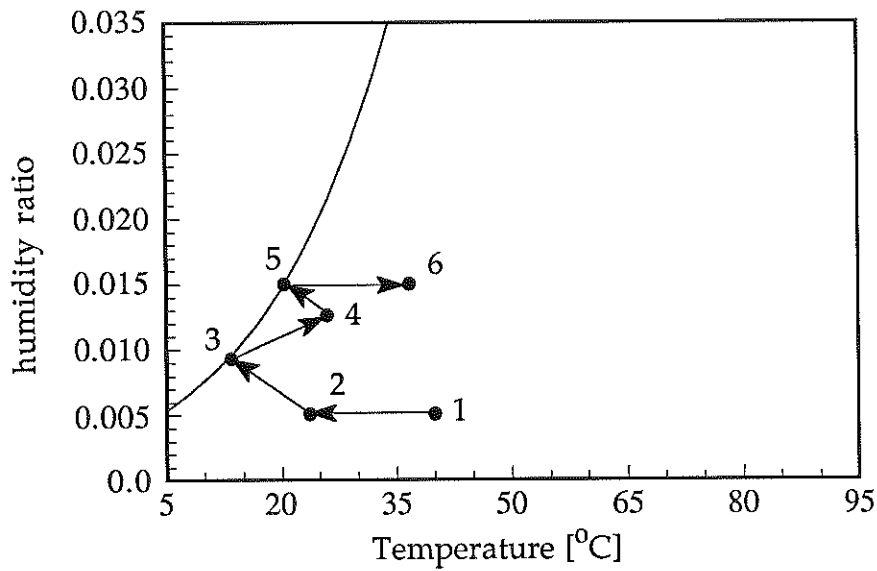


Figure 1.6. Schematic Diagram of an Evaporative Cooler

Regenerative evaporative coolers of this type are sufficient in dry and hot climates and meet almost during the whole year the cooling load. They are very cost effective since the only costs during operation are electrical costs for fans, pumps, and water. Regenerative coolers operate only well if the ambient is drier than the desired room state.



*Figure 1.8 Psychrometric Diagram of a Evaporative Regenerative Cooler*

### 1.4 Ventilation Cycle Desiccant Cooling System

In the classical ventilation cycle a rotary dehumidifier dries the ambient air (state 1) and heats it (state 2) due to the condensation effects involved in the adsorption process. The process stream (state 3) enters a rotary sensible heat exchanger and cools down (state 4). An adiabatic humidifier cools this air stream further and humidifies it to the desired room inlet conditions (state 5). The load of the zone heats and humidifies the air to the room state (state 6). The exhaust stream (regeneration stream) of the zone is cooled by a evaporative cooler in order to provide the sensible heat exchanger with a deeper heat sink (state 7). The heat exchanger heats the regeneration stream up (state 8). The temperature at state 8 is not high enough for the regeneration of the dehumidifier therefore an additional heater is necessary to heat the regeneration stream to the regeneration temperature (state 9).

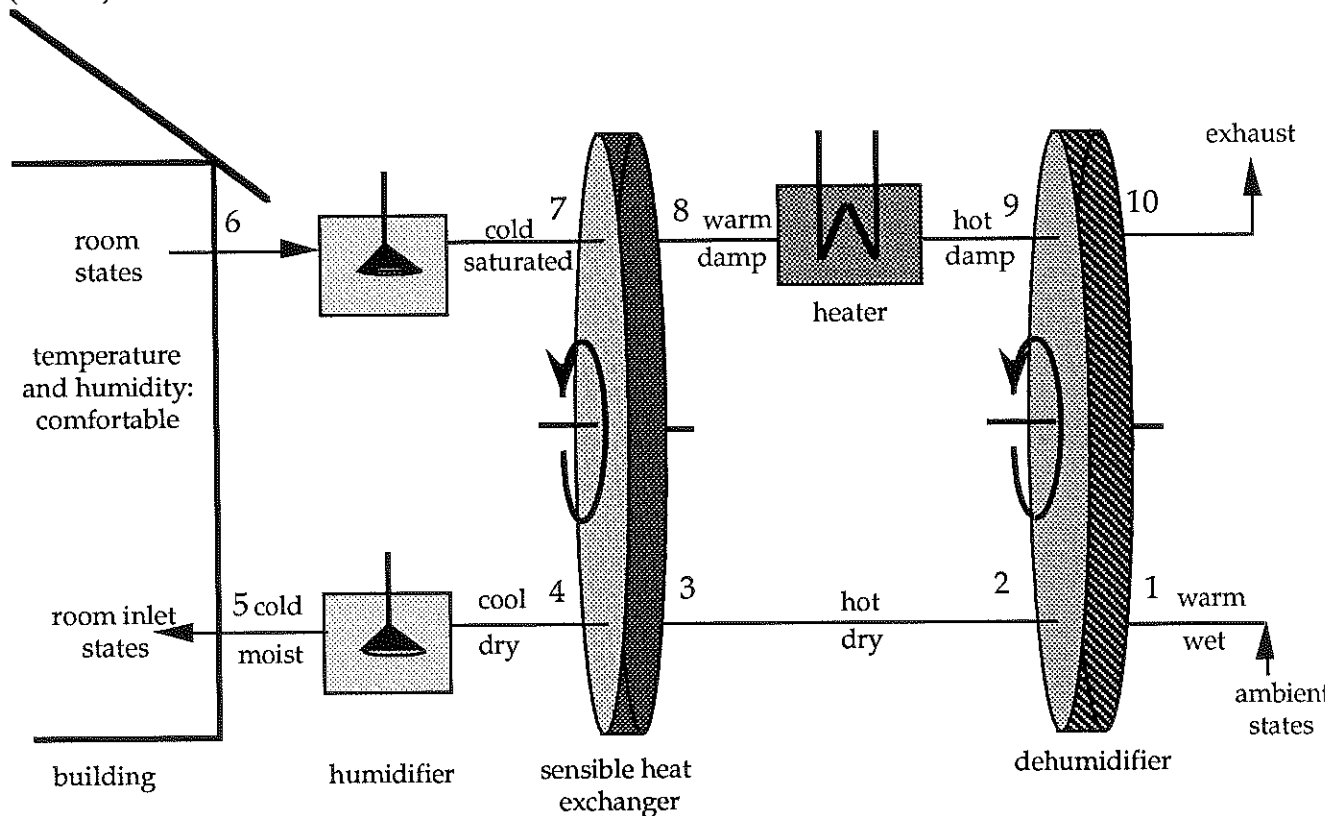
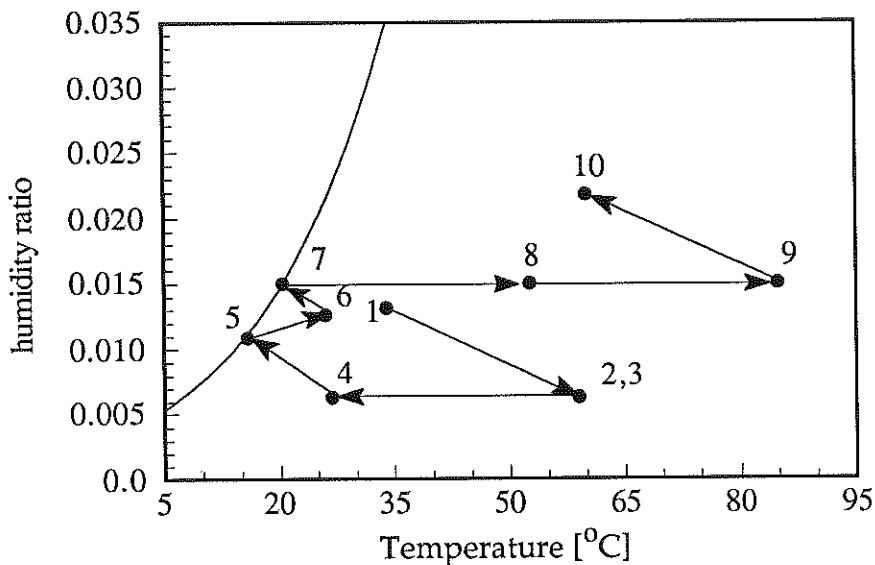


Figure 1.10 Schematic Diagram of a Ventilation Cycle

Through the dehumidifier the hot regeneration stream with a very low relative humidity picks up the moist from the dehumidifier matrix and cools down due to the evaporation process involved with the desorption of water (state 10).



*Figure 1.11 Psychrometric Diagram of a Ventilation Cycle*

The ventilation cycle works better compared to the single regenerative cooler at higher ambient humidity. The thermal COP of the system, the ratio between zone load and auxiliary heat provided to the heater, is highly dependable on the heat exchanger effectiveness and ambient state. A low heat exchanger effectiveness has double the impact on the performance. With a small heat exchanger the process air is cooled down less and must be therefore drier before it enters the evaporative cooler to meet the desired conditions at the room inlet. The other impact is the fact that the regeneration stream is heated less and therefore more heat is required by the auxiliary heater.

A high humidity of the ambient air causes trouble since the adsorption process is a 'condensation' process. This means that the adsorbed water heats the air stream up and, due to the increased temperature, reduces the relative humidity of the process air.

The relative humidity is the driving force of an adsorption process. With a smaller driving force the absolute outlet humidity is higher and the temperature of the process stream after the dehumidifier is higher. Both effects make the performance of the cooler worse. The ventilation cycle is therefore suitable for small humidity of the ambient and the COP gets much worse with only little humidity increase. The highest humidity which can be handled with a ventilation cycle is about 40% relative humidity.

### **1.5 Recirculation Cycle**

The recirculation cycle uses the same equipment as the ventilation cycle. In contrast to the ventilation cycle, which supplies fresh air to the zone, the recirculation cycle circulates the room air in a closed loop.

The recirculation cycle works at low ambient humidity with a lower COP than the ventilation cycle. This is caused by the fact that at low ambient humidity the regeneration stream of a ventilation cycle is less moist than the regeneration stream of a recirculation cycle. At higher ambient humidity the effect of the higher dehumidification load of the process stream of a ventilation cycle is more important than the higher initial humidity of the regeneration stream. The benefit of a process air stream with constant dehumidifier inlet states is greater than the problems involved with a more moist regeneration stream.

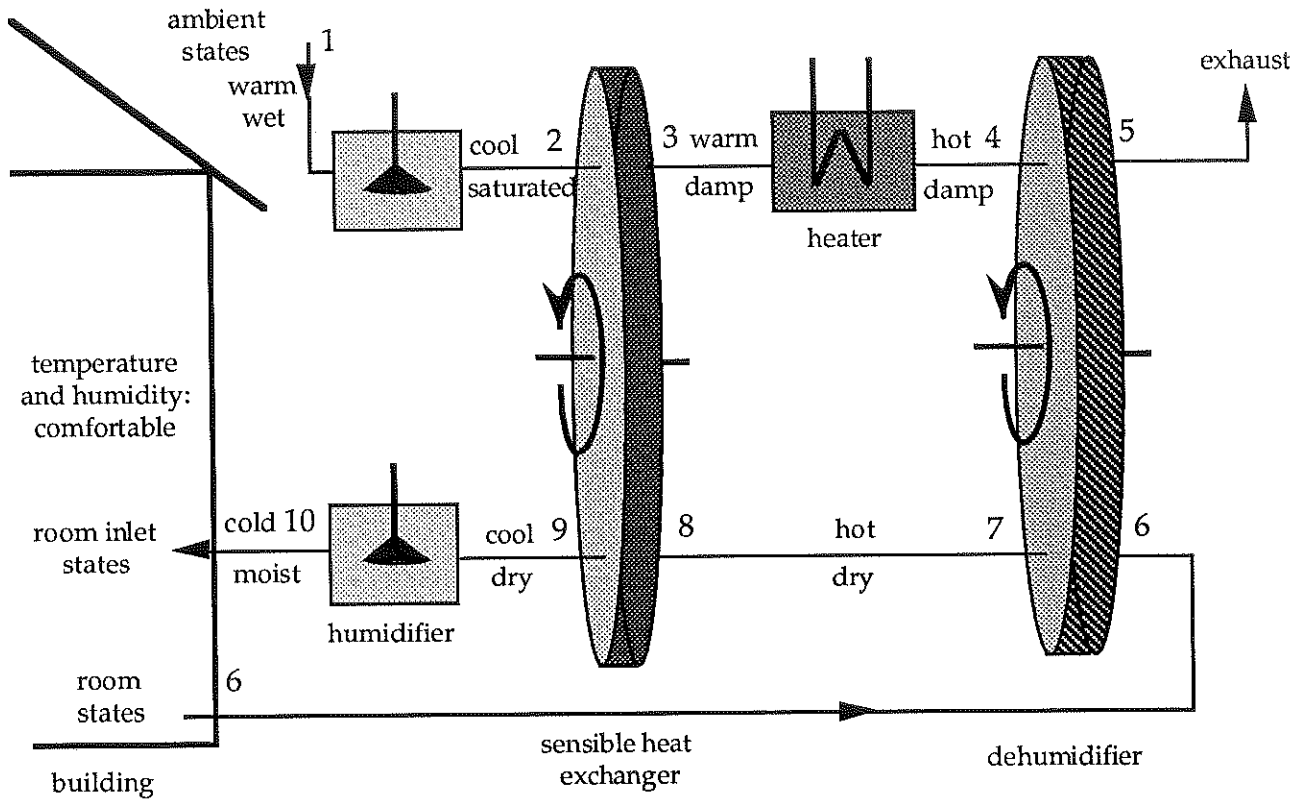


Figure 1.11. Schematic Diagram of a Recirculation Cycle

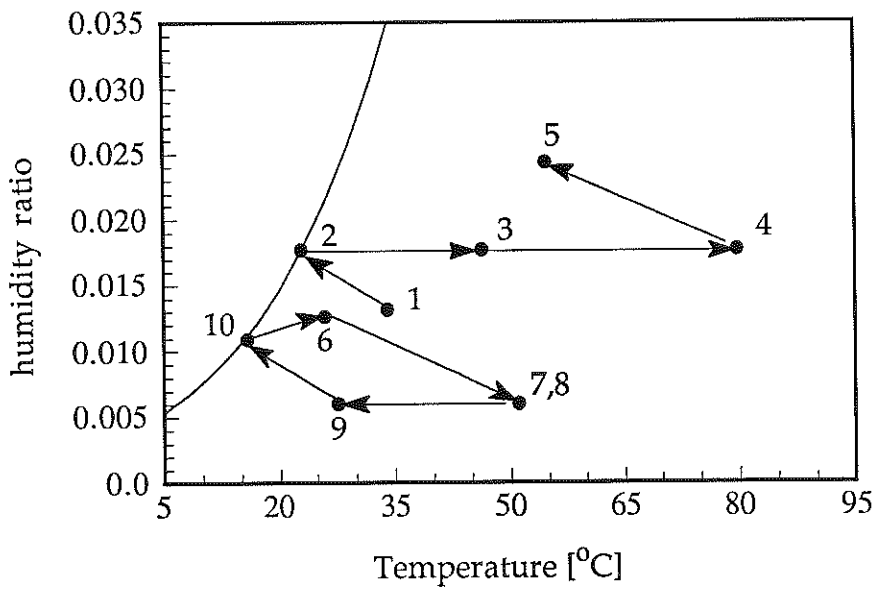


Figure 1.12. Psychrometric Diagram of a Recirculation Cycle

The recirculation cycle shows still limits for the maximum ambient humidity which can be handled by the cooling device. These are about 5 to 10% higher than the limits of the ventilation cycle with the same equipment.

The recirculation cycle is not desirable for modern air conditioning requirements since it provides the zone with no fresh air from the ambient. The ASHRAE handbook requires at least 2.5 l/s per person out door air.

### **1.6 Dunkle Cycle**

The Dunkle cycle works with one additional sensible heat exchanger. The Dunkle cycle described here is connected like a recirculation cycle, whereas the heat sink for the heat exchanger of the process air stream loop is similar to the one of a ventilation cycle. Besides this connection it is possible to feed the dehumidifier directly with air from the ambient instead of recirculated heat from the second heat exchanger (state 7). This stream is then dumped to the ambient. In chapter 5 this connection is referred to as 'open' Dunkle cycle.

The Dunkle cycle is able to combine the advantages of ventilation and recirculation cycle for the price of one more heat exchanger. It works well even at slightly higher humidity ratios than the recirculation cycle.

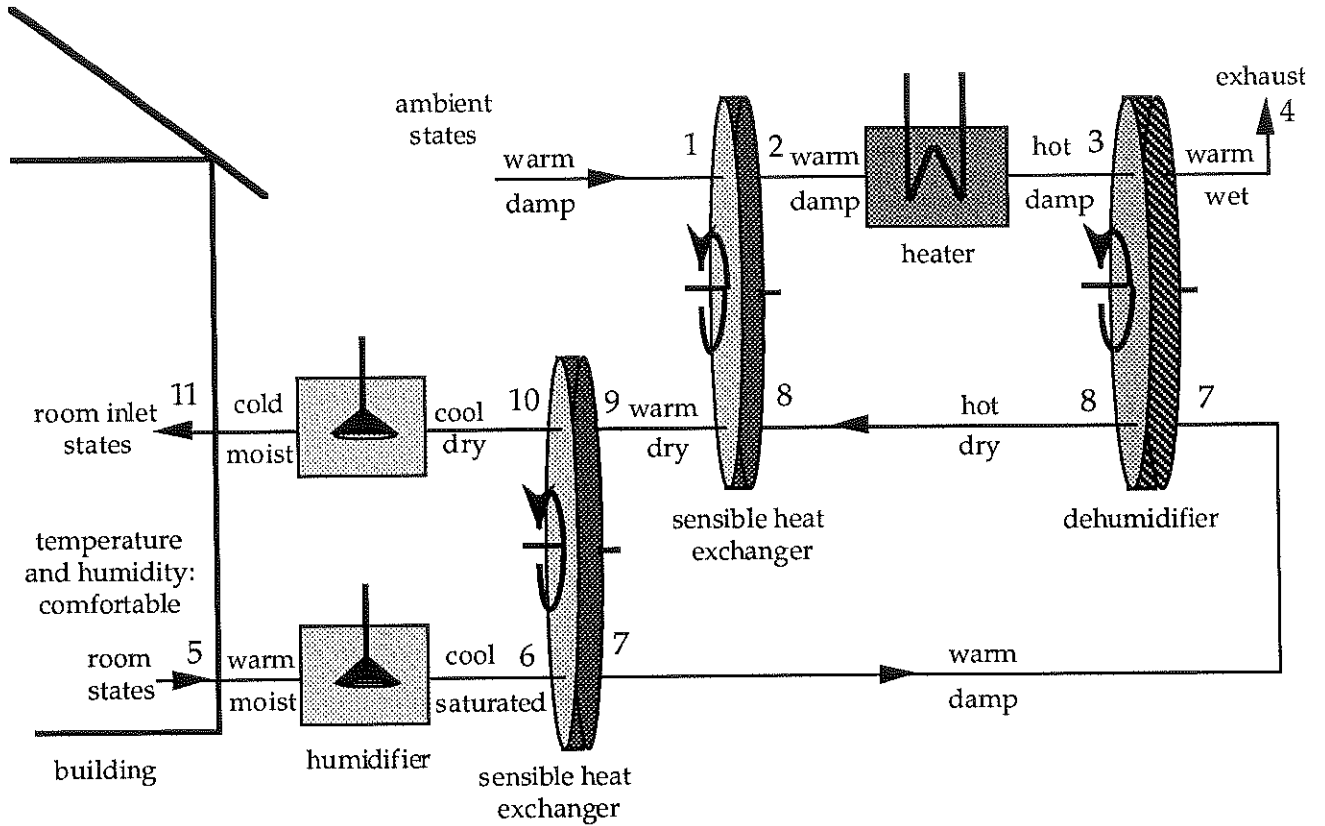


Figure 1.13. Schematic Diagram of a Closed Dunkle Cycle

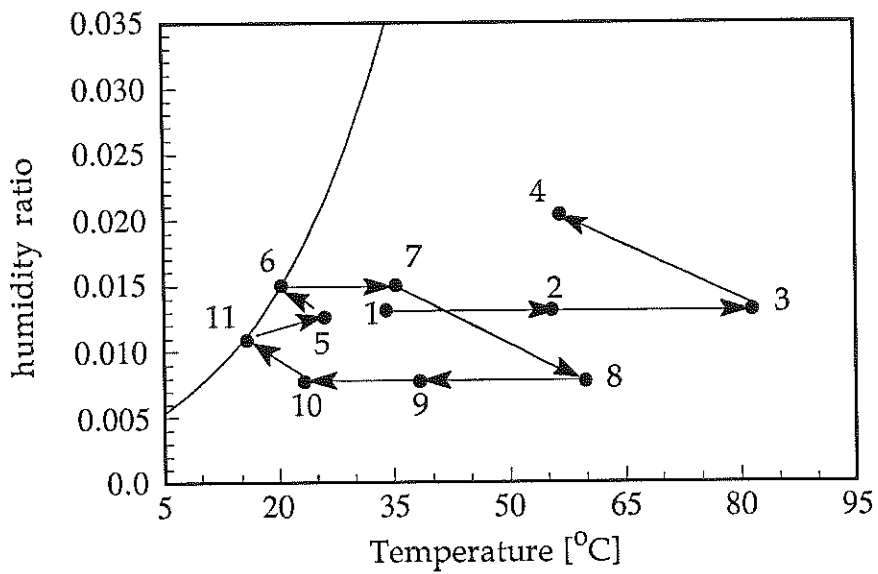


Figure 1.14 Psychrometric Diagram of a Dunkle Cycle

## 1.7 Report Objectives

The primary goal of this study is the evaluation of new desiccants for desiccant cooling cycles. This investigation is based on isotherm measurements taken by the Solar Energy Research Institute (SERI). The results and problems which are involved with the SERI measurements are presented in Chapter 2.

An isotherm model should be developed which allows the simulation of the behavior of the desiccants studied by SERI. Chapter 3 discusses two different formulations for isotherms and suggests curve fits for the SERI data.

The isotherm model is then implemented in an adiabatic rotary dehumidifier model, which is discussed in Chapter 4.

The evaluation of these new desiccants compared to regular silica gel should show the advantage of these new desiccants. The reaction of the classical cooling cycles introduced in this chapter is presented in Chapter 5 in terms of thermal COPs, and regeneration temperatures.

Finally, new desiccant cooling cycles with staged dehumidification are introduced in Chapter 5.

---

## Chapter two

---

### **Analysis of SERI/NREL Isotherm Measurements**

#### Polymers as Advanced Materials for Desiccant Cooling Applications

### **2.1 Background**

The analysis of polymers for desiccant cooling applications began in 1985 as a subtask of the Solar Desiccant Cooling Program done by the Solar Energy Research Institute (SERI).

The US. Department of Energy (DOE) supports a variety of programs to promote a balanced and mixed energy resource system. It is the goal of this program to establish a proven technology base to allow industry to develop solar products and designs for buildings that are economically competitive and can contribute significantly to building energy supplies nationally.

The research activities which are sponsored by this program are conducted in four major areas: 1 Advanced Passive Solar Materials Research, 2 Collector Technology Research, 3 Cooling Systems Research, and 4 Systems Analysis and Applications Research.

The polymer analysis done by SERI fits in the third area: *Cooling Systems Research*. This activity involves research on high-performance dehumidifiers and chillers that can operate efficiently with the thermal output and delivery temperatures associated with solar collectors. It also includes work on advanced passive cooling techniques. [1]

## 2.2 The Polymers PSSA, PSSALS, PSSASS , PSSAKS

The SERI institute studied several polymers based on multiple phenyl groups. The different desiccants can be distinguished by the percentage of sulfonation, one hundred percent sulfonation means one sulfonate ion is attached to each phenyl group, and by the different counterions attached to the  $\text{SO}_3^-$  group. Figure 2.1 shows the chemical structure of the investigated polymers. Strong acid ion exchange resins [3] have the same chemical structure.

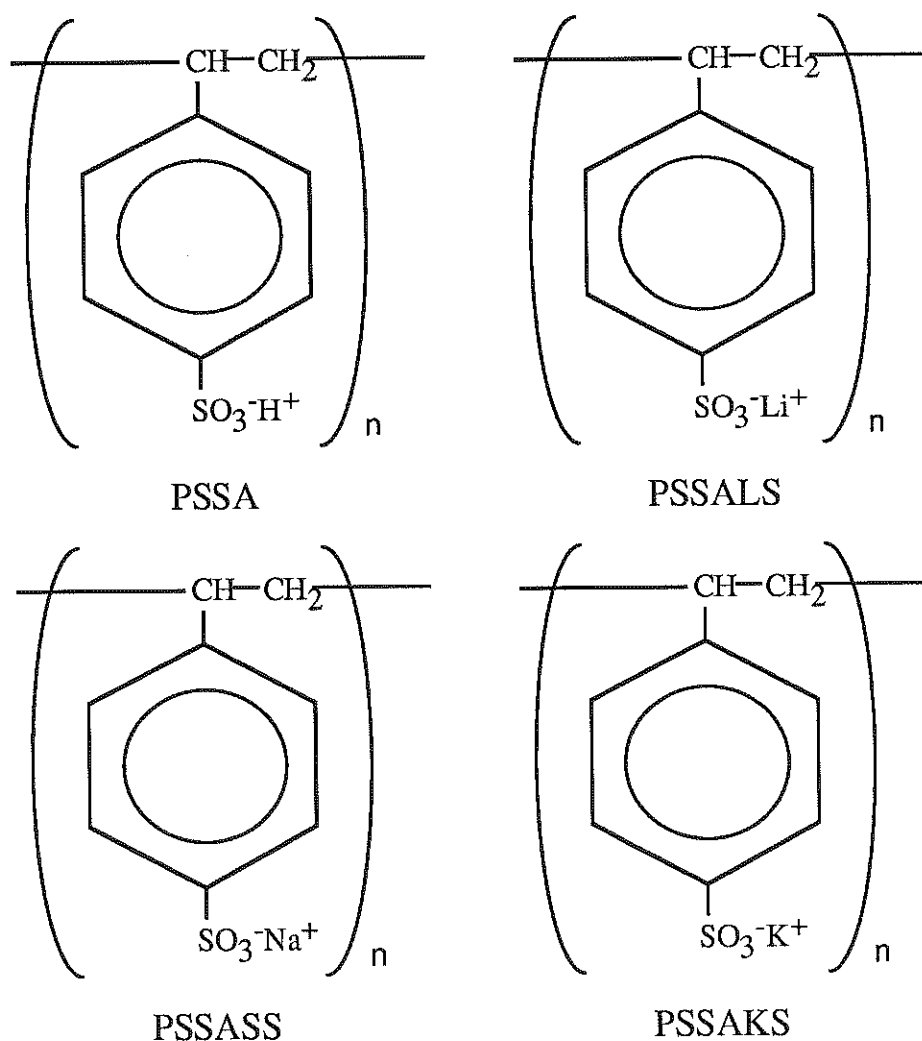


Figure 2.1 Structural repeating units for PSSA, PSSALS, PSSASS and PSSAKS, where  $n$  is the number of repeating units

Polystyrene sulfate sodium salt (PSSA) is the base structure of all polymers above. The alkali ionic salts of PSSA are made by exchanging  $H^+$  of PSSA with a different counterion. Polystyrene sulfonic acid lithium salt (PSSALS), polystyrene sulfonic acid sodium salt (PSSASS), polystyrene sulfonic acid potassium salt (PSSAKS), and sodium polystyrene sulfonate (SPSS), which is a commercially available form of PSSASS with 90% sulfonation, were investigated by SERI during the years 1988 and 1989.

### **2.3 The Intention of the SERI Research**

The primary objective was the discovery and evaluation of new and better desiccants for desiccant cooling applications. The SERI laboratory based their investigation activities on a computer parametric systems analysis study (Collier, Cale, and Lavan 1986). This study concluded that if an "ideal" desiccant can be identified, the thermal COP of a desiccant cooling system can be improved from the range 0.85 to 1.05, which can now be obtained with a silica gel dehumidifier, to a minimum of 1.3 to 1.4 or closer to the theoretical maximum of about 2.5. From these studies SERI concluded that a Brunauer Type 1 moderate is the best isotherm shape for the adsorption step, and a Type 3 extreme is the best shape during regeneration or desorption of water. Therefore, they declared a temperature dependent isotherm to be desirable for desiccant cooling systems which changes its shape from a Type 1 at adsorption temperature to a Type 3 at regeneration temperature.

### **2.4 The Brunauer Isotherm Classification**

Brunauer classified experimentally observed isotherms into five types. Here, only two of these types are introduced: Type 1 moderate and Type 3 together with a linear isotherm. "Normal" desiccants have a constant ratio between the relative humidity of the air and the water uptake of the desiccant. This ratio is usually almost independent of

temperature. It can be concluded from Figure 2.2 that a Type 1 isotherm will adsorb water vapor more easily than a linear shape since a low relative humidity which will be reached at the outlet of an dehumidifier is related to a high desiccant water content. The driving force for the adsorption process is the difference between the relative humidity of the air and the equilibrium water vapor concentration (relative humidity of air in equilibrium with desiccant). This driving force is higher compared to a linear isotherm. The same is true for the regeneration process and a Brunauer Type 3 isotherm shape, where the desorption is supported by the isotherm shape. Figure 2.2 shows normalized isotherms as functions of relative humidity. Normalized means that the actual water content which represents the ratio between the mass of water adsorbed to the mass of the dry matrix ( $W$ ) is divided by the maximum water content ( $W_{\max}$ ; water content at 100% relative humidity).

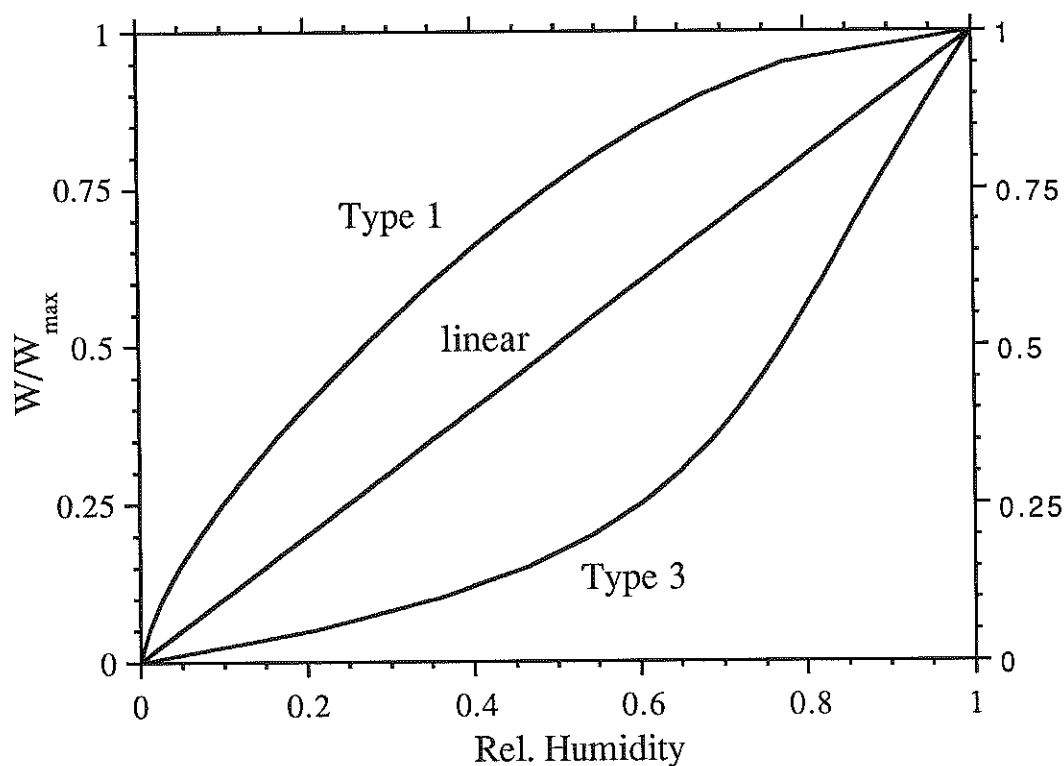
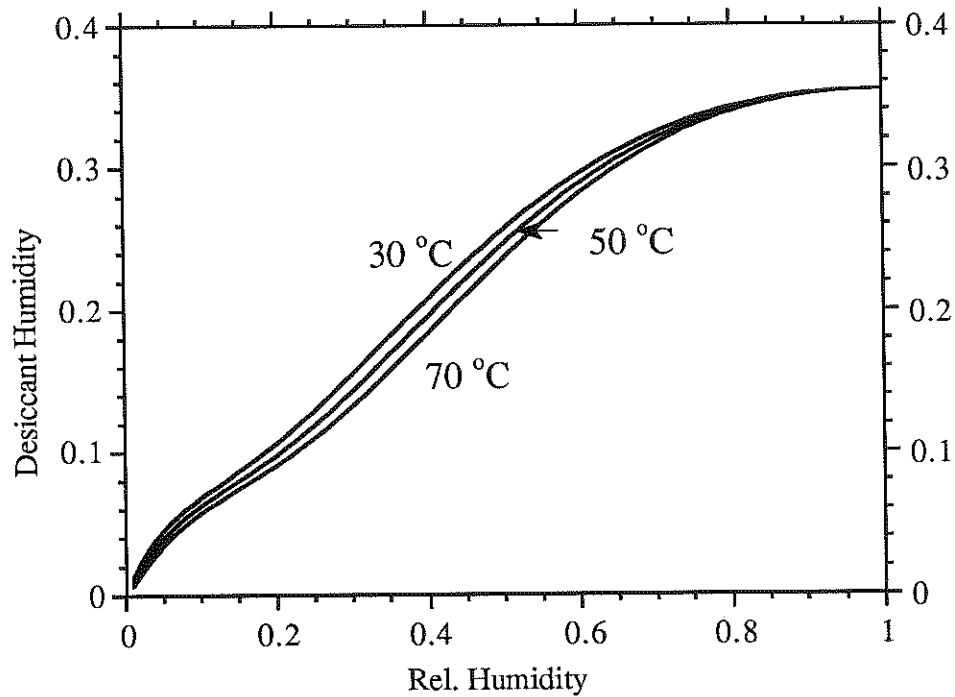


Figure 2.2 Brunauer Type 1, Type 3, and Linear Isotherms

## 2.5 The Results of the SERI Isotherm Measurements Compared to Silica Gel

### Silica Gel



*Figure 2.3 Silica Gel Isotherm*

The typical isotherm for silica gel is almost linear. Figure 2.3 presents a isotherm correlation for regular silica Gel based on the Dubinin - Polanyi theory for silica gel. The isotherms for 30°C, 50°C, 70°C are curve fits for experimental data [Van den Bulk 1987]

## SPSS, Scientific Polymer

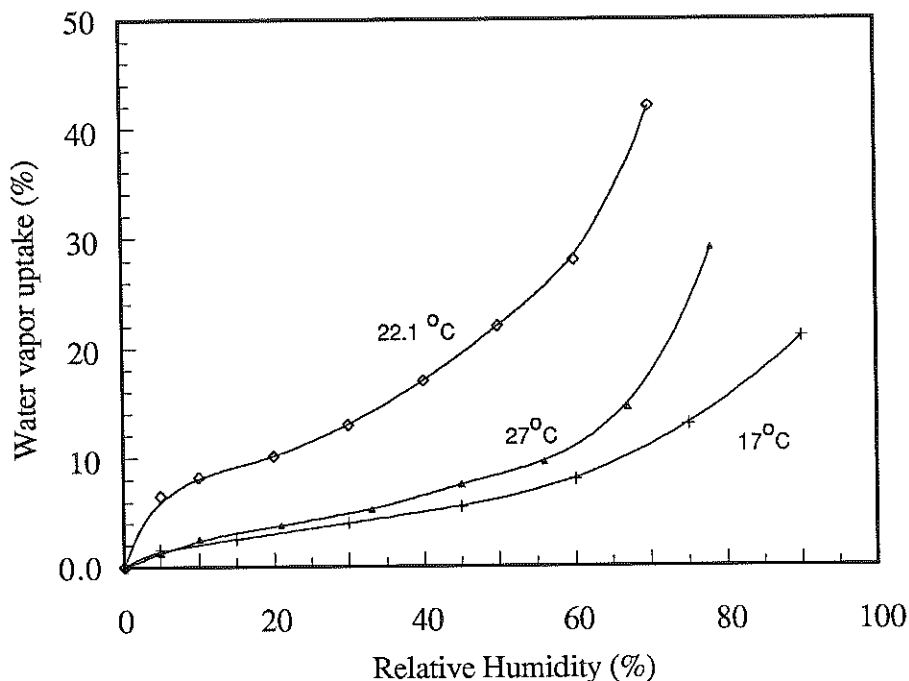


*Figure 2.4 Isotherm Measurement for SPSS Taken by SERI*

Figure 2.4 shows the measured isotherms for SPSS replotted in terms of relative humidity. The isotherm measurements for PSSASS and for PSSALS show the same pattern for the water uptake. The original isotherm charts are unconventional, since SERI presented the water uptake with respect to the partial water vapor pressure.

### Silica Gel versus Scientific Polymer

Silica gel has almost no temperature dependence of the isotherm shape compared to SPSS. The fact that between 17°C and 22.1°C the water uptake of SPSS increases is new and cannot be seen by conventional desiccants like Silica Gel. The temperature dependence is extreme. A five degree Celsius increase results in totally new isotherm shapes. PSSALS, PSSASS, and SPSS even show a maximum percentage of desiccant

water content at one discrete temperature and constant relative humidity. The fact that these polymers adsorb less water with decreasing temperature raises the question of whether this behavior fits in our normal picture of physical adsorption and obeys the laws of thermodynamics.

The following investigation deals with the relationship between temperature and desiccant water content in a closed system. A thermodynamic cycle is introduced which identifies the range of possible isotherm shapes from the viewpoint of the Second Law of Thermodynamics.

## 2.6 General Behavior of Desiccant and Humid Air in a Closed Adiabatic System

### The Closed System

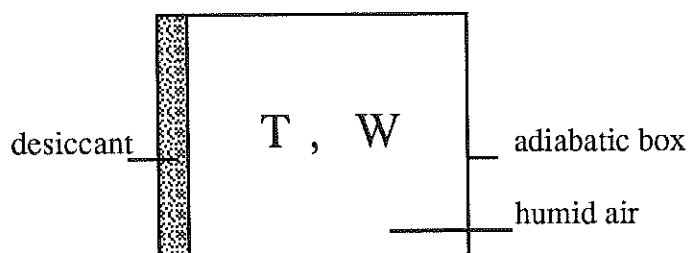


*Figure 2.5 Closed Adiabatic System*

A closed system consisting of humid air and a desiccant bed is considered as shown in Figure 2.5. There is an adiabatic boundary separating the air and desiccant from the surroundings. The system is not in equilibrium initially. It is assumed that the desiccant water content is slightly lower or higher than the equilibrium state. The heat of adsorption should be in a range which is usual for physical adsorption. This means that the heat of adsorption is positive and the value is only slightly different from the heat of vaporization. In other words the process of adsorption has the same behavior as conden-

sation and releases heat in the same way as condensation. (see Appendix A The Nature of Adsorption)

In Chemistry the heat of adsorption for physical sorption is defined as negative. Chemists treat the adsorption process like a reaction with the reactants **water vapor** and **dry desiccant** and the product **wet desiccant**.

$$dH_{\text{reaction}} = H_{\text{products}} - H_{\text{reactants}}$$

Adsorption:  $H_{\text{reactants}} = H_V + H_{\text{dry matrix}}$

$$H_{\text{products}} = H_{\text{wet matrix}}$$

$$dH_{\text{reaction}} = \text{heat of adsorption}$$

In this study internal energy of adsorption is the liberated internal energy during the adsorption process and is defined as **positive**.

## 2.7 Application of the First Law of Thermodynamics on This System

The system is adiabatic and closed. The first law of thermodynamics states:

$$dU = 0$$

The energy terms can be separated into the desiccant and the humid air energy change.

$$dU = dU_A + dU_D \quad (2.1)$$

$$dU_D = [ c_D m_D dT + c_w m_D W_D dT + u_L m_D dW_D + ((u_V - u_L) - u_s) m_D dW_D ] \quad (2.1a)$$

$$dU_A = [ c_A m_A dT + c_v m_A w dT + u_V m_A dw ] \quad (2.1b)$$

$U_D$  : energy of desiccant

$U_A$  : energy of air

$U_V$  : energy of water vapor at system temp.

$U_L$  : energy of liquid water at system temp.

$U_s$  : energy released during the adsorption process,

differential energy of adsorption

The principle for the energy calculations of desiccant, pure water on desiccant and the energy of humid air is as follows. For example, for the  $U_D$  calculation,  $dU_D$  can be separated in the energy change of the water on the desiccant and the energy change of the desiccant matrix.

$$dU_D = dU_{water} + dU_{matrix}$$

$$U_{water} = f(T, W_D) \quad dU_w = \left( \frac{\partial U_w}{\partial T} \right)_w dT + \left( \frac{\partial U_w}{\partial W_D} \right)_T dW_D$$

$$U_{matrix} = f(T, W_D) \quad dU_m = \left( \frac{\partial U_m}{\partial T} \right)_w dT + \left( \frac{\partial U_m}{\partial W_D} \right)_T dW_D$$

comparison with (2.1) yields

$$c_D m_D = \left( \frac{\partial U_m}{\partial T} \right)_w ; ((u_V - u_L) - u_S) m_D = \left( \frac{\partial U_m}{\partial W_D} \right)_T ; c_W m_D W_D = \left( \frac{\partial U_w}{\partial T} \right)_w ; u_L m_D = \left( \frac{\partial U_w}{\partial W_D} \right)_T$$

Explanation of the partial derivatives above.

$c_D m_D = \left( \frac{\partial U_m}{\partial T} \right)_w$  : This term expresses the energy change of the matrix with temperature due to the specific internal energy capacity of the desiccant.

$((u_V - u_L) - u_S) m_D = \left( \frac{\partial U_m}{\partial W_D} \right)_T$  : This term expresses the energy change of the matrix with water content due to energy bonded in the matrix by adsorption. For example, the adsorption process liberates less energy than a condensation process. This energy difference is conserved in a water-matrix bond and increases the energy of the matrix.

$c_W m_D W_D = \left( \frac{\partial U_w}{\partial T} \right)_w$  : This term expresses the energy change of the bonded water on the desiccant with temperature due to its internal energy capacity.

$u_L m_D = \left( \frac{\partial U_w}{\partial W_D} \right)_T$  : This term expresses the energy change of the bonded water on the desiccant with water content due to its internal energy.

In the closed box the total water mass is conserved.

$$0 = dwm_A + dW_D m_D \quad (2.2)$$

substitute (2.2) into (2.1a) and /  $m_D$

$$0 = c_D dT + c_w W_D dT + u_L dW_D + [(u_V - u_L) - u_S] dW_D + c_A m_A / m_D dT - u_V dW_D + c_v m_A / m_D w dT \quad (2.3)$$

It is now possible to summarize all expressions with  $dT$  in one term with an overall mass-average heat capacity  $\bar{c}$

$$\bar{c} = \frac{\sum_i m_i c_i}{\sum_i m_i}$$

or

$$\bar{c} = \frac{c_D + c_w W_D + c_A \frac{m_A}{m_D} + c_v \frac{m_A w}{m_D}}{1 + W_D + \frac{m_A}{m_D} + \frac{m_A w}{m_D}} \quad (2.4)$$

substituting (2.4) into (2.3)

$$0 = \bar{c} dT + u_L dW_D + [(u_V - u_L) - u_S] dW_D - u_V dW_D$$

$$0 = \bar{c} dT - u_S dW_D \quad (2.5)$$

Expression (2.5) shows that a decrease of the water content of the desiccant is always connected with a decrease of the system temperature as long as  $u_S$ , the differential energy of sorption, is positive. Physical adsorption processes have a positive  $u_S$  (compare Appendix A The Nature of Physical Adsorption).

## 2.8 The General Behavior of a Desiccant and Temperature Dependent Adsorption Isotherm Shapes.

There are two possibilities for the temperature dependent properties of an isotherm.

Case a) The isotherm water content decreases with temperature and has an overall water content gradient  $\frac{dW_D}{dT} < 0$ .

This means that the water content of the adsorbent increases with decreasing temperature at equilibrium.

This system is stable! For small deviations from the equilibrium the following will occur:

The temperature of the system in the box is smaller than the temperature at equilibrium  $\Rightarrow$  the water capacity of the adsorbent increases  $\Rightarrow$  water will condense on the surface of the desiccant ( $dW_D > 0$ )  $\Rightarrow$  system temperature will rise ( $dT > 0$  equation (2.5) ; general behavior).

The little push stops.

Case b) The isotherm water content increases with temperature and has an overall water content of  $\frac{dW_D}{dT} > 0$

This means that the water content decreases with decreased temperature at equilibrium.

This system is unstable! For small deviations from equilibrium the following occurs:

The temperature is smaller than the temperature at equilibrium  $\Rightarrow$  the water capacity of desiccant decreases  $\Rightarrow$  water evaporates from the adsorbent.

Because ( $dW_D < 0$ ) the system temperature continues to fall (general behavior; equation (2.5)). The temperature of the closed system will fall until the overall isotherm gradient  $\frac{dW_D}{dT}$  is smaller than zero. The calculation of this gradient is shown in Appendix C.

Thus for case b) the system temperature will spontaneously fall!

## 2.9 The Proposed Thermodynamic Cycle and Second Law of Thermodynamics.

If a desiccant exists for which  $\frac{dW_D}{dT} > 0$ , a thermodynamic cycle can be constructed that will continuously produce work using only heat from the atmosphere.

### The Proposed Cycle :

1. The system described above is initially in equilibrium with the ambient.

$$w_1 = w_{ambient}; T_1 = T_{ambient}$$

2. The system is then separated from the ambient by an adiabatic box. It cools down spontaneously as described in the previous section. (Case b)

$$w_2 > w_a, T_2 < T_a$$

3. The air and the desiccant in the box is then separated by an impervious box. The adiabatic wall is removed and the box is heated up to ambient temperature by energy rejected by a heat engine. The heat supply for the engine is from the ambient, and the engine thus produces useful work.

$$T_3 = T_a, w_3 > w_a$$

4. The box and the wall is removed and the system is in equilibrium with the ambient again. Mass exchange occurs between desiccant and ambient. The air has ambient properties since there is no box.

final state = state 1,  $w_4 = w_a$ ,  $T_4 = T_a$

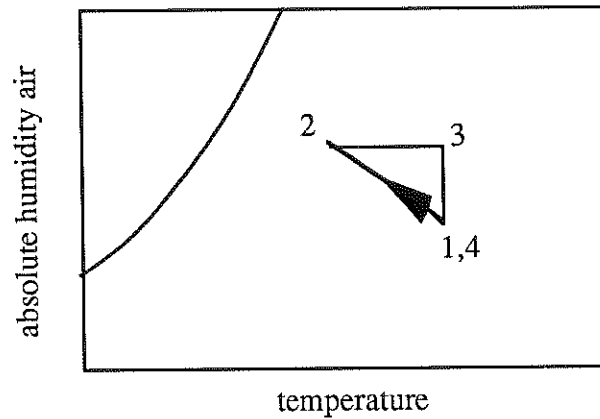


Figure 2.6 The Theoretical Cycle

Figure 2.6 shows the cycle of the heat engine on a psychrometric chart.

### Second Law Calculation for Process 2 to 3.

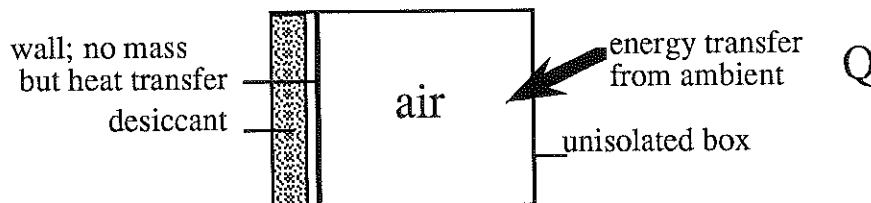


Figure 2.7 The Process Conditions for Process 2 to 3.

### First Law of Thermodynamics:

$$u_3 - u_2 = q$$

$$\bar{c}(T_3 - T_2) = q ; T_a = T_3 \quad (2.6)$$

### Second Law of Thermodynamics:

$$s_3 - s_2 = \frac{q}{T_3} + is \quad (2.7)$$

$$s_3 - s_2 = \int_{T_2}^{T_3} \bar{c} \frac{dT}{T} + \int_{V_2}^{V_3} R \frac{dV}{V}; \quad V_2 = V_3 \quad (2.8)$$

substitute (2.8) and (2.7) in (2.6)

$$\bar{c} \ln \frac{T_3}{T_2} = \frac{\bar{c} (T_3 - T_2)}{T_3} + is$$

$$\bar{c} \ln \frac{T_3}{T_2} - \frac{\bar{c} (T_3 - T_2)}{T_3} = is$$

$$-L_{ex} = T_3 is \quad (2.9)$$

The term 'is' is the entropy production, when the box is heated by the ambient irreversibly.  $-L_{ex}$  is the work which could be gained in a reversible process.

The second law of thermodynamics states that it is impossible to run a heat machine using only one energy source. Therefore the proposed cycle with the assumptions of section 3, case b) produces heat using only ambient as a source and thus violates the second law.

## 2.10 Conclusions from the Second Law Analysis

With the knowledge that every thermodynamic cycle must follow the rules of the Second Law only one conclusion remains that one of the assumptions is wrong.

Case a)

Energy of adsorption is negative; not positive as assumed. This means that there is energy required to cause water to condense on the desiccant.  $\Rightarrow$  no physical adsorption  $\Rightarrow$  chemical absorption. The absorption of water on the desiccant is involved with an endothermic reaction. (compare Appendix A)

Case b)

The measured gradient  $\frac{dW_D}{dT}$  is negative; not positive as assumed. This means, that the measurements of the water uptake for the polymer isotherms are incorrect.

### Assessment of the Cases

A negative heat of adsorption is most unlikely since the magnitude of the endothermic reaction between water and desiccant must be on the order of the heat of vaporization for these data. The fact that the isotherms show a maximum for the water uptake somewhere between 17°C and 27°C is also not reasonable. The Second Law analysis above will not lead to a violation if the internal heat of adsorption is below the maximum negative and above the maximum positive value. This makes no sense! The reaction changes its nature from endothermic to exothermic with only a 10°C temperature increase! The remaining conclusion is that the measurements are incorrect.

---

## Chapter three

---

### **Isotherm Formulations**

The results presented in Chapter 2 show that the SERI measurements cannot be used directly for numerical simulations in rotary dehumidifiers. Therefore, the goal of this study switched towards the evaluation of isotherms with shapes similar to the trends of the SERI measurements. This involved the formulation of a new isotherm model which allows the simulation of different shapes, different temperature dependencies, and obeys the Second Law of Thermodynamics.

In the literature there are two different isotherm formulations which are widely applied for desiccants. One isotherm formulation is based on the theory of the adsorption potential. The other formulation simply applies the Clausius-Clapeyron relationship for perfect gas on the adsorption - desorption process. The following sections give a brief introduction in both theories.

#### **3.1 Dubinin - Polanyi Equilibrium for Microporus Adsorbents.**

The adsorption potential theory was originally proposed by Polanyi (1932). Based on the gas-kinetic theory of Boltzmann, Polanyi derived a theoretical relationship between the average potential energy of the adsorbed molecules and the adsorbed amount.

$$A = R T \ln(r), \text{ for } W_D = \text{constant} \quad (3.1)$$

Where  $A$  is the adsorption potential,  $r$  the relative humidity,  $R$  the perfect gas constant, and  $T$  the absolute temperature. The Polanyi theory predicts that  $W_D$  is a function of  $A$ .

From thermodynamic relationships it can be derived that the adsorption potential is equal to the difference between the differential heat of adsorption and the heat of vaporization.

$$A = h_S - h_{VL}$$

Dubinin showed that the amount adsorbed can often be approximated by a Weibull expression.

$$W_D = W_o \exp(- (A/E_o)^n)$$

Where  $W_D$  is the total micropore volume, and  $E_o$  is the characteristic energy of adsorption. For most microporous systems the parameter  $n=2$  is recommended. This expression applies only for "one sided" microporous systems. This means only one pore size. A heterogeneous system with pore size distribution can be approximated by the superposition of microporous substructures. In most cases a "two sided" Weibull expression is used to represent smaller micropores (twigs) and larger supermicropores (branches) in a pore system.

$$W_D = W_{o1} \exp(-(A/E_{o1})^n) + W_{o2} \exp(-(A/E_{o2})^n) \quad (3.2)$$

Equation (3.2) states that the amount adsorbed is related only to the adsorption potential and the functional relationship is independent of temperature as an independent variable. The main advantage of expressing the sorption isotherm in terms of  $A$  is that adsorption data may be collected at one temperature and a limited set of vapor pressures. Expression (3.2) gives then a function for interpolation for intermediate vapor pressures and the adsorption potential theory extrapolates for different temperatures. However, the Polanyi theory is restricted to systems where the temperature dependence of the isotherm shape is only due to the adsorption potential change with temperature. The Polanyi theory has been applied successfully for adsorption equilibrium data for activated carbon and

zeolites or molecular sieves. The highly temperature dependent isotherms which are required for the evaluation of the dehumidifier performance can not be simulated with this theory. Therefore, this formulation is used to double check the results which were achieved with the Jurinak - Polynomial isotherm expression.

### 3.2 The Jurinak - Polynomial Formulation

The Jurinak isotherm formulation is a curve fit for desiccant isotherms. It relates the amount of adsorbed water to the equilibrium concentration of water vapor.

Adsorption isotherms usually express the amount adsorbed to sorbent mass ratio depending on the concentration of the adsorbate at one temperature. In the desiccant humid air system a common expression which represents the concentration of water vapor is relative humidity. The formulation of isotherms with respect to relative humidity has the advantage of a normalization, since it relates the concentration of water vapor (partial pressure) to the highest possible concentration at system temperature. (water vapor saturation pressure). In other words the potential for condensation on a desiccant surface depends on the fraction of the partial vapor pressure and the saturation vapor pressure. At pressures equal to one, adsorption becomes a simple condensation process, whereas at lower water vapor concentrations the ability to adsorb water depends on the attractive molecular forces between vapor molecules and the desiccant surface. (see Appendix A The Nature of Physical Adsorption)

The adsorption process is always connected with a heat effect. This effect is due to the nature of adsorption which can be understood as a condensation process at partial vapor pressures below saturation pressure.

The Clausius - Clapeyron equation (1850) relates the saturation temperature  $T$ , the heat of vaporization  $h_V - h_L$  to the volume change  $v_V - v_L$ , and the derivative of the saturation vapor pressure curve for a pure substance.

$$\frac{h_V - h_L}{v_V - v_L} = T \frac{dp_S}{dT} \quad (3.3)$$

At small pressures, where water vapor is almost a perfect gas and  $v_L$  can be neglected compared to  $v_V$ , the perfect gas equation  $v_V = RT/p_S$  can be substituted into (3.3).

$$\frac{dp_S}{p_S} = \frac{h_{VL}}{R} \frac{dT}{T^2} \quad (3.4)$$

where  $h_{VL}$  is the heat of vaporization and  $p_S$  is the saturation water vapor pressure.

At a constant amount adsorbed the desiccant water vapor system must follow the same Clausius Clapeyron equation.

$$\frac{dp_V}{p_V} = \frac{h_S}{R} \frac{dT}{T^2} \quad (3.5)$$

The restriction that  $W_D$  is a constant excludes effects caused by different matrix properties due to the amount adsorbed (multilayer, dependence of heat of adsorption).

Dividing (3.5) by (3.4) yields

$$\frac{dp_V}{p_V} \frac{p_S}{dp_S} = \frac{h_S}{h_{VL}} \quad (3.6)$$

It is now assumed that the ratio  $\frac{h_S}{h_{VL}}$  is independent of temperature. With this assumption equation (3.6) may be integrated between a reference temperature  $T_o$  and a temperature  $T$ .

$$\int_{T_o}^T d \ln p_V = \int_{T_o}^T \frac{h_S}{h_{VL}} d \ln p_S$$

or

$$\frac{p_V(T)}{p_V(T_o)} = \left( \frac{p_S(T)}{p_S(T_o)} \right)^{\frac{h_S}{h_{VL}}}$$

Division of both sides with  $\frac{p_S(T)}{p_S(T_o)}$  yields

$$\frac{r(T)}{r(T_o)} = \left( \frac{p_S(T)}{p_S(T_o)} \right)^{\frac{h_S}{h_{VL}} - 1} \quad (3.7)$$

Equation (3.7) gives the relationship between an isotherm shape at temperature  $T_o$  and a unknown temperature  $T$  with respect to the ratio between heat of adsorption and heat of vaporization. Jurinak calls  $r(T_o)$  the equilibrium isotherm function  $G(W_D)$  at reference temperature  $T_o$ . The ratio  $\frac{h_S}{h_{VL}}$  is approximately independent of temperature and a function of the matrix water content only.

This assumption makes sense and is consistent with other isotherm formulations such as the Brunauer, Emmett, and Teller (1938) isotherm formulation (BET) which is based on the assumption that molecules could be adsorbed more than one layer thick on the surface of the adsorbent. Moreover, the BET equation assumes that the energy of adsorption holds for the first monolayer but that the condensation energy of the adsorbate is responsible for adsorption of successive layers.

Brandemuehl postulated a relationship between the ratio heat of adsorption to heat of vaporization and the amount adsorbed which is valid for silica gel and physical adsorption.

$$\frac{h_S}{h_{VL}} (W_D) = 1 + dh^* \exp(kW_D) \quad (3.8)$$

where  $1 + dh^*$  is  $\frac{h_S}{h_{VL}}$  at  $W_D = 0$  and  $k$  is a constant. Both constants  $dh^*$  and  $k$  are scaling parameters. For positive  $dh^*$  and negative  $k$  the ratio  $\frac{h_S}{h_{VL}}$  declines rapidly with the amount adsorbed. The heat of adsorption for the first molecules adsorbed on the desiccant surface is  $(1 + dh^*)h_{VL}$ . With increasing matrix water content the heat of adsorption decays rapidly, but never reaches  $h_{VL}$ .

Jurinak modified Brandemuehl's approach slightly. He introduced a normalized water content  $W_D^*$ . This normalized water content is now in the range zero to one and is defined as the ratio  $W_D$  to  $W_{Dmax}$ , where  $W_{Dmax}$  is the amount adsorbed at 100% relative humidity. He termed the ratio  $\frac{h_S}{h_{VL}}$  as  $h^*$  and expressed  $h^*$  in terms of  $W_D^*$ .

$$h^* = 1 + dh^* \frac{\exp(kW_D^*) - \exp(k)}{1 - \exp(k)} \quad (3.9)$$

The advantage of (3.9) over (3.8) is that at  $r = 1$ ,  $W_D^* = 1$  regardless of temperature. The physical assumption implicit in the variation of  $h^*$  given by equation (3.9) is that at saturated air states, adsorption becomes a normal condensation process on the matrix with  $h_{VL} = h_S$ .

The Jurinak Isotherm Equation

$$r(T, W_D^*) = G(W_D^*) \left( \frac{p_S(T)}{p_S(T_o)} \right)^{h^* - 1} \quad (3.10)$$

$$\text{where } h^* = 1 + dh^* \frac{\exp(kW_D^*) - \exp(k)}{1 - \exp(k)}$$

$$W_D^* = \text{ratio } W_D \text{ to } W_{Dmax}$$

$$dh^*, k, W_{Dmax} \text{ are scaling parameters}$$

$$G(W_D^*) \text{ is curve fit for isotherm shape at reference temperature } T_o.$$

The Jurinak isotherm expression allows the simulation of a highly temperature dependent desiccant behavior. The scaling parameter  $dh^*$  and  $k$  affect the isotherm shapes at temperatures different from the reference temperature  $T_o$ .

### 3.3 The Function $G(W_D^*)$

The function  $G(W_D^*)$  is a curve fit for the equilibrium adsorption isotherm at the reference temperature  $T_o$ . This formulation describes the correlation desiccant water up-

take and relative humidity (water vapor concentration) in an unconventional way. Here, the dependent variable is the relative humidity and the independent variable is the dimensionless water content. Usually isotherm correlations are formulated in terms of adsorbent load depending on concentration ( $W_D = f(r)$ ).

$$r = G(W_D^*) \text{ at } T = T_o$$

In order to give function  $G(W_D^*)$  a maximum flexibility for the requirements of all possible isotherm shapes a fifth order polynomial expression was chosen for the curve fits. The constant parameter of a polynomial expression is not included since all isotherms must meet the requirement of zero water uptake at zero relative humidity.

$$G(W_D^*) = a_1 W_D^* + a_2 W_D^{*2} + a_3 W_D^{*3} + a_4 W_D^{*4} + a_5 W_D^{*5} \quad (3.11)$$

where

$$a_1, a_2, a_3, a_4, a_5, \text{ scaling parameter}$$

### 3.4 Isotherm Curve Fits for Silica Gel and SERI Isotherm Measurements

In the previous chapter it was shown that the isotherms measured by SERI can not be applied for dehumidifier simulations since the measurements turned out to be inconsistent with the Second Law of Thermodynamics. Another problem is the low temperature range at which the measurements were taken. These do not provide any information at regeneration temperatures.

However, despite these problems, a closer look at the measured isotherm shapes might help to assess the possibilities for the improvement of a dehumidification process and finally the desiccant cooling cycles. Therefore, one of the most promising polymers SERI R19-52-3, a PSSASS sample prepared by SERI, is chosen for the curve fits at reference temperature. The sample SERI R19-52-3 is a Brunauer Type 2 in shape and has

the best isotherm of the various PSSASS samples SERI has measured to date. (SERI Progress Report, p. 4-5)

SERI made measurements for this sample in the range 5% to 60% relative humidity. The measured results are shown in Figure 3.1. (The desiccant humidity is defined as  $W_D$ , the ratio mass of water adsorbed to mass of dry desiccant)

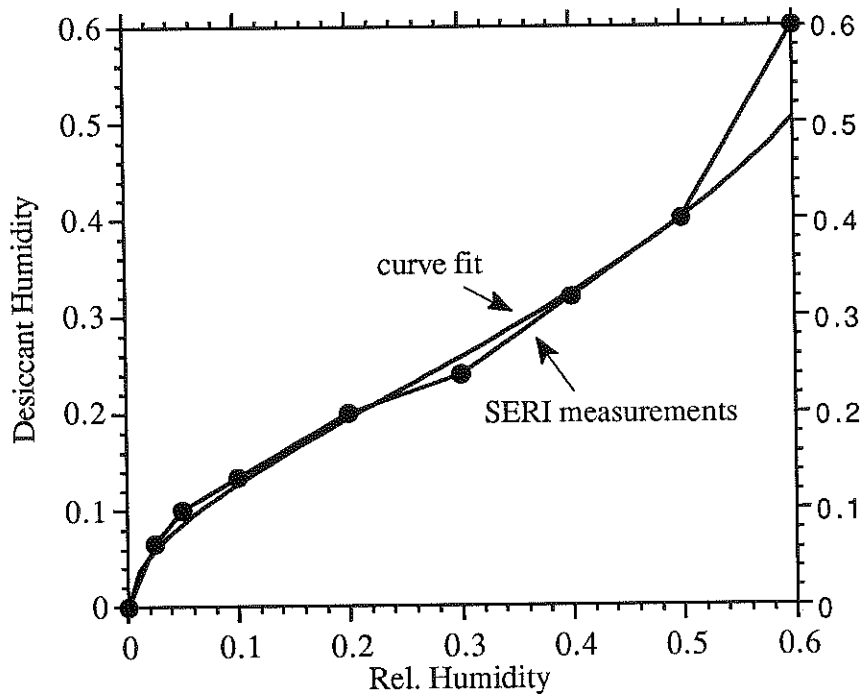


*Figure 3.1 SERI R19-52-3 and Fifth Order Polynomial Curve Fit*

The approximation procedure uses measured data up to 50% relative humidity. The last SERI measurement at a humidity of 60% is not included in the approximation since a approximation of the data in the measured range between 5% and 60% leads to a polynomial function which makes no sense at a humidity above 70% ( $W_D$  increases to about 20 at 100% humidity.).

The approximation had to meet the requirements of 100% desiccant humidity at 100% relative humidity in order to avoid simulation program crashes due to undefined matrix property evaluations. Figure 3.2 shows the approximation of the SERI measurements without the measurement at 60% relative humidity and the assumed isotherm shape above the measured values.

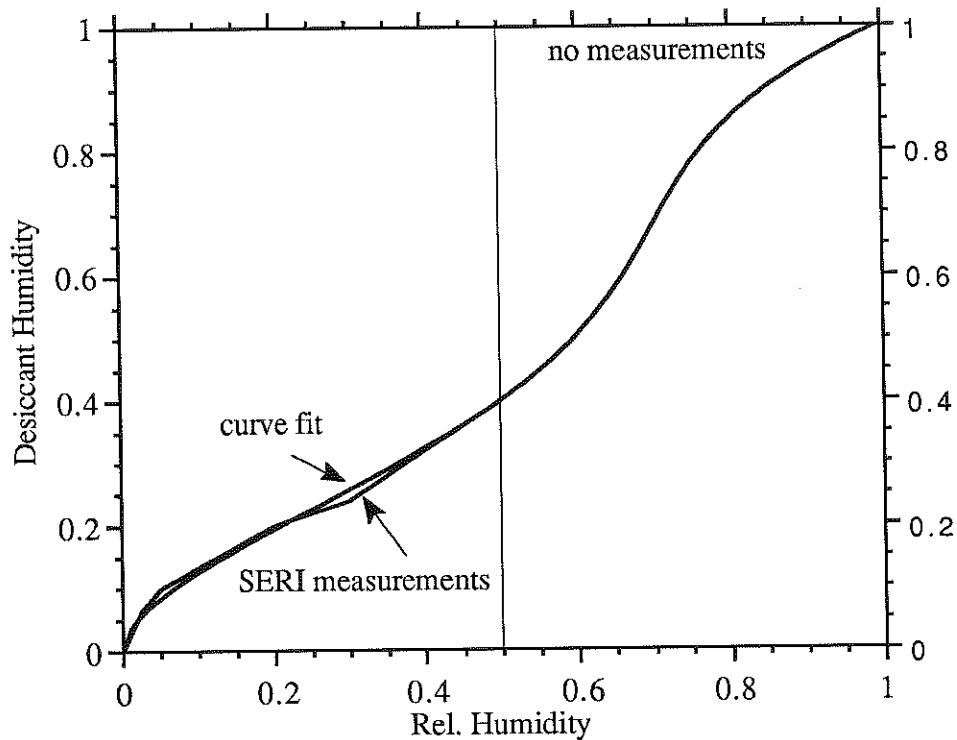


Figure 3.2 The Approximation of the SERI Measurements.

The curve above 50% relative humidity has no impact on the final results of dehumidifier simulations and performance since no inlet or outlet state reach values for the relative humidity above 50%. Table 3.1 gives the parameter of the function  $G(W_D^*)$  for SERI R19-52-3

$a_1$	$a_2$	$a_3$	$a_4$	$a_5$	$W_{Dmax}$
0.0	9.340175	-21.82200	18.75017	-5.148716	1.06

Table 3.1 SERI Approximation Parameters

Silica gel was used as the basis of comparison for the SERI polymers. The Dubinin-Astakov two sided isotherm curve fit for silica gel was applied for the Jurinak polynomial isotherm model. In this study the Dubinin-Astakov isotherm formulation is used as a reference formulation. Since the Dubinin-Astakov theory correlates relative humidity and desiccant humidity ( $W_D=f(r)$  compared to  $r=f(W_D)$ ) the necessary calculations for the matrix properties are totally different. This fact makes a double check of the results very effective and gives some confidence in the validity of the results.

Eric van den Bulck (1987) made isotherm measurements for silica gel. The validity of these measurements is proven by other data found in literature. Figure 3.3 shows his Dubinin-Astakov curve fit for silica gel at 50°C and the approximation of this curve fit with the Jurinak polynomial formulation. In Table 3.2 the parameters of the Dubinin-Astakov curve fit (equation 3.2) are presented. Table 3.3 summarizes the parameters for the silica gel approximation with Jurinak's model for isotherms at reference temperature 50°C.

$W_{o1}$	$E_{o1}$	$W_{o2}$	$E_{o2}$
0.117	7740	0.237	2500

*Table 3.2 Van den Bulck Parameters for Silica Gel*

$a_1$	$a_2$	$a_3$	$a_4$	$a_5$	$W_{Dmax}$
0.494717	0.727943	1.662559	-6.052235	4.109001	0.354

*Table 3.3 Jurinak Polynomial Approximation Parameters*

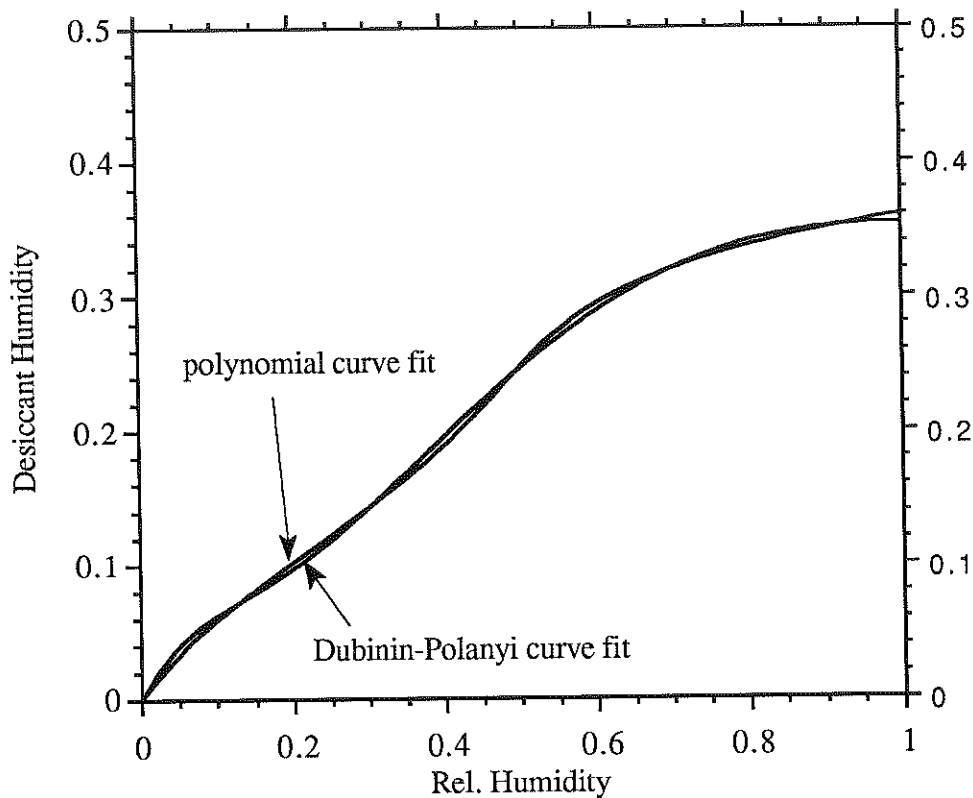
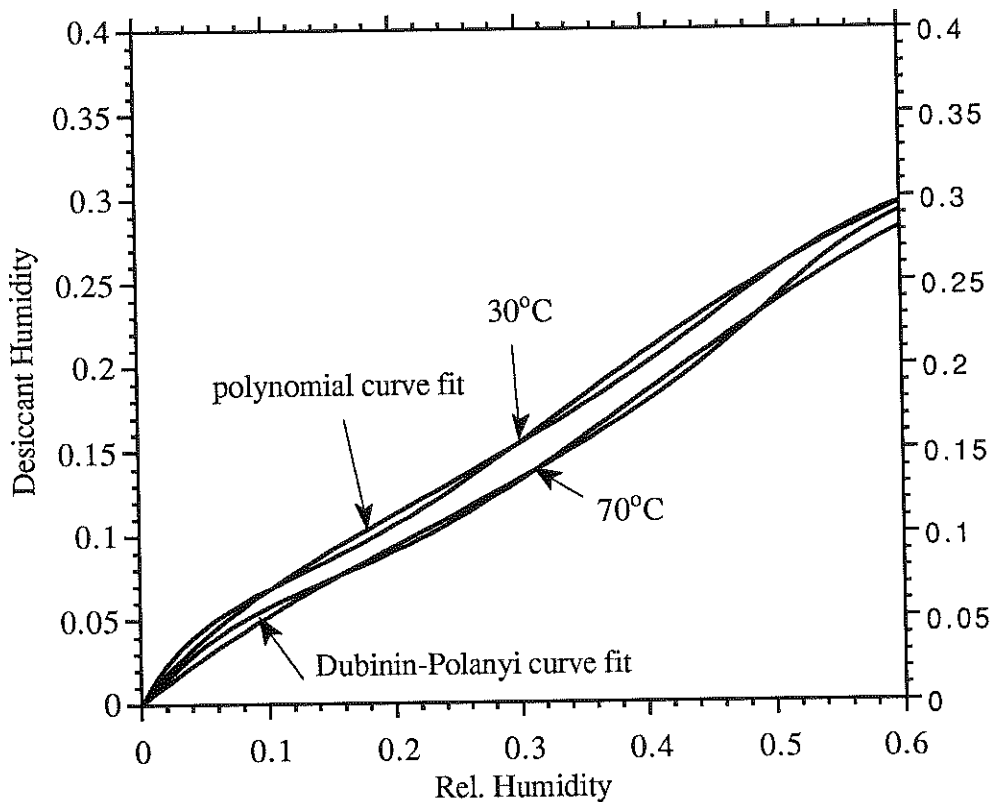


Figure 3.3 Polynomial Curve Fit and Van den Bulck Curve Fit at 50°C

### 3.5 Temperature Dependent Isotherms Based on Jurinak's Model

Typical adiabatic rotary dehumidifiers work at adsorption inlet temperatures of about 30°C and regeneration temperatures of about 70°C. In order to achieve the maximum benefit from temperature dependent desiccants, the reference temperature for the function  $G(W_D)$  is chosen to be 50°C. The scaling parameters for the temperature dependence  $k$  and  $dh^*$  are varied from -2.2 to -4.0 and 0.25 to 1.4, respectively. The scaling parameter  $dh^*$  affects directly the heat of adsorption (compare equation 3.9). Increasing values for  $dh^*$  means higher heat of adsorption compared to the heat of vaporization. Theory predicts that adsorbents with an ionic structure have high heats of adsorption (compare Appendix A). Thus, the variation of  $dh^*$  to values up to 1.4 is reasonable with

respect to theory. The temperature dependent behavior of the Dubinin-Astakov formulation is approximated by the parameter pair  $k = -2.2$  and  $dh^* = 0.25$ . Figure 3.4 shows the results of the approximation at 30°C and 70°C only up to 60% relative humidity, since isotherms above this limit are of minor interest for dehumidification applications.



*Figure 3.4 Polynomial Curve Fit and Van den Bulck Curve Fit at 30°C and 70°C.*

The following Figures show the resulting theoretical isotherm shapes that are simulated. Figure 3.5 to Figure 3.8 present the results for the SERI curve fits at 50°C reference temperature and  $k = 2.2$ . Figure 3.9 to Figure 3.12 show the silica gel approximation with artificial temperature dependence. Finally Figure 3.13 shows the effect of  $k = -4.0$  compared to  $k = -2.2$  at  $dh^* = 1.0$  for the SERI curve fits with extreme temperature dependence.

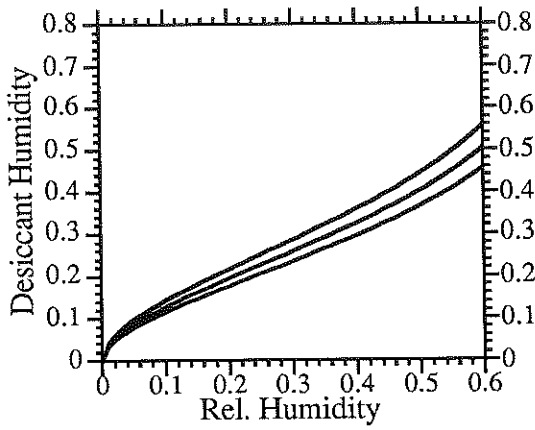


Figure 3.5 SERI R19-52-3  $dh^* = 0.25$

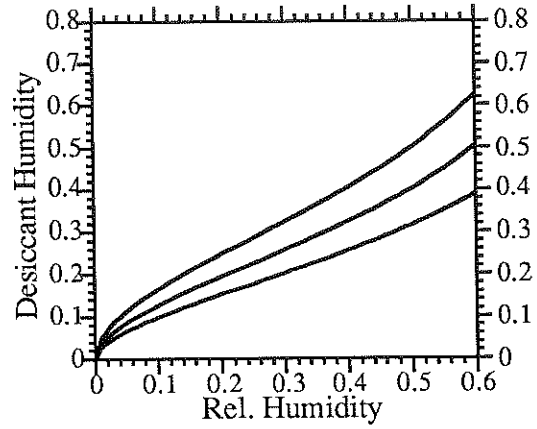


Figure 3.6 SERI R19-52-3  $dh^* = 0.6$

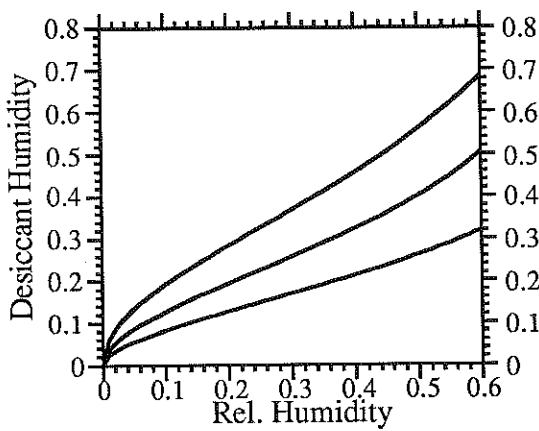


Figure 3.7 SERI R19-52-3  $dh^* = 1.0$

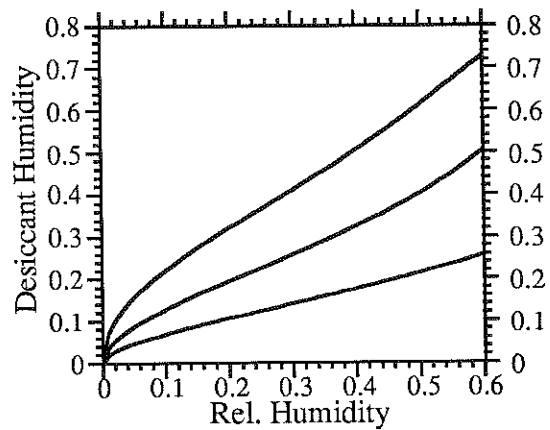


Figure 3.8 SERI R19-52-3  $dh^* = 1.4$

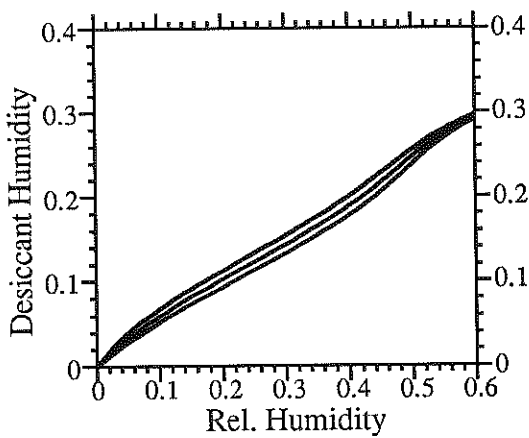


Figure 3.9 Artificial Silica Gel  $dh^* = 0.25$

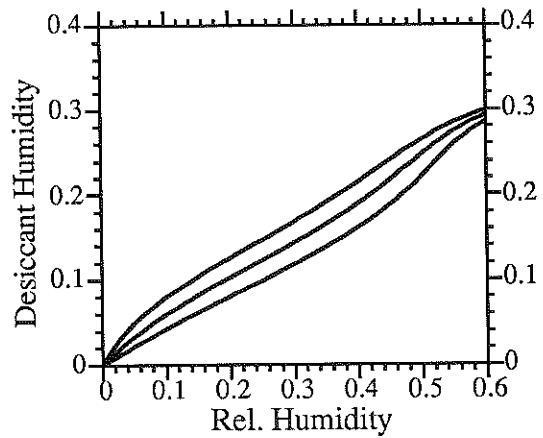


Figure 3.10 Artificial Silica Gel  $dh^* = 0.6$

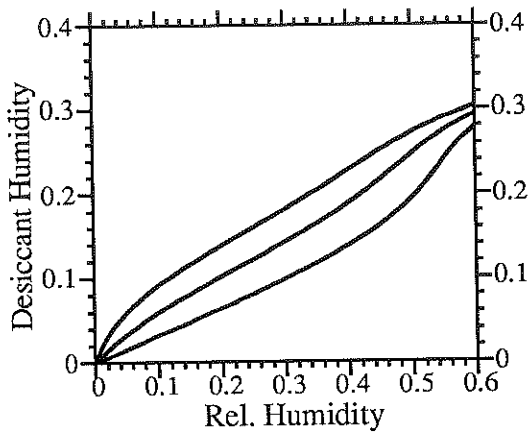


Figure 3.11 Artificial Silica Gel  $dh^* = 1.0$

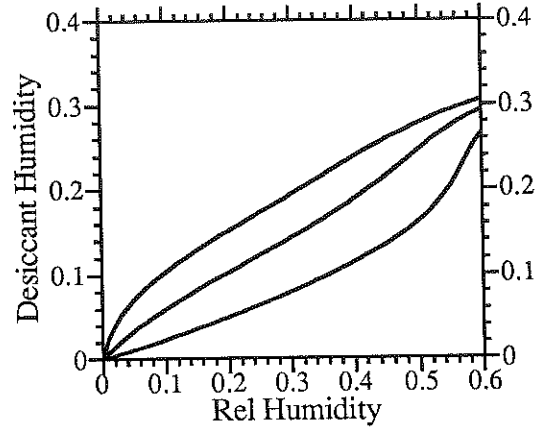


Figure 3.12 Artificial Silica Gel  $dh^* = 1.4$

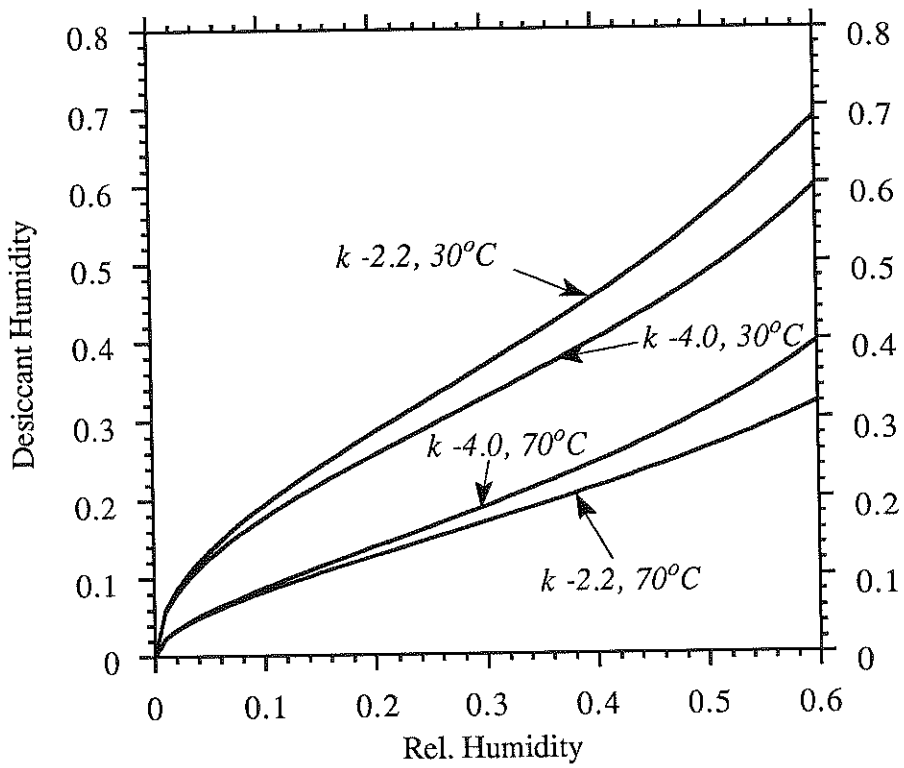


Figure 3.13 SERI R19-52-3 Variation of  $k$  at  $dh^* = 1.0$

### 3.6 Conclusions

The Dubinin-Polanyi isotherm formulation can be applied only for adsorbents where the temperature dependence of the shape follows the theory of the adsorption potential. This theory does not apply for highly temperature dependent isotherm shapes.

The polynomial Jurinak formulation allows the simulation of almost every isotherm shape. The temperature dependence is a result of the thermodynamic relationship stated by the Clausius-Clapeyron equation between heat of adsorption and isotherm shape. The formulation obeys the Second Law of Thermodynamics since it is derived from a Second Law relationship.

The approximation with this formulation for the basic shape of the SERI measurements for PSSASS is close to the measured values in the range which is important for desiccant cooling application. The approximation provides a good base for the comparison between silica gel and PSSASS isotherm. Furthermore with the polynomial Jurinak formulation isotherms can be modeled which fulfill all the requirements of a 'optimum' isotherm with a Type 1 shape for the adsorption step and a Type 2 shape at regeneration temperature.

---

## Chapter four

---

### **The Models of the System Components**

This chapter presents the theory of a rotary dehumidifier and sensible heat exchanger as well as the model of an adiabatic humidifier. The main focus in this chapter is on the model of an adiabatic regenerative dehumidifier which represents the central component in a desiccant cooling system.

#### **4.1 The Dehumidifier Model**

The dehumidifier theory reviewed in this chapter draws on the extensive work published by researchers in Australia (McLain- Cross and Banks, 1972) and researchers from the Solar Energy Laboratory of the University of Wisconsin - Madison (Jurinak, 1982; Harald Klein and John Mitchell, 1987; Van Den Bulk, 1987)

##### **4.1.1 The Dehumidifier Matrix Geometry**

Rotary adiabatic dehumidifiers basically consist of a desiccant matrix. The rotary wheel is built by two components, the desiccant and support material. The matrix is exposed to two separate air streams in counterflow arrangement. Figure 4.1 illustrates the coordinate system and nomenclature of the dehumidifier wheel.

where

$L$  = length in flow direction

$M_D$  = mass of dry desiccant

$m_{air}$  = mass flow of dry air

subscripts:

$c$ : period 1 or colder stream (here process steam)

$h$ : period 2 or hotter stream (here regeneration stream)

$j$ : either period 1 or period 2

$o$ : outlet

$i$ : inlet

$D$ : desiccant (here desiccant material alone)

$m$ : matrix (desiccant together with support)

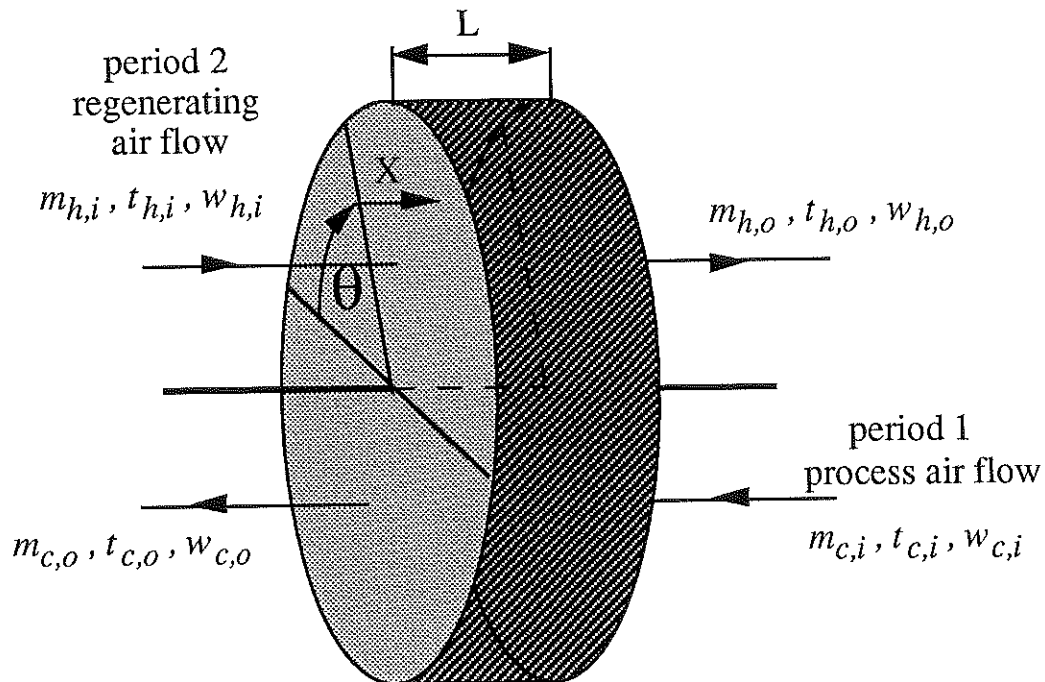


Figure 4.1 Nomenclature and Coordinate System for a Regenerative Dehumidifier

For each period the axial coordinate  $x$  is defined as positive in flow direction, while the rotary position of a matrix element is measured by the time coordinate  $\theta$ . The duration of one whole rotation is  $T$ . The duration of period  $j$  is  $T_j$ .

$\theta_c$ : dwell time of process stream (time coordinate).

$\theta_h$ : dwell time of regeneration stream

#### 4.1.2 Assumptions for the Models

The following assumptions are made for the process.

1. State properties are uniform in time and the inlet streams are ideal mixed.
2. The pressure drop in the dehumidifier is small, so that thermodynamic properties are not affected.
3. The mass of air entrained in the matrix is small compared to matrix mass. The capacitance of the entrained air is neglected.
4. No leakage or carry over between the air streams.
5. Fluid and matrix states are considered to be uniform in the radial coordinate.
6. Angular and radial heat conduction and diffusion due to gradients in temperature and concentration are neglected.
7. The matrix is homogeneous.
8. Heat and mass transfer can be described by convection transfer coefficients which are constant with distance and time through all the system.
9. The dehumidifier is overall adiabatic.

#### Assessment of the Assumptions

Assumption 1 makes sense for steady state simulations.

Assumption 4 might have the largest impact on differences in the performance of a real dehumidifier and this model. It is a question of the dehumidifier design how well carry over losses can be avoided.

Assumption 5 reduces the problem to a one dimensional problem.

Assumption 6 reduces the numerical effort required to solve the equations essentially. Without this assumption second derivatives would appear in the model equations.

Assumptions 7 and 8 are critical since the matrix is not homogeneous due to the compound structure desiccant - desiccant support. Local variations in the air flow

velocity and surface inhomogenities will cause different convection transfer coefficients in flow direction.

### 4.1.3 The Model Equations

With the assumptions listed above, the overall conservation and transfer rate equation for each period can be written as follows.

1. water vapor conservation

$$\dot{m}_{air} \frac{\partial w_{air}}{\partial x} + \frac{M_D}{L} \frac{\partial W_D}{\partial \theta} = 0 \quad (4.1)$$

2. energy conservation

$$\dot{m}_{air} \frac{\partial h_{air}}{\partial x} + \frac{M_D}{L} \frac{\partial h_m}{\partial \theta} = 0 \quad (4.2)$$

3. rate of water vapor mass transfer

$$\frac{M_D}{L} \frac{\partial W_D}{\partial \theta} = D_m \frac{A}{L} (w_{air} - w_{eq}) \quad (4.3)$$

4. rate of energy transfer

$$\frac{M_D}{L} \frac{\partial h_m}{\partial \theta} = \alpha \frac{A}{L} (t_{air} - t_m) + D_m \frac{A}{L} (w_{air} - w_{eq}) \quad (4.4)$$

where

$D_m$ : convective mass transfer coefficient based upon A

$\alpha$ : convective heat transfer coefficient

$w_{eq}$ : local humidity ratio of air in equilibrium with desiccant at temperature  $t_m$  and adsorbed amount  $W_D$ .

A: total transfer area of regenerator for each period

Introducing dimensionless coordinates

$$\Gamma_j = \frac{M_D}{T \dot{m}_{air,j}} \quad (4.5)$$

where

$\Gamma_c, \Gamma_h$  : capacitance ratios of the cold and hot stream, respectively.

for position

$$z = \frac{x}{L}; \quad \text{where } 0 \leq z \leq 1 \quad (4.6)$$

for time

$$\tau = \frac{\theta}{T_j \Gamma_j}; \quad \text{where } 0 \leq \tau \leq \frac{1}{\Gamma_j} \quad (4.7)$$

The conservation laws can be written in these dimensionless coordinates

water vapor conservation

$$\frac{\partial w_{air}}{\partial z} + \frac{\partial W_D}{\partial \tau} = 0 \quad (4.8)$$

energy conservation

$$\frac{\partial h_{air}}{\partial z} + \frac{\partial h_m}{\partial \tau} = 0 \quad (4.9)$$

rate of water vapor mass transfer

$$\frac{\partial W_D}{\partial \tau} = NTU_{w,j} (w_{air} - w_{eq}) \quad (4.10)$$

rate of thermal energy transfer

$$\frac{\partial h_m}{\partial \tau} = NTU_{t,j} c_{air,j} (t_{air} - t_m) + NTU_{w,j} (w_{air} - w_{eq}) \quad (4.11)$$

where

$$NTU_{w,j} = \frac{D_m A_j}{\dot{m}_{air,j}} \quad (4.12)$$

$$NTU_{t,j} = \frac{\alpha A_j}{\dot{m}_{air,j} c_{p,air}} \quad (4.13)$$

$NTU_{w,j}$  and  $NTU_{t,j}$  are the *Number of Transfer Units* for the regeneration stream and the process stream,  $NTU_{w,j}$  for mass and  $NTU_{t,j}$  for heat transfer.

The introduction of an overall effective Lewis number reduces the number of parameter further.

$$Le = NTU_{t,j} / NTU_{w,j}$$

All the equations above are coupled through the thermodynamic property relationships for desiccant-air-water vapor mixture.

$$w_{eq} = w_{eq}(W_D, t_m)$$

$$h_{air} = h_{air}(t_{air}, w_{air})$$

$$H_m = H_m(t_m, W_D)$$

The conservation and transfer equation above need a set of boundary conditions, formed by the inlet states of the air streams.

at  $z = 0$

$$w_{air} = w_{j,i} \text{ and } t_{air} = t_{j,i} \quad \text{for } 0 \leq \tau \leq \frac{1}{\Gamma_j}; j = c, h (1, 2)$$

The initial conditions are defined by the periodical turnover of the process stream to the regeneration mode and of the regeneration stream to the process mode. Therefore, the initial matrix conditions for the regeneration stream are the final matrix properties of the process side at the end of the adsorption process. Furthermore the flow direction is changed and the last outlet element of the process side becomes the first inlet element of the regeneration side. In the finite difference numerical solution scheme this means that the numbering of the matrix elements is reversed each time when the periods change.

at  $\tau_1 = 0$ ,

$$\lim_{\tau_1 \rightarrow 0^+} W_D = \lim_{\tau_2 \rightarrow (1/\Gamma_2)} W_D$$

for  $0 \leq z \leq 1$

$$\lim_{\tau_1 \rightarrow 0^+} t_m = \lim_{\tau_2 \rightarrow (1/\Gamma_2)} t_m$$

at  $\tau_2 = 0$ ,

$$\lim_{\tau_2 \rightarrow 0^+} t_m = \lim_{\tau_1 \rightarrow (1/\Gamma_1)} t_m$$

for  $0 \leq z \leq 1$

$$\lim_{\tau_2 \rightarrow 0^+} W_D = \lim_{\tau_1 \rightarrow (1/\Gamma_1)} W_D$$

The coupled non-linear system of equations are solved using numerical solution techniques. For a complete solution the determination of the state property distributions of fluid and the matrix is necessary in order to gain the outlet states.

#### 4.1.4 The Solution of the Model Equations

In this chapter only the finite difference scheme is introduced in some detail, whereas the equilibrium model based on the combined transfer potentials is skipped here. Van den Bulck 1987 and Harald Klein 1988 discuss this theory extensively. Maclain-Cross (1972) developed a finite difference scheme for the solution of the equation system presented above. Since this model was extensively used in this study and modified for a new exchanger model with two process streams and one regeneration stream for staged dehumidification, some features of the program MOSHMX are presented here.

MOSHMX divides the matrix of the dehumidifier into a grid of discrete space and time steps. Each element can be treated as a small heat and mass exchanger. Maclain-Cross developed a second order finite difference representation with is conceptionally analogous to a second order Runge-Kutta method. Figure 4.2 shows one finite difference element. The computation in the program proceeds in the way that the air "outlet" states and the matrix "outlet" states of the previous element become the inlet states of the present element. The first guess value for the outlet states is computed based on the inlet property states. Then, the second order Runge Kutta accuracy is achieved by a second evaluation of the matrix and air properties and derivatives at the middle of the element. The matrix and air states in the middle of the element are the mean of the inlet states and the first guess of the outlet states gained by the evaluation of the inlet states. The outlet property states are recalculated based on the properties in the middle of the element.

The initial conditions of the matrix have to be guessed. The program distributes the initial matrix states between the inlet states linearly at higher rotation speeds. At low

rotation speeds the initial states are equal to the inlet conditions. At the turnover from process to regeneration the numbering of the elements is inverted.

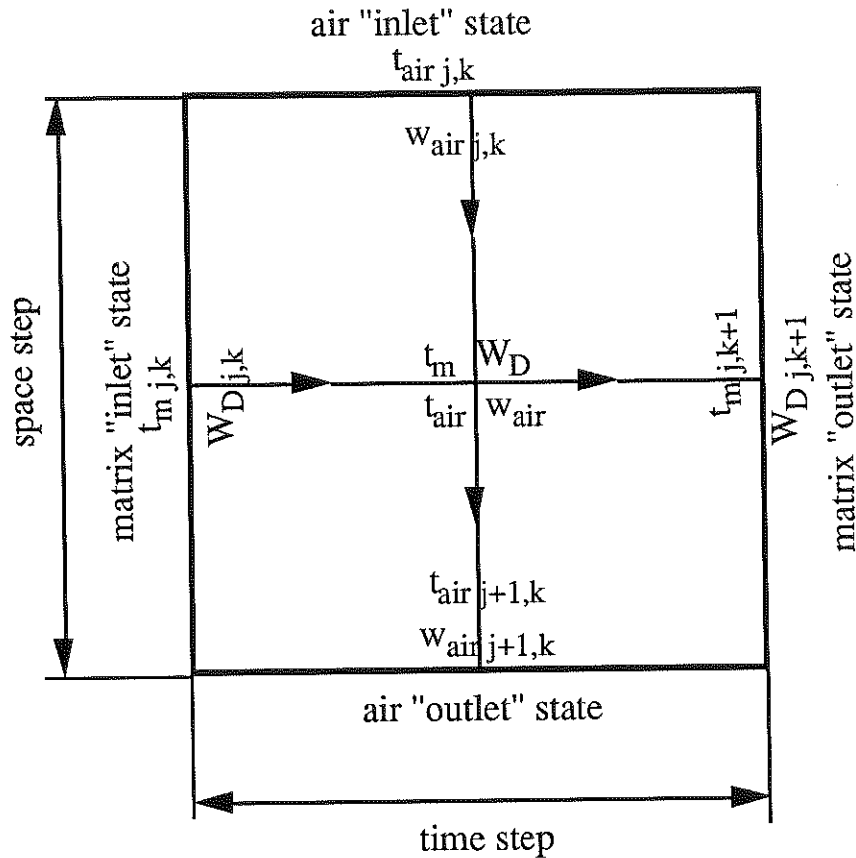


Figure 4.2 One Finite Difference Element

where:

j: space step index

k: time step index

Convergence is reached when the fluid and matrix states do not vary within specified criteria for two consecutive rotations. MOSHMX allows a variety of different convergence criteria. One criteria is a water balance between the regeneration stream and the process stream. If the overall mass balance is within a defined limit the iteration process is stopped. The same is possible for an energy balance and an enthalpy effectiveness criteria.

The simplest iteration method is to rotate the wheel as long as it takes till the convergence criteria are satisfied. This method is called transient method. Another method is the matrix method. After two total rotations of the wheel with the transient scheme a modified Newton Raphson guesses the final states of each matrix element. This method converges much faster at high rotation speeds.

The discretization of the time and space steps is optimized with respect to accuracy and CPU time. Maclaine-Cross found an empirical correlation between NTU and number of space steps. At higher NTU a smaller discretization is required. The number of time steps depends on the wave speeds determined by the analogy solution. Thus, MOSHMX always calls the ANALOGY solution for this calculation first. It is also possible to specify the number of time and space steps explicitly.

For a more accurate solution the calculation procedure can be run for three different space step discretizations and the final solution is extrapolated by a Richardson extrapolation scheme.

When the final solution is reached the mass and energy balance errors are equally distributed between the process and the regeneration outlet state properties.

The dehumidifier with two process stream inlets at one side of the wheel and one regeneration stream inlet at the other side of the wheel works only with the water balance and enthalpy balance convergence criteria. The major difference to the normal MOSHMX version is the addition of a third stream with index 3. Figure 4.3 illustrates the configuration of this dehumidifier type. The MOSHMX code analysis the first process stream (index 1) and regeneration stream (index 2) with the analogy solution and the resulting discretization is applied for the regeneration stream and for the first process stream as well as for the second process stream. The parameter which indicates that a third inlet is used is the capacitance ratio  $\Gamma_3$ .  $\Gamma_3$  bigger than zero results in the simulation

of the dehumidifier with three inlets. The new MOSHMX version skipped the possibility of a Richardson extrapolation since this leads to CPU times above 25 minutes for desiccant cooling systems. Another feature is that the number of time steps can be chosen by the parameter NFX which multiplies the number of space steps with a constant value for the determination of the time steps. NFX should be in the range of 5 to 10 for sufficient accuracy. In order to achieve faster convergence the code initializes the matrix if the regeneration inlet temperature changes more than 3°C, otherwise the solution of the last simulation is the start initialization of the matrix. This leads to faster convergence within a Newton iteration loop where the consecutive regeneration temperature is almost the same.

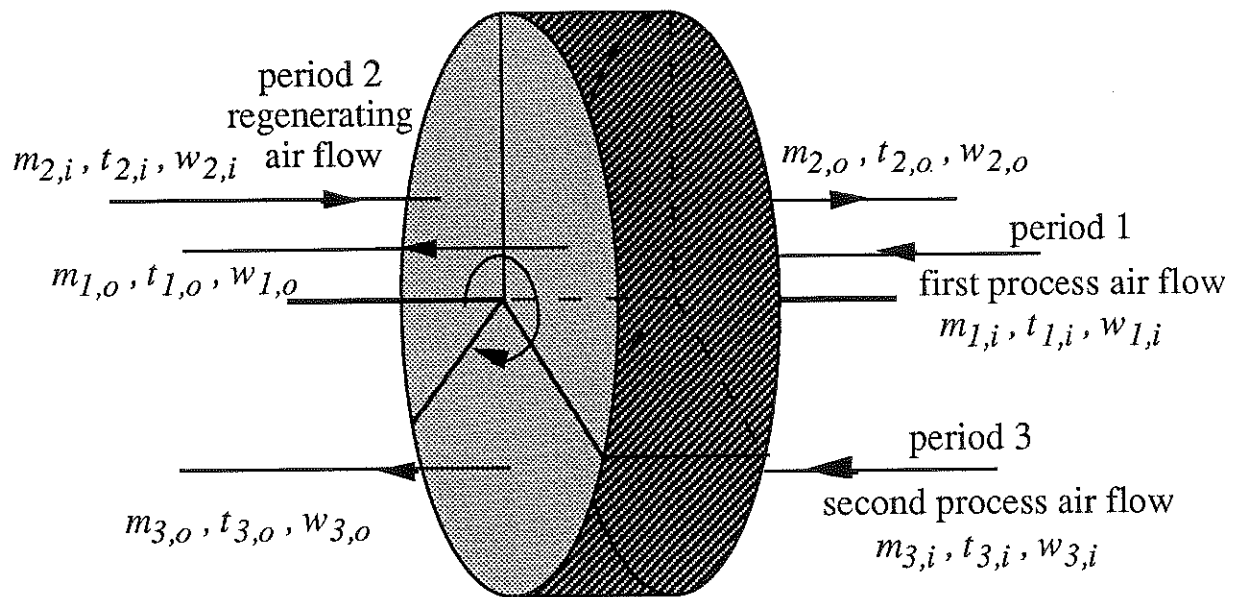


Figure 4.3 Dehumidifier with Three Inlets

The mathematical formulation of the new initial conditions and the turnover between the periods.

at  $\tau_l = 0$

$$\lim_{\tau_1 \rightarrow 0^+} W_D = \lim_{\tau_2 \rightarrow (1/\Gamma_2)} W_D$$

for  $0 \leq z \leq 1$

$$\lim_{\tau_1 \rightarrow 0^+} t_m = \lim_{\tau_2 \rightarrow (1/\Gamma_2)} t_m$$

at  $\tau_3 = 0$

$$\lim_{\tau_3 \rightarrow 0^+} W_D = \lim_{\tau_1 \rightarrow (1/\Gamma_1)} W_D$$

for  $0 \leq z \leq 1$

$$\lim_{\tau_3 \rightarrow 0^+} t_m = \lim_{\tau_1 \rightarrow (1/\Gamma_1)} t_m$$

at  $\tau_2 = 0$

$$\lim_{\tau_2 \rightarrow 0^+} W_D = \lim_{\tau_3 \rightarrow (1/\Gamma_3)} W_D$$

for  $0 \leq z \leq 1$

$$\lim_{\tau_2 \rightarrow 0^+} t_m = \lim_{\tau_3 \rightarrow (1/\Gamma_3)} t_m$$

## 4.2 Sensible Heat Exchanger Model

The model of a regenerative sensible heat exchanger is similar to the dehumidifier model introduced above. The solution of the model equations is a lot easier than the solution of the dehumidifier equations. This is due to the fact that mass exchange does not occur and the differential equations are uncoupled. Therefore, equation (4.2) and equation (4.4) with the energy transfer term due to mass effects omitted are sufficient for the description of the model.

$$\dot{m}_{air} \frac{\partial h_{air}}{\partial x} + \frac{M_D}{L} \frac{\partial h_m}{\partial \theta} = 0 \quad (4.2)$$

$$\frac{M_D}{L} \frac{\partial h_m}{\partial \theta} = \alpha \frac{A}{L} (t_{air} - t_m) \quad (4.4b)$$

In this study a curve fit for the computation of the heat exchanger effectiveness is used to describe the performance of a rotary sensible heat exchanger (Kays and London).

$$\epsilon_t = \epsilon_{direct} \left( 1 - \frac{1}{9(C_r^*)^{1.93}} \right) \quad (4.14)$$

where

$\epsilon_{direct}$ : effectiveness of a countercurrent heat exchanger (not regenerative)  
 $C_r^*$ :  $\frac{c_{pm}}{c_{pair}} \Gamma_{max}$ ; ratio of matrix capacitance rate to minimum fluid capacitance rate.

Equation (4.14) is derived by Kays and London. It describes the results of Lambertson [4] and Bahnke and Howard [5] for regenerative heat exchanger.

The effectiveness for a direct transfer sensible heat exchanger is given by

$$\epsilon_{direct} = \frac{1 - \exp[-NTU_d(1-C^*)]}{1 - C^* \exp[-NTU_d(1-C^*)]} \quad (4.15)$$

where

$C^*$ :  $\frac{\dot{m}_{min}}{\dot{m}_{max}}$  or  $\frac{\Gamma_{min}}{\Gamma_{max}}$ ; ratio of minimum to maximum heat capacitance at equal specific heat capacity of the air.

$NTU_o$ : number of transfer units of a direct heat exchanger

The number of transfer units for direct heat exchanger can be related to the number of transfer units of a regenerative heat exchanger with equation (4.16).

$$\frac{1}{NTU_o} = \frac{1}{NTU_{tc}} + \frac{C^*}{NTU_{th}} \quad (4.16)$$

where :

$NTU_{tc/h}$ :  $NTU_t$  for the "cold"/"hot" stream of the heat exchanger (compare equation (4.13))

Equations (4.15 - 4.16) apply only for unbalanced heat exchangers. For balanced rotary heat exchangers with equal heat capacitance streams and equal heat transfer areas ( $NTU_{tc} = NTU_{th}$ ) the relations simplify to:

$$\epsilon_{direct} = \frac{NTU_o}{1 + NTU_o} \quad (4.17)$$

and

$$NTU_o = \frac{NTU_t}{2} \quad (4.18)$$

With the definition of the heat exchanger effectiveness  $\varepsilon_t$  the outlet states can be computed by the knowledge of the inlet states.

$$\varepsilon_t = \frac{(t_{c,o} - t_{c,i})/\Gamma_c}{(t_{h,i} - t_{c,i})/\Gamma_{max}} = \frac{(t_{h,i} - t_{h,o})/\Gamma_h}{(t_{h,i} - t_{c,i})/\Gamma_{max}} \quad (4.19)$$

This concept works well in the range of  $C_r^*$  above 0.4. For very low rotation speeds of the regenerative wheel equation (4.14) can not be applied, but  $C_r^*$  below 0.4 does not occur in normal heat exchanger applications. The usual range for  $\Gamma$  is between 5 and 30.

### 4.3 The Evaporative Cooler Model

Assumptions:

1. The evaporative cooler is adiabatic.
2. The air pressure is the same at inlet and outlet (no pressure drop)
3. There is no work necessary to blow the air through the equipment.

Assumptions 2 and 3 are critical, since pressure drop in the cooler occurs and converts mechanical energy in terms of pressure differences between inlet outlet into thermal energy.

The main equation for the whole humidifier model is derived from a energy balance and mass balance:

Energy Balance:

$$H_{a,i} + H_{water,i} = H_{a,o} \quad (4.20)$$

Mass Balance:

$$\dot{m}_{air}w_{air,i} + \dot{m}_{water} = \dot{m}_{air}w_{air,o} \quad (4.21)$$

Main equation:

$$h(t, w_{air,i}) + (w_{air,o} - w_{air,i})h_L(t) = h(t, w_{air,o}) \quad (4.22)$$

Basically equation (4.22) and some thermodynamic relationships between absolute humidity, relative humidity, total pressure and temperature define the model. The widely used humidifier effectiveness model is not applied in this study, but the relative humidity of the outlet stream can be specified as well as the inlet temperature of the liquid water. This gives more flexibility in terms of the water temperature which can be changed in order to increase or decrease the enthalpy stream which enters the adiabatic component (a more or less adiabatic humidifier can be simulated). This humidifier model would have a 100% effectiveness if the water temperature is equal to the wet bulb temperature, and the relative humidity of the outlet is set to 100%.

#### 4.4 Conclusions

The dehumidifier model with its assumptions is widely used and the validity of the numerical results is proven by experiments (Van den Bulck 1987).

The MOSHMX program code allows the simulation of an adiabatic rotary dehumidifier. The main features are accuracy, flexibility in terms of convergence criteria /method, and simplicity due to the auto discretization routines. The MOSHMX program code has the disadvantage of a high CPU consumption and is not applicable for long term system simulations.

The rotary regenerative heat exchanger model is based on an effectiveness model. The heat exchanger effectiveness is a curve fit of measured and of simulated data. The exactness of this model is not critical for the solutions in a desiccant cooling cycle since the resulting heat exchanger effectiveness can be used for system comparisons as well as the input parameters NTU and  $\Gamma$ .

The humidifier model is very simple and flexible. It is not based on an effectiveness model or NTU correlations.

---

## Chapter five

---

This chapter deals with the simulation of the classical desiccant cooling cycles. In the first sections some general limits for cooling cycles are discussed with respect to ambient states, room inlet states, and equipment size for regular silica gel dehumidifiers.

The second part of this chapter deals with the new theoretical desiccants introduced in chapter three.

Finally the last section illustrates some new equipment configurations which are designed to improve the COP and operational range of a desiccant cooling system without increasing of the size of the equipment.

### 5.1 Simulation Conditions

The ASHRAE Application Handbook (1991) gives general design criteria for commercial buildings. In this study the suggested design conditions for dining and entertainment centers are chosen. Table 5.1 shows some design data.

Specific Category	Inside Design Conditions Winter	Inside Design Conditions Summer	Circulation, Air Changes per Hour
Cafeterias and Luncheonettes	21 to 23°C 20 to 30% rh	26°C 40% rh	12 to 15
Restaurants	21 to 23°C 20 to 30% rh	23 to 26°C 55 to 60% rh	8 to 12
Bars	21 to 23°C 20 to 30% rh	23 to 26°C 50 to 60% rh	15 to 20

*Table 5.1 Design Data for Commercial Buildings*

Here the upper limit for restaurants is picked in this study with 26°C and 60% relative humidity.

For the comparison of the different cycles three locations in the US are selected: Miami, Chicago Midway, Los Angeles CO. The 1% design dry-bulb and mean coincident wet-bulb temperature for these areas are the parameters which define the ambient conditions of the simulations. The design conditions are defined by the ASHRAE Fundamentals Handbook (1989) as the percentage of hours in summer with exceed the specified ambient states. Table 5.2 illustrates the 1% ambient design conditions with the corresponding relative humidity.

	$T_{dry}$	$T_{wet}$	rh	$w_{air}$	$h_{air}$
Miami	33°C	25°C	52.6%	0.0167	75.9kJ/kg
Chicago	34°C	23°C	39.3%	0.0131	67.9kJ/kg
Los Angeles	34°C	21°C	30.1%	0.0102	60.4kJ/kg

*Table 5.2 ASHRAE 1% Design Conditions for Chicago, Los Angeles, and Miami*

These three locations are selected due to their different level of relative humidity. Los Angeles has the lowest humidity and almost needs no dehumidification. Chicago is very hot but not as humid as Miami, which represents the toughest design condition for cooling machines.

The cooling load due to one kg dry air is 10 kJ/kg. This value is fixed in all simulations and represents a common design compromise between necessary air flow and enthalpy difference to meet a given cooling load. Higher cooling loads per kg conditioned process air result in very low inlet temperatures and therefore in uneven temperature distributions in the room. Lower enthalpy differences between room and inlet states require high mass flow rates and large air duct systems with large pumping costs.

In this study the enthalpy difference is separated into 8 kJ/kg sensible heat difference and 2 kJ/kg latent heat difference. This means, that 2 kJ/kg of the load is due to a lower absolute humidity of the inlet and 8 kJ/kg of the load is due to a lower temperature of the inlet. The resulting inlet and room states are summarized in Table 5.3.

States	$T_{air}$	rh	$w_{air}$	$h_{air}$
Inlet	18.22°C	90.5%	0.0119	48410kJ/kg
Room	26°C	60%	0.0126	58410kJ/kg

*Table 5.3 Room States and Process Air Inlet states*

The input parameter for a typical simulation run with silica gel as desiccant are summarized in Table 5.4

Room States	$T_{dry}$ : 26°C	rh: 60%
Room inlet	delta $h_{air}$ : 10kJ/kg	sensible heat ratio: 0.8
Ambient States	$T_{dry}$ : 34°C	$T_{wet}$ : 23°C
Air Properties	total Pressure: 1013hPa	$C_{pair}$ : 1.005kJ/kgC
Dehumidifier	$C_{pm}$ : 1.009kJ/kgC	Le: 1.0
	NTU <sub>2</sub> : 10	$\Gamma_1$ : 0.1
		NTU <sub>1</sub> : 10
		$\Gamma_2$ : 0.1
Heat Exchanger	NTU <sub>h,t</sub> : 10	$\Gamma_h$ : 20

*Table 5.4 Simulation Inputs*

In the following simulations these parameters are the standard parameters for each simulation.

## 5.2 The Simulation Method

With the simulation conditions above all output and input parameters for the cooling devices are specified. The link of the cooling equipment for the ventilation, recirculation, and closed Dunkle cycle is similar to the presentation in Chapter One, Figure 1.11, 1.13, 1.15, respectively.

For all cycles the simulation programs varies the dehumidifier regeneration temperature. With this specification the ventilation cycle and recirculation cycle can be solved without iterations. The closed Dunkle cycle requires one more iteration loop since one additional temperature must be guessed (compare;  $t(7)$ ; Figure 1.13). One simulation run calculates the room inlet temperature. When the program algorithm finds a regeneration temperature that leads to lower room inlet temperatures than required, a modified Newton iteration is started to find the exact regeneration temperature at the dehumidifier inlet.

The output of each simulation run consists of all air states and the COP. The coefficient of performance includes only thermal energy and is defined as the ratio of the cooling load of the house and the required heat for regeneration. Parasitic power of the fans in the air duct system to overcome the pressure drop of the equipment is skipped in this study.

$$COP = \frac{\Delta H_{house}}{\Delta H_{heater}} \quad (5.1)$$

The simulation program is described in much more detail in Appendix B Program Description.

### 5.3 The Performance of the Different Cycles

In this section the limits of the conventional cooling cycles are illustrated with respect to equipment size, ambient state properties, and room inlet state properties. The dehumidifier models used are based on the Dubinin-Astakov isotherm formulation and Van den Bulck's parameters. (compare Chapter 3) The indices ve, rc, do, dc distinguish between ventilation cycle, recirculation cycle, open Dunkle cycle, and closed Dunkle cycle, respectively.

#### 5.3.1 Desiccant Cooling Cycle Performance with Respect to Equipment Size

The classical ventilation cycle and regeneration cycle are both very sensible with respect to the equipment size. In dry climates the ventilation cycle always performs better than the regeneration cycle. Figure 5.1 illustrates the COP and regeneration temperature with respect to a variation of NTU for the heat exchanger and dehumidifier simultaneously.

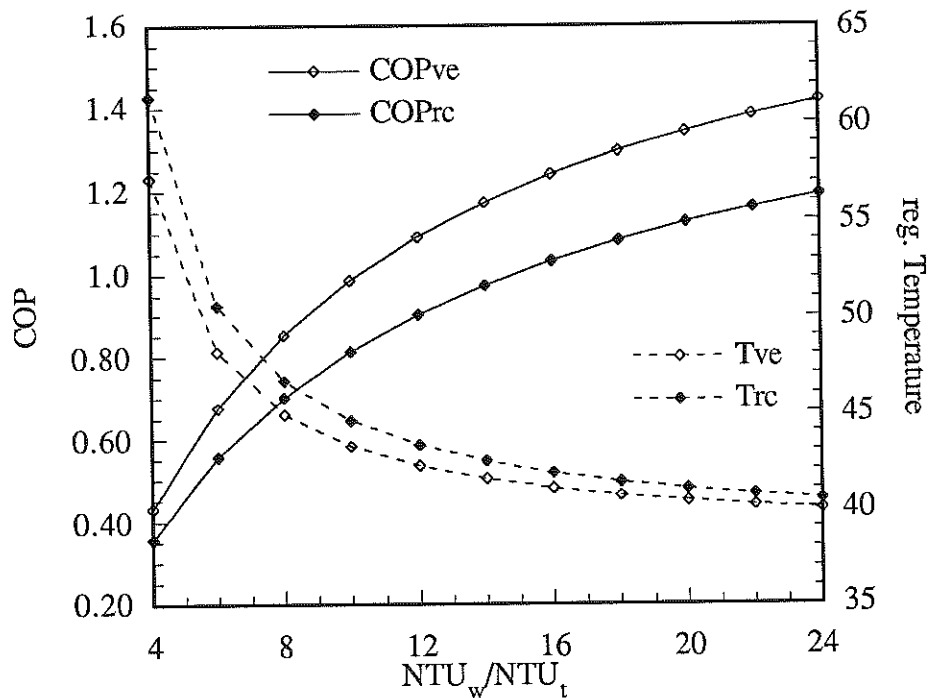


Figure 5.1 Equipment Size, Recirculation and Ventilation Cycle, Los Angeles

The outside conditions are equal to the Los Angeles design conditions and the regeneration heating for the cooling device is relatively low compared to other locations like Miami. Even in this case the cooling cycles do not work well below NTU equal to 8. NTU equal to 10 might be already the upper limit for reasonable equipment size.

In the case of low ambient humidity the regeneration temperature for the regeneration cycle is always higher, but with tougher ambient conditions such as Miami the picture changes and the recirculation cycle becomes better at small equipment size. The necessary regeneration temperature is much lower than the corresponding temperature for the ventilation cycle. Figure 5.2 shows that at large equipment size the ventilation cycle performs better than the recirculation cycle.

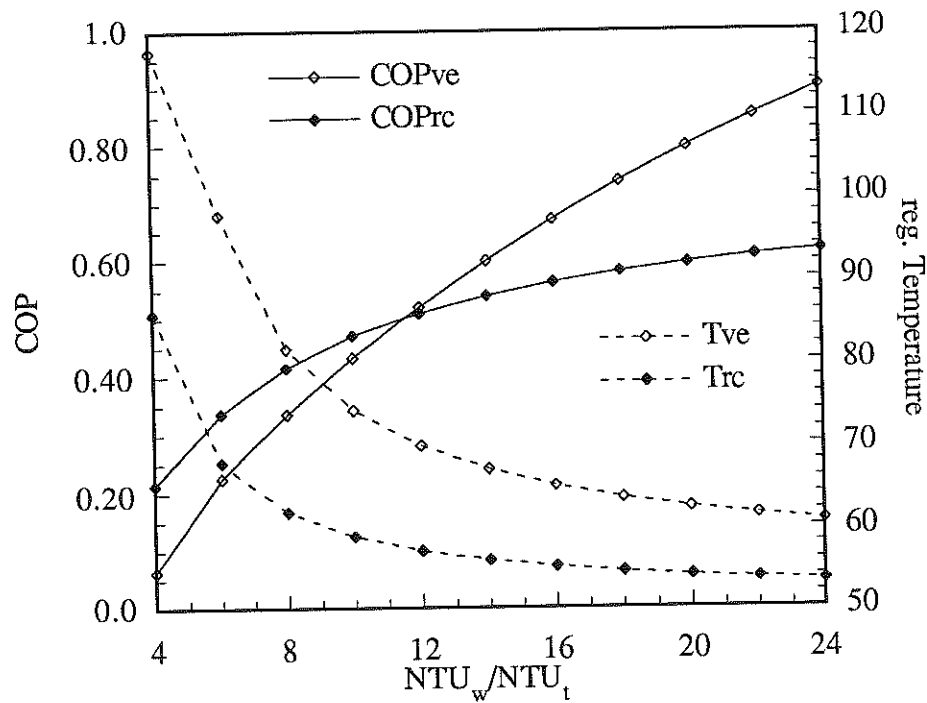


Figure 5.2 Equipment Size, Ventilation and Recirculation Cycle, Miami

This is due to the fact that the heat sink for both cycles is different. In the case of the recirculation cycle the heat sink for the heat exchanger is the wet bulb temperature of the ambient; in the case of the ventilation cycle the heat sink is the wet bulb temperature

of the room state. At very high heat exchanger effectiveness the ventilation cycle recovers almost all energy from the process stream and even with a high regeneration temperature a smaller regeneration heat is necessary since the wet bulb temperature of the room is lower than the wet bulb temperature of the ambient and therefore reduces the necessary cooling load. (compare Figure 1.10; state 9 is never cooler than state 2).

The Dunkle cycle, open in the case of low ambient humidity or closed in the case of high ambient humidity, shows a much better COP than recirculation and ventilation cycle. Figure 5.3 illustrates all cycles considered for the Chicago design conditions.

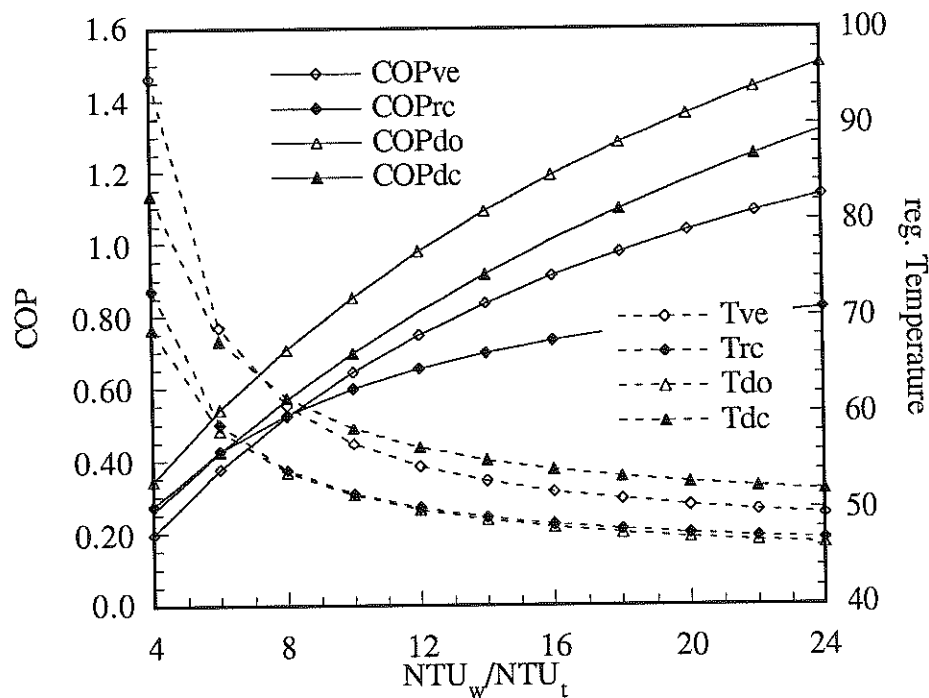


Figure 5.3 Equipment Size, All Cycles, Chicago Design Conditions

### 5.3.2 Desiccant Cooling Cycle Performance with Respect to Ambient Conditions

In this section the ambient states are varied in two different ways. Figure 5.4 and Figure 5.5 show the dependence of the performance of the cycles with respect to ambient

temperature at constant relative humidity. Here, the humidity is chosen to be 50% which is close to the Miami design conditions. The ventilation cycle can not meet the requirements above 38°C with a regeneration temperature below 120°C. Both Figures show that at 32°C the closed cycles perform better than the open cycles. In the case of the recirculation cycle this is accidental since the point of equal performance depends on the enthalpy difference between room inlet and room state as well (compare Figure 5.4), whereas the combination open/closed Dunkle Cycle behaves always the same at the point, where the enthalpy of state 7 becomes lower than the enthalpy of the ambient state (compare Figure 1.13).

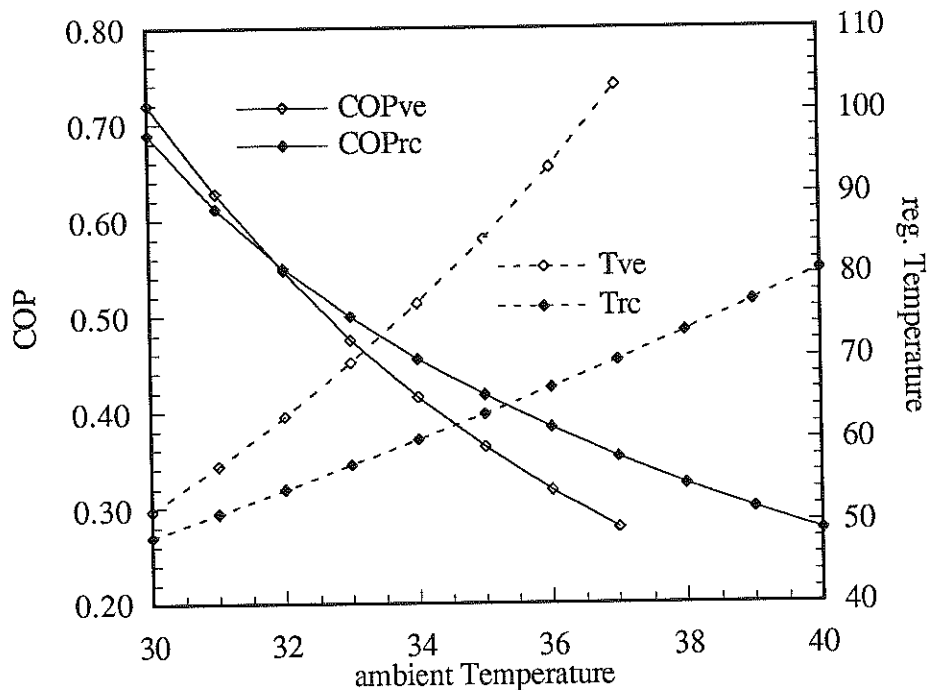


Figure 5.4 Variation of the Ambient Temperature at Constant Relative Humidity

The variation of the relative humidity at constant temperature gives no new information. The ambient state where the closed configurations become better than the open cycles has the same enthalpy in both cases. At a fixed ambient temperature equal to 34°C the corresponding ambient humidity is about 43% at that point.

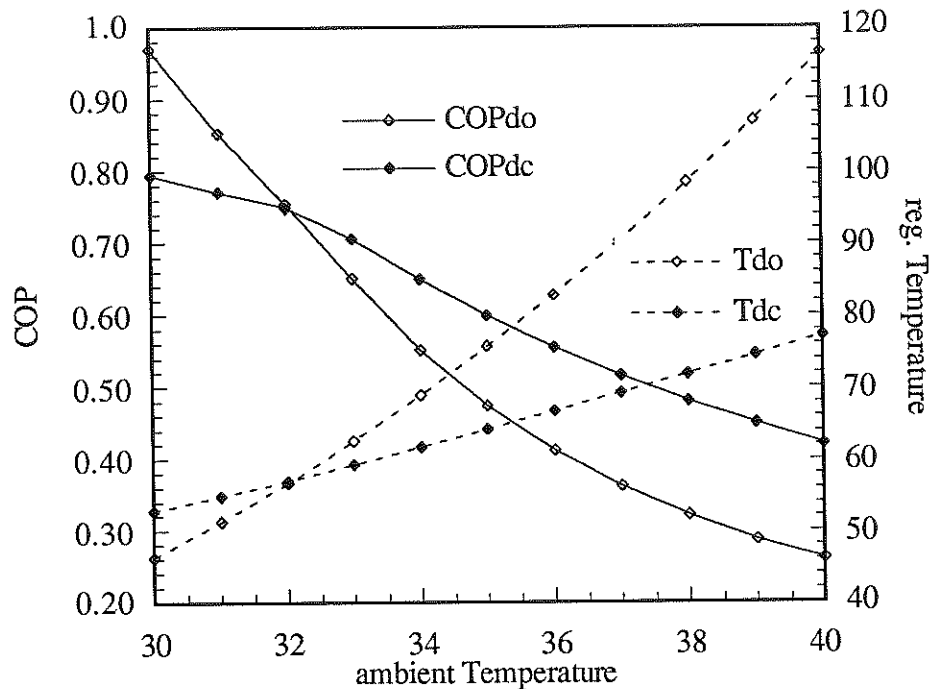


Figure 5.5 Variation of the Ambient Temperature at Constant Relative Humidity

### 5.3.3 Desiccant Cooling Cycle Performance with Respect to Inlet Conditions

In this section the enthalpy difference between room state and inlet state is varied. To reduce the enthalpy difference, a greater air flow is required to meet the load. The sensible load factor is adjusted in the simulations to 0.7 since the standard value 0.8 leads to room inlet humidity above 100% at high enthalpy differences. The ventilation and recirculation cycle show both a maximum in the COP for one discrete cooling load per kg process air when the enthalpy difference between room and ambient state is high enough. In locations such as Los Angeles, where the room state can be reached without the dehumidifier, it is beneficial to decrease the enthalpy difference of the room inlet as far as possible in order to gain the maximum COP. This method is limited due to the total cooling load with must be met by the air conditioner. Half the enthalpy difference per kg process air means twice the mass flow in order to achieve the same cooling effect. The decrease of the COP at higher enthalpy differences is caused by the dependence of the

enthalpy difference on the regeneration temperature. The enthalpy difference increases slower than the regeneration temperature. Thus, the required heat for the regeneration increases more than the cooling enthalpy difference. At a low enthalpy difference the effect of the added 'load' by the humidifier (the required regeneration temperature is higher due to the moist added to the regeneration stream) which serves as heat sink of the heat exchanger increases the actual regeneration effort. In other words the ventilation and regeneration cycle consume energy to remove the moisture added by the humidifiers. Another fact that contributes to the effect of decreasing COP at low enthalpy differences in the case of the ventilation cycle is that there is a negligible enthalpy difference between the room state and the inlet state compared to the difference between the ambient states and the room states. Thus, the cooling device consumes energy in order to reach the room state, but provides no usable enthalpy difference for the conditioning requirements of the house. Figure 5.6 illustrates the COP depending on the enthalpy difference between room state and inlet state.

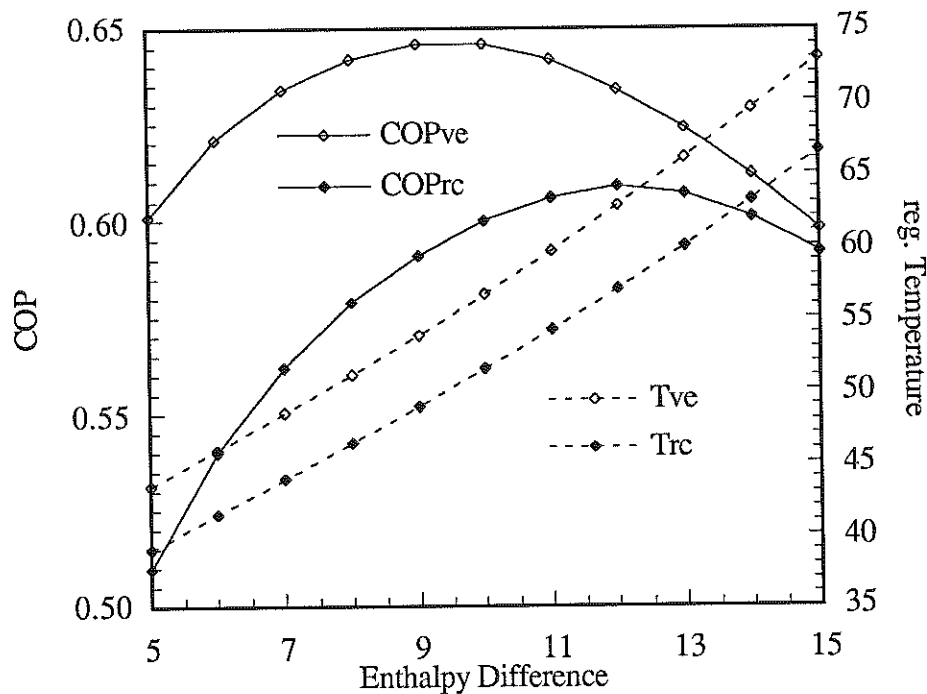


Figure 5.6 Variation of the Enthalpy Difference at Chicago Design Conditions

At Chicago design conditions the open Dunkle cycle shows still the behavior of the ventilation cycle at Los Angeles design conditions. This is due to the fact that the open Dunkle cycle operates with two heat exchangers and the second heat exchanger with the wet bulb temperature of the room state as heat sink does not increase the humidity of the regeneration stream compared to the ventilation cycle. In the case of 5 kJ/kg enthalpy difference almost no water has to be added in the adiabatic humidifier in front of the room inlet, the dehumidifier does not work much, almost the total load can be met by the regenerative evaporative cooler component (second heat exchanger and the humidifiers). At higher enthalpy differences additional cooling capacitance must be provided and the humidifier in front of the room inlet adds more moist to cool the room inlet further down. All this moist that is added in the humidifier must be removed by the dehumidifier which causes higher regeneration temperatures and results in a lower COP. In other words, at low enthalpy differences the open Dunkle cycle works as a regenerative evaporative cooler which cools without regeneration effort. Figure 5.7 shows the COP of an open and closed Dunkle cycle depending on the enthalpy difference.

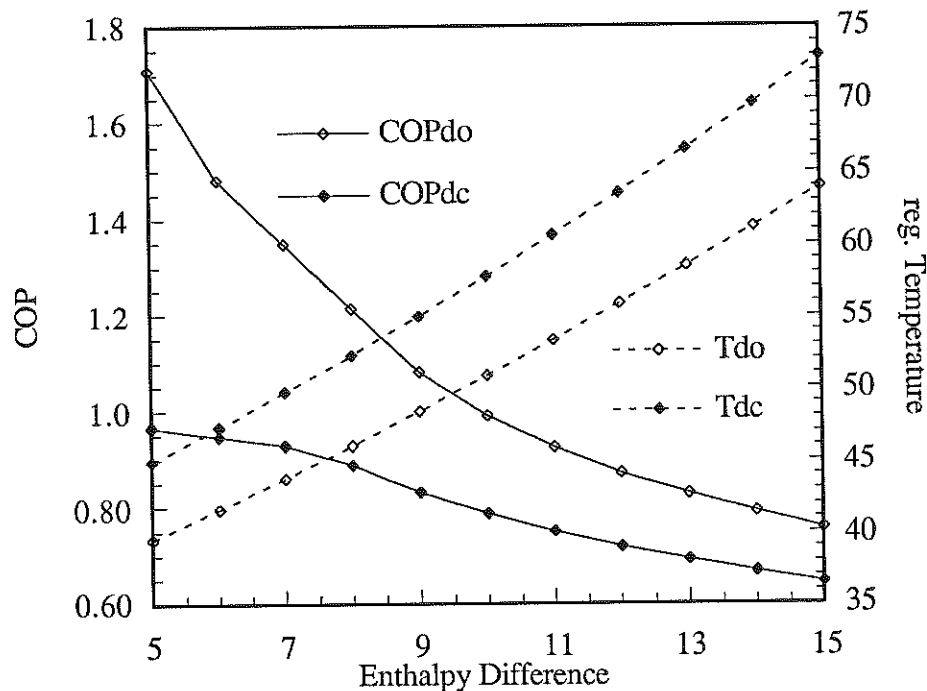


Figure 5.7 Variation of Enthalpy Difference at Chicago Design Conditions

At very high ambient humidity for the open and closed Dunkle cycle the optimum changes towards higher enthalpy differences. This is due to the fact that significant energy is required just to reach the room states and every additional enthalpy difference between the room and the inlet state is extremely beneficial for the COP. Figure 5.8 illustrates the COP depending on the enthalpy difference for the open and closed Dunkle cycle at 34°C and 69% relative humidity ambient state.

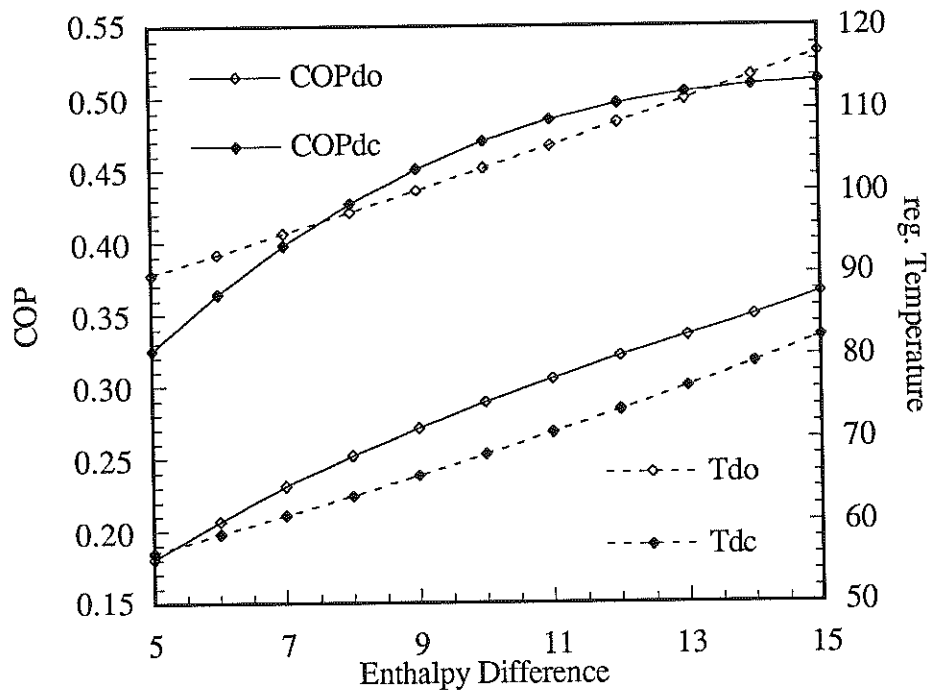


Figure 5.8 Variation of Enthalpy Difference at 69% rh and 34°C

### 5.3.4 Cycle Performance with Respect to the Regeneration Mass Flow

For all cases it turned out that a slightly smaller regeneration stream connected with a higher regeneration temperature results in higher COPs. The heat exchangers operate always balanced since unbalanced heat exchangers reduce the available heat sink capacitance dramatically. Therefore the surplus air is dumped before the auxiliary heater and right after the heat exchanger. Figure 5.9 illustrates the COP and regeneration temperature depending on the percentage of the mass flow through the regeneration side of

the dehumidifier based on the process air flow for ventilation, recirculation, and open Dunkle cycle. The results presented in this section agree with Jurinak's results.

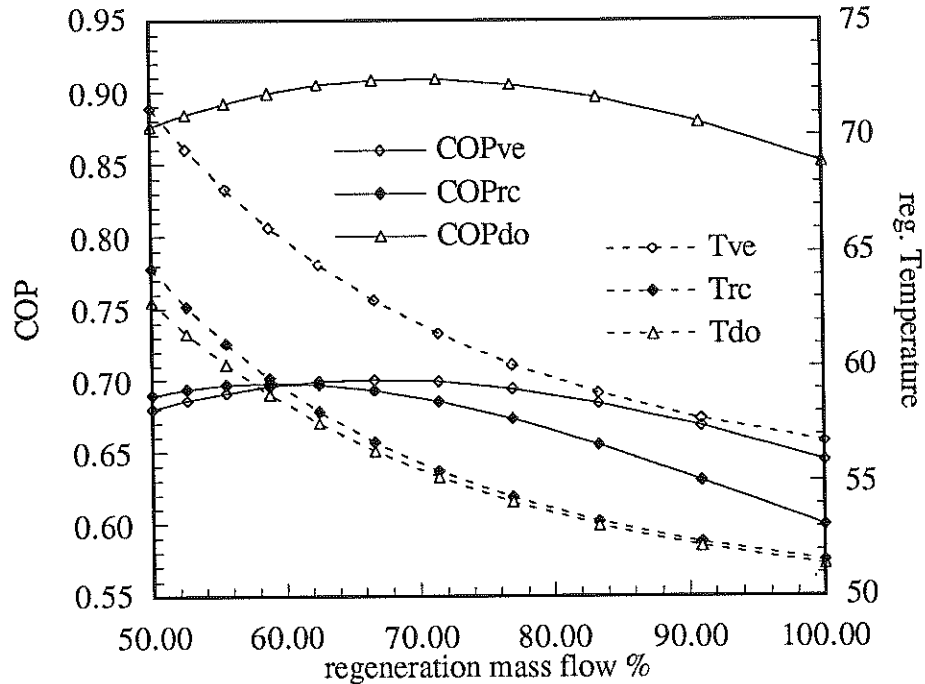


Figure 5.9 Regeneration Mass Flow Variation at Chicago Design Conditions

### 5.3.5 Assessment of the Different Cycles.

The classical cooling cycles ventilation and recirculation cycle work always with low COPs. At low ambient humidity the ventilation cycle is better than the regeneration cycle. Already at slightly higher cooling loads than the maximum cooling load, which can be handled by a regenerative evaporative cooler alone, the ventilation and regeneration cycle operate with low COPs of about 1.0 and 0.8, respectively. (compare Figure 5.1 Los Angeles Design Conditions) This low performance is caused by the increase of the necessary regeneration temperature due to the humidity increase of the regeneration stream. This increase in humidity is necessary in order to provide a deeper heat sink for the sensible heat exchanger. The Dunkle cycle does not have these problems compared to the simple cycles. The open Dunkle cycle does not increase the humidity of the regen-

eration stream and operates like an evaporative cooler with a dehumidifier in front which is able to reduce the humidity alone without temperature increase (the temperature of the dehumidified air is slightly higher than the ambient temperature because of the heat exchanger effectiveness.)

The Dunkle Cycle has thermodynamic advantages compared to the simple cycles which might predominate the disadvantage of one additional heat exchanger. Furthermore the option to operate the Dunkle cycle open, closed, or in any combination gives enough flexibility to adjust this cycle for a variety of ambient conditions and indoor air quality requirements.

A reduced mass flow of the regeneration stream relative to the process stream is beneficial for the COP of all cycles. For gas fired regeneration equipment any improvement of the COP is beneficial for the cooling machine performance. Another advantage of the reduced mass flow through the regeneration side is the fact that the actual dehumidifier size decreases with decreasing mass flow at constant NTU (equation 4.13). When the regeneration energy is provided by a solar system the advantage of a lower regeneration temperature might predominate the disadvantage of more total energy consumption. In this case the balanced dehumidifier is preferred.

In the simulations the Dubinin-Polanyi isotherm formulation for regular silica gel and the approximation of this formulation with the Jurinak polynomial expression are so close that the highest difference in the regeneration temperature is in the range of 1°C and the coincident COP is off only 1%. This result shows that the polynomial curve fit is close enough and that both formulations can be exchanged without major effect on the simulation results. Furthermore this gives confidence in the program code.

## 5.4 The Evaluation of the Isotherms Based on the SERI Measurements

In the following sections the approximation to the SERI measurements is compared to regular silica gel for the Chicago Design conditions. The highly temperature dependent isotherms introduced in Chapter 3 are implemented in the simulation program code (Figure 3.5 to 3.12). The ventilation and open Dunkle cycles are chosen for the simulation comparisons.

### 5.4.1 Variation of the Isotherm Shape with Respect to Equipment Size

In this section the number of transfer units is varied for the different isotherm shapes. Figure 5.10. illustrates the COP and regeneration temperature depending on the NTU of the dehumidifier and of the heat exchanger for four isotherm shapes. Here the basic shape is the shape of the approximated silica gel correlation introduced in Chapter 3.4. The shapes are distinguished by the scaling parameter  $dh^*$  equals 0.25, 0.6, 1.0, 1.4, respectively.

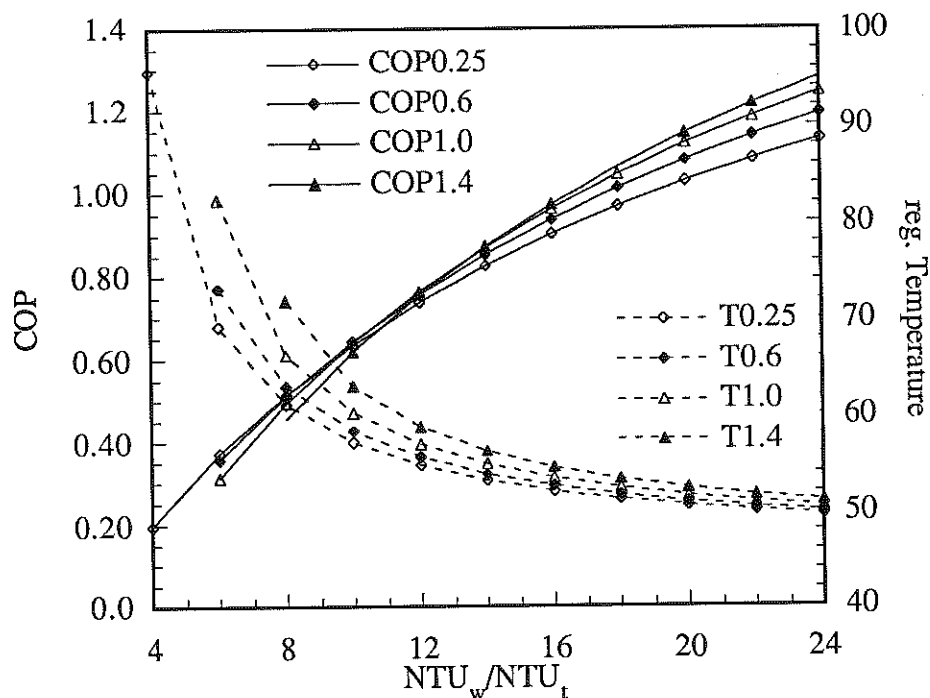


Figure 5.10. COP Silica Gel Isotherm Set, Ventilation Cycle, Chicago Design

Figure 5.11 illustrates the same correlations as Figure 5.10, but for the SERI approximation. In the simulations the heat capacity of the matrix for silica gel and for the approximation of the SERI sample R19-52-3 is assumed to be the same. Other assumptions are equal NTU and Lewis numbers.

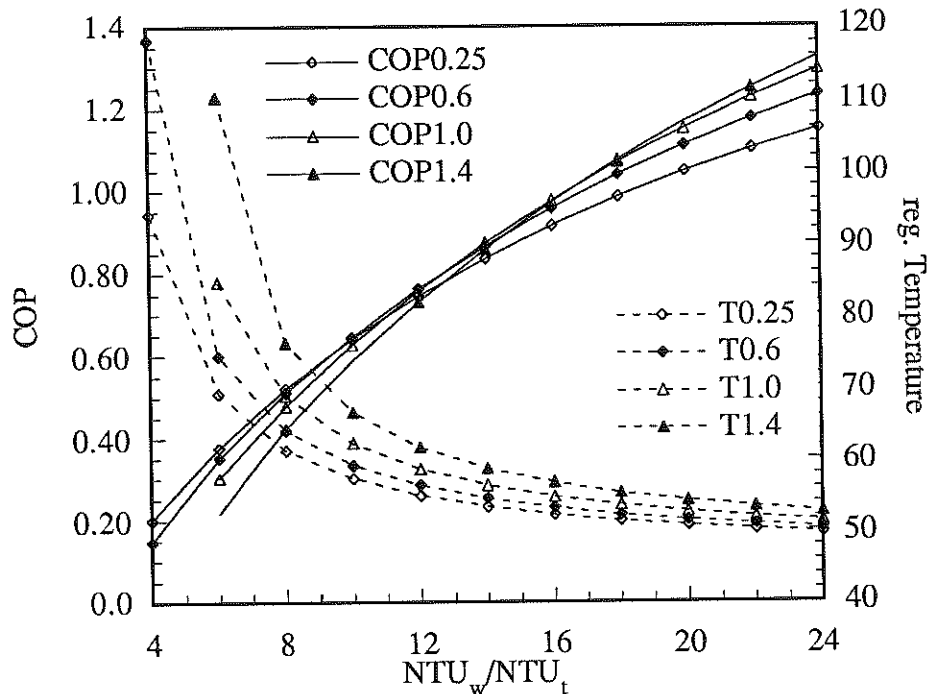


Figure 5.11. COP of SERI Isotherms, Ventilation Cycle, Chicago Design

Both base isotherms behave almost identical regardless of the temperature dependence. The isotherms with the same parameter set which affect the temperature dependence result in almost the same COP and regeneration temperature. The SERI base shape is slightly better than the silica gel approximation since the SERI sample has at low relative humidity a higher water uptake. Thus, the base shape tends to be a Brunauer Type 1 extreme in the range of low humidity. (compare section 5.4.4)

The artificial temperature dependence is designed to operate with the optimum results for adsorption temperatures around 30°C with an adsorption shape equal to a Type 1 isotherm and an isotherm shape with is close to a Type 3 shape at a regeneration of about 70°C. For NTUs in the range 5 to 8 where the regeneration temperature is close to these

design values the highly temperature dependent isotherms are worse. The necessary regeneration temperature is higher and the COP is lower. At higher NTUs the graphs are reversed and the highly temperature dependent isotherms become better. A closer look at Figure 5.11/5.10 shows that the artificial isotherms operate at NTUs above 12 with regeneration temperatures below 60°C. The regeneration temperature remains higher for all cases regardless of NTU for the more temperature affected shapes.

Figure 5.12 illustrates the correlations for the artificial silica gel set implemented in the open Dunkle cycle for Chicago design conditions. Since the Dunkle cycle shows the same pattern as the ventilation cycle the Dunkle cycle is not included in the following investigations.

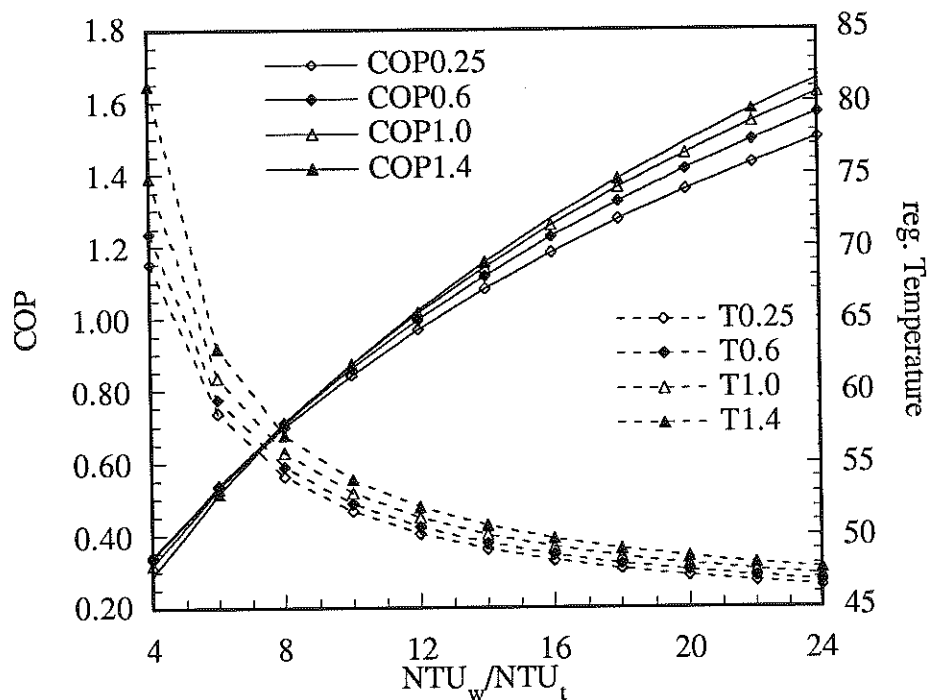


Figure 5.12. COP Silica Gel Isotherm Set, Dunkle Cycle, Chicago Design

#### 5.4.2 Variation of the Isotherm Shape with Respect to Ambient Conditions

In this section the same simulation procedure as in section 5.3.2 is applied for the various isotherm shapes. Figure 5.13 shows the COP and regeneration temperature of the

ventilation cycle with an increase of the ambient temperature at constant relative humidity.

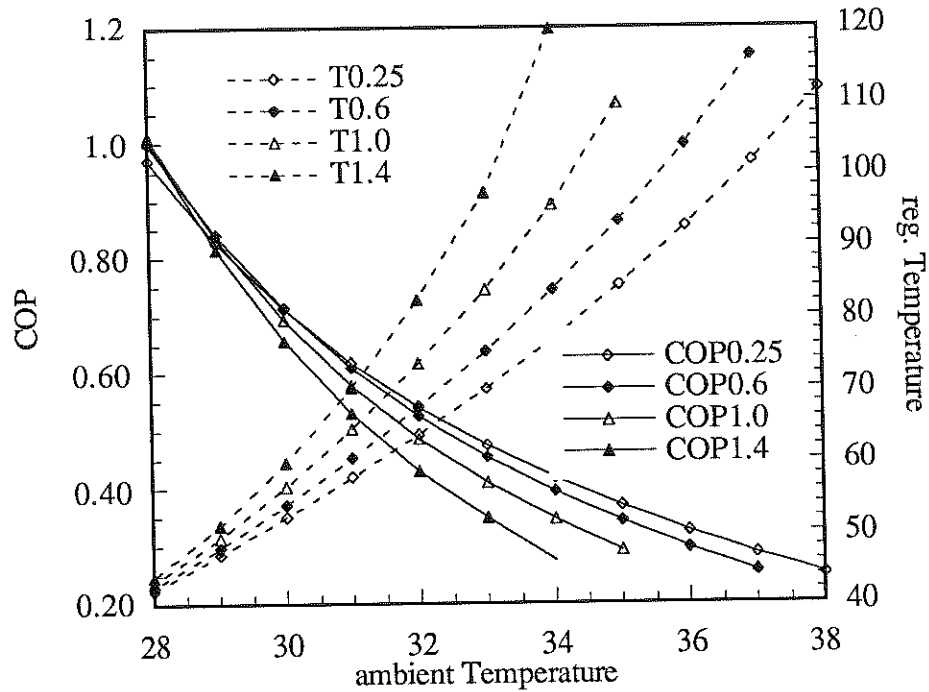


Figure 5.13 Variation of Ambient Temperature for Various Isotherm Shapes

In this case the highly temperature dependent isotherms perform worse at tougher ambient conditions and perform better at conditions where the difference between ambient and room state is small.

#### 5.4.3 Variation of the Isotherm Shape with Respect to the Room Inlet State

Figure 5.14 illustrates the COP and regeneration temperature depending on the enthalpy difference between room state and room inlet state for the Chicago design conditions.

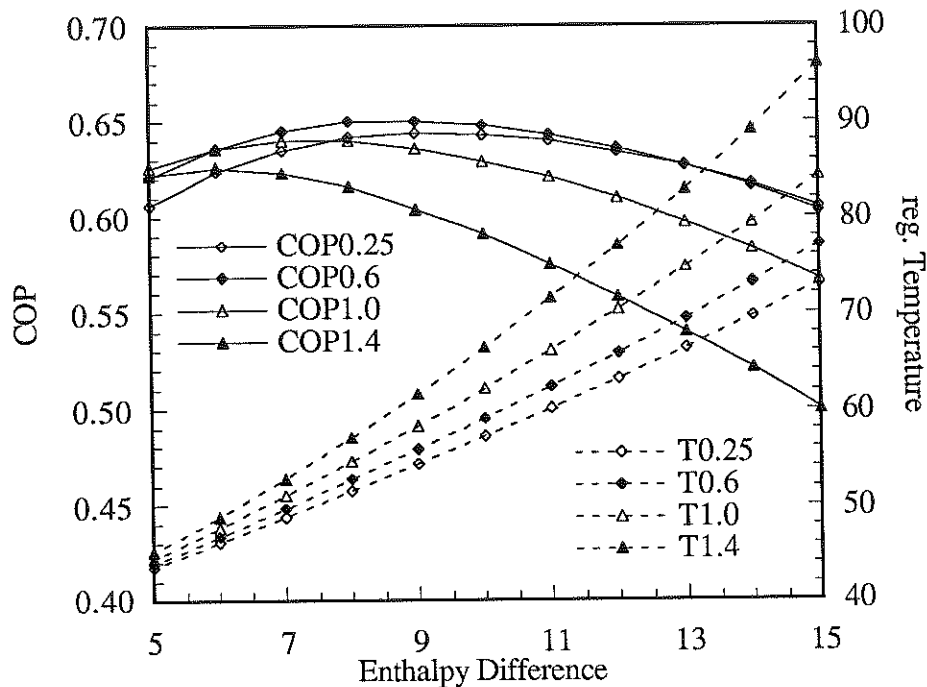


Figure 5.14 Enthalpy Difference Variation for Different Shapes at Chicago Design

The graph above supports the general tendency that at higher enthalpy difference between the ambient and the room inlet state the highly temperature dependent isotherms become worse. Here, the slightly more on temperature depending isotherm with  $dh^*=0.6$  produces the highest COPs for all conditions.

#### 5.4.4 Assessment of the Simulation Results and Interpretation

The graphs above show all the same pattern: at a low regeneration temperature the COP of the cooling cycles is high for highly on temperature dependent isotherms. The isotherms with small  $dh^*$  work much better at more difficult ambient conditions or with smaller equipment.

At design regeneration temperatures (30-40°C for the adsorption step and 60-70°C for the regeneration step) the highly temperature dependent isotherms are always worse.

The cause for this unexpected behavior of the temperature dependent isotherms can be understood by looking at the temperature of the dehumidifier outlet of the process stream. With increasing  $dh^*$  (temperature dependence) the outlet temperature increases. Table 5.5 shows the regeneration temperature  $T_{rg}$ , process stream outlet temperature  $T_{pr}$ , and COP with respect to the isotherms depending on temperature for three different NTUs.

<i>NTU 6/dh*</i>	<i>COP</i>	<i>T<sub>rg</sub></i>	<i>T<sub>pr</sub></i>
0.25	0.377	69.11	52.14
0.6	0.352	74.30	55.72
1.0	0.303	84.58	63.42
1.4	0.217	110.28	80.79
<i>NTU 10/dh*</i>	<i>COP</i>	<i>Trg</i>	<i>Tpr</i>
0.25	0.642	57.23	46.53
0.6	0.646	59.12	48.92
1.0	0.628	62.20	52.09
1.4	0.589	66.53	56.04
<i>NTU 20/dh*</i>	<i>COP</i>	<i>T<sub>rg</sub></i>	<i>T<sub>pr</sub></i>
0.25	1.048	50.64	43.52
0.6	1.111	51.40	44.94
1.0	1.152	52.61	46.62
1.4	1.167	54.11	48.38

*Table 5.5 SERI Approximation Dehumidifier Outlet Temperatures*

The higher outlet temperature has several impacts on the performance of the cooling cycles. The most obvious is that the process stream which is used for cooling is hotter after the dehumidifier and has to be cooled down more by the sensible heat exchanger. Some heat cannot be transferred from the hot process outlet to the regeneration side due to the finite heat exchanger effectiveness. Thus, the higher temperature increases the cooling load on the process side and the heater load on the regeneration side.

The other problems involved with the higher outlet temperature are caused by thermodynamic relationships. Near the dehumidifier outlet of the process stream the relative humidity which is the driving force for the adsorption process becomes lower at the

same absolute humidity with higher temperatures. Therefore the adsorption process gets very ineffective at the end of the dehumidifier. The isotherm shape which is beneficial at the inlet temperature of the adsorption side of the dehumidifier switches with the increasing air and matrix temperature in flow direction from a Type 1 more towards a Type 3 at the end of the dehumidifier. In other words, most of the mass exchange of the dehumidifier occurs at the beginning of the dehumidifier right after the inlet where the air temperature is low, the relative humidity is high, and the isotherm has a beneficial Type 1 shape for the adsorption step. At the end of the humidifier is the relative humidity of the air very low, the air temperature very high and the isotherm shape switches with the increasing temperature towards a shape which is more preferable for regeneration than for adsorption. In summary; the benefit of the isotherm shape is more than offset by the higher dehumidifier outlet temperature.

At very high NTU numbers or at a low cooling load (small enthalpy difference between room state and ambient state or low enthalpy difference between room and room inlet) the necessary regeneration temperatures are low and the temperatures of the process outlet is not much higher than the inlet. Thus, the temperature dependent isotherms operate in a range where the shapes do not change much, the effects of the higher outlet temperatures are small, and the highly temperature dependent isotherms have a Type 1 extreme shape on average (the dehumidifier operates always below 50°C). The Type 1 extreme with a very high water uptake at low relative humidity supports the adsorption step at the end of the dehumidifier more than the opposite effects of the higher outlet temperature. In the case of very high NTU the effect of the high temperature at the outlet is further diminished by a very high heat exchanger effectiveness.

Figure 5.15 and 5.16 illustrate the outlet state of a balanced dehumidifier for various rotational speeds in terms of  $\Gamma$  (equation 4.5) for the SERI approximation with  $dh^*=0.25$ , and  $dh^*=1.4$ , respectively. The chosen inlet states of the regeneration stream

(hot stream) and of the process stream (cold stream) are similar to a typical simulation of a ventilation cycle at Chicago design conditions.

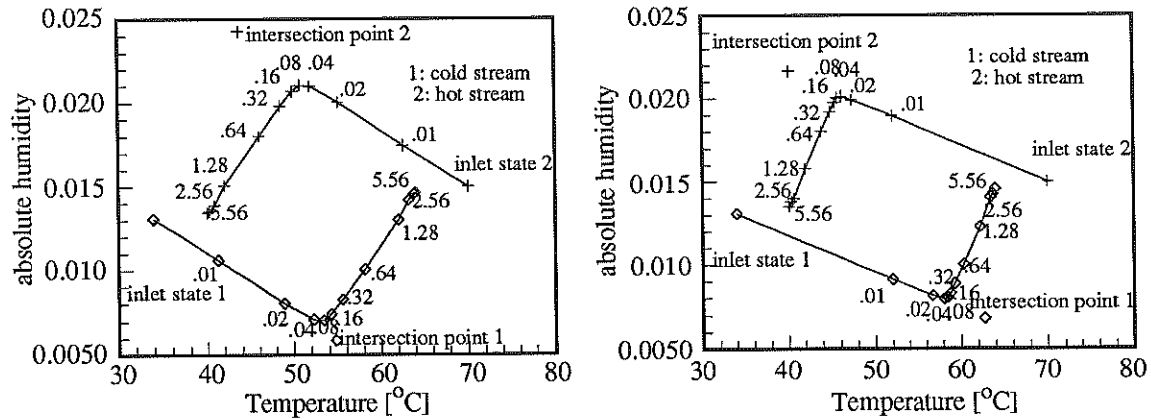


Figure 5.15 SERI Approximation,  $dh^*=0.25$  Figure 5.16 SERI Approximation,  $dh^*=1.4$

The graphs above show that with increasing temperature dependence the optimum rotation speed for the dehumidification is lower and the maximum possible outlet state which can be reached with infinite transfer coefficients in the case of isotherms with a high value for  $dh^*$  is hotter and more moist. (Intersection point 1, outlet state with infinite transfer coefficients).

#### 5.4.5 The Heat of Adsorption and Isotherm Shape

In Chapter 3 the Jurinak formulation is derived from the Clausius-Clapeyron equation. The result is a thermodynamic relationship between the ratio of the heat of adsorption to the heat of vaporization and the isotherm shape change due to a temperature change. The isotherms that are highly dependent on temperature must have a  $\frac{h_S}{h_{VL}}$  ratio which is essentially higher than one.

This is a result of the application of the Second Law of Thermodynamics to the adsorption process; the Clausius-Clapeyron equation is derived from a Second Law analysis. There is no way to change an isotherm shape from a Brunauer Type 1 at

adsorption temperature to a Brunauer Type 2 at regeneration temperature without an increase in the heat of adsorption.

This means that the temperature difference between the dehumidifier inlets and outlets increases with the temperature dependency of the isotherm shapes since the temperature difference is proportional to the amount adsorbed (desorbed) and to the heat of adsorption.

#### **5.4.6 Summary of the Performance of the Theoretical Isotherms based on the SERI/ NREL Results**

The highly temperature dependent isotherms are not beneficial for adiabatic rotary dehumidifiers since the process stream outlet temperatures are always higher. For all usual applications the COP is lower and the regeneration temperatures are always higher. Only in some special cases, (large NTU, low ambient enthalpy, or low difference between room and room inlet states) where the regeneration temperature is very low, does the temperature dependence result in higher COPs. Even at these special situations the improvement of the COP is not directly a result of the temperature dependence, but a result of the beneficial impact of the Type 1 extreme isotherm shape which is created at lower temperatures by the temperature dependency. Furthermore the limit for the ambient conditions which can be handled by a cooling cycle is lower and the dependence on the ambient state of the COP and of the regeneration temperature increases dramatically.

The measured base shape of PSSASS is beneficial for desiccant cooling applications since the isotherm has a relatively high water uptake at low relative humidity and is therefore closer to a Brunauer Type 1 than regular silica gel which has a more linear isotherm shape. The difference between the base shape for silica gel and the base shape for PSSASS is in the range of one to two percent. This is negligible compared to the major impact of equipment size and inlet state on performance.

### 5.5 New Cooling Cycles with Staged Dehumidification

The principal problem of all adiabatic dehumidifiers is the fact that the process stream heats up during the adsorption process. The relative humidity which is responsible for the adsorption potential is therefore reduced not only due to the smaller absolute humidity at the end of the dehumidifier but also due to the temperature increase of the process air. One approach to overcome this problem is the method of staged adsorption.

In this study two different approaches in dehumidifier design and cooling cycle configuration are discussed.

The first cycle with staged dehumidification works with two dehumidifiers and two heat exchangers. The dehumidifier can be designed in a way that both dehumidifiers operate with only one wheel. Figure 5.17 illustrates one possible design for the face of the regenerator wheel with the nozzles for the inlets and outlets. In the following sections this dehumidifier type is called Four Way dehumidifier.

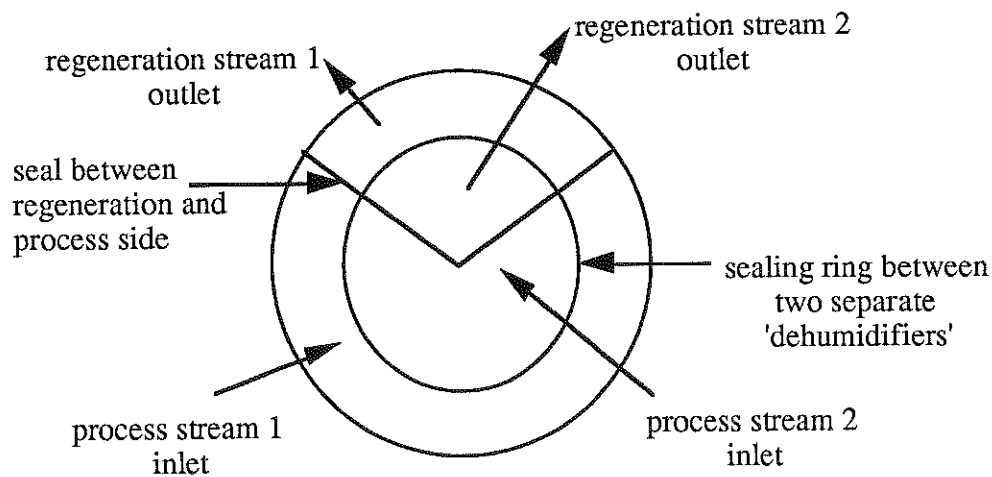


*Figure 5.17 Inlet and Outlet Nozzles of a Four Way Dehumidifier Wheel*

The wheel is divided into two parts for the process side and one part for the regeneration side. This method is chosen in order to achieve equal NTU for all air streams.

Since the regeneration stream is split into two equal streams the regeneration side needs only half the transfer area for the same NTUs. (compare equation 4.12, 4.13)

In the schematic diagram the four way dehumidifier wheel is separated into two dehumidifiers for more clarity.

The other approach uses a dehumidifier with three inlets, one inlet on the regeneration side, and two inlets on the process stream side. This dehumidifier configuration is described in detail in Chapter 4. In the following sections this dehumidifier type is called Three Way dehumidifier.

Both systems for staged dehumidification work with the same principle. After the process stream leaves the dehumidifier the first time, it is cooled down by a heat exchanger. The heat sink of this heat exchanger is the ambient temperature. At the outlet of the first dehumidifier the process stream has almost ambient temperature and reenters the dehumidifier for further regeneration. The rest of the cooling cycle is a regenerative evaporative cooler component with the wet bulb temperature of the room state as the heat sink of the sensible heat exchanger.

The major difference of these dehumidifier configurations is the regeneration principle. The dehumidifier with the three inlets which separates the wheel area into three sections works one regeneration stream, whereas the configuration with two dehumidifiers has to share the regeneration stream between the dehumidifiers. The Four Way arrangement has the advantage of counter flow for both process streams. In the case of the Three Way dehumidifier the matrix is already loaded when the process stream passes the dehumidifier the second time. This makes the second stage of this dehumidifier less effective. Figure 5.18 illustrates the schematic diagram of the open configuration with two dehumidifiers. An alternative closed link of this configuration is achieved by a connection of the heat exchanger outlet (state 9) with the dehumidifier inlet (state 1).

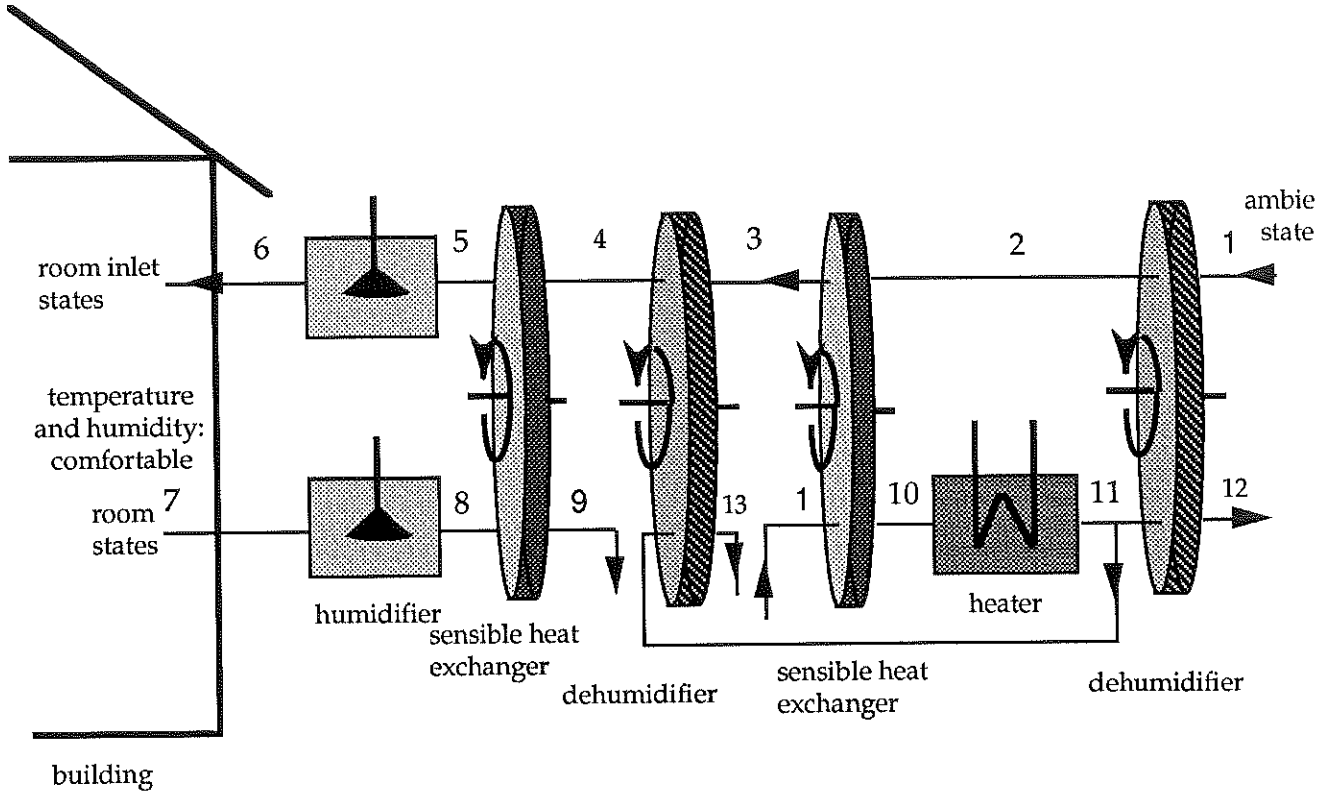


Figure 5.18 Open Cycle with Staged Dehumidification and a Four Way Dehumidifier

Figure 5.19 shows the schematic diagram of the cycle with the dehumidifier with two process streams and one regeneration stream. The closed variant can be converted into an open system by disconnecting the heat exchanger outlet with the dehumidifier inlet and by feeding the dehumidifier inlet with ambient air.

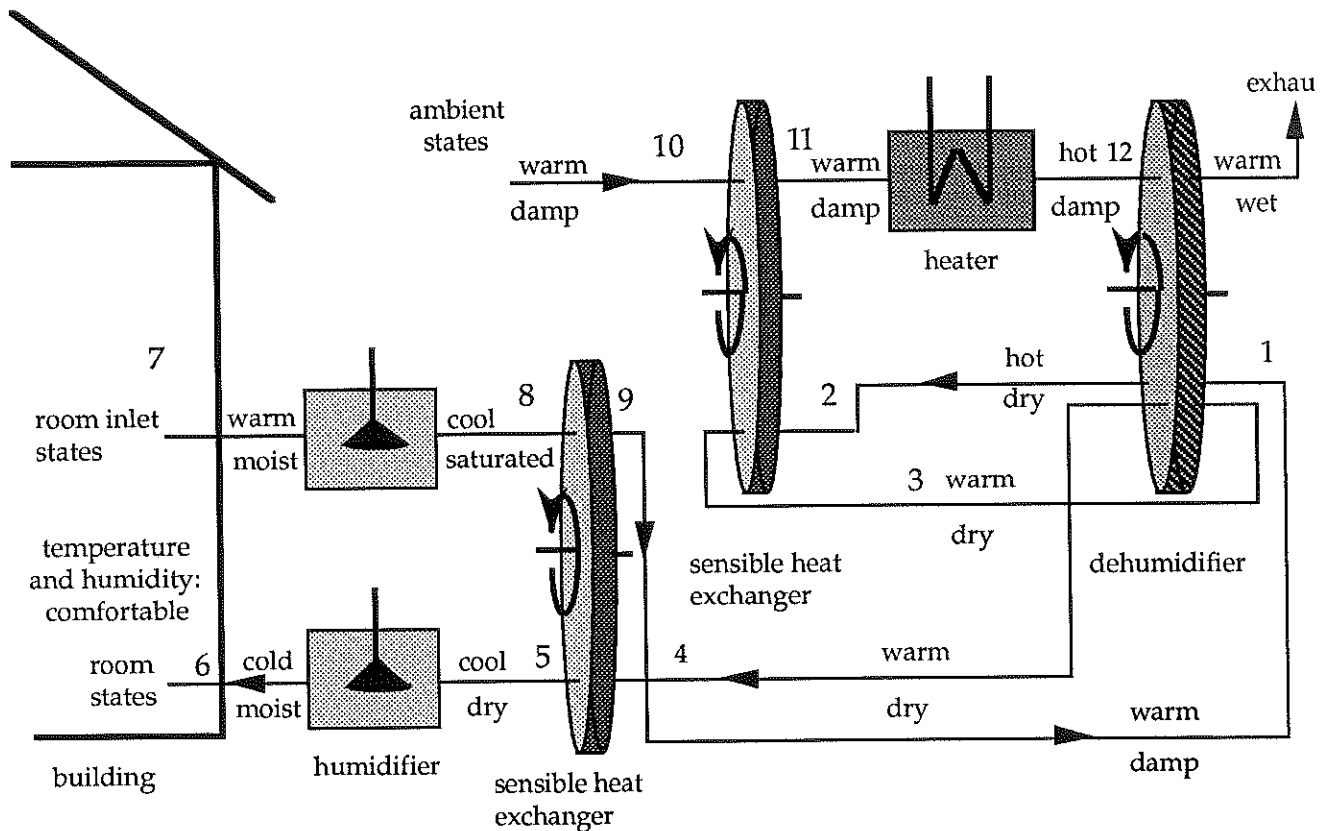


Figure 5.19 Closed Cycle with Staged Dehumidification and a Three Way Dehumidifier

### 5.5.1 Simulation Results of the New Cooling Cycles

This section gives the results of the simulations for the Los Angeles, Chicago, and Miami design condition. The system comparisons are based on the open/closed Dunkle cycle with NTUs for heat exchanger and dehumidifier equal to 10. The resulting transfer area for the dehumidifier is split between the Three Way and Four Way dehumidifier. The effective NTUs which lead to the same total transfer area of the Four and Three Way dehumidifier are equal to 6.67.

COP/ Location	open Dunkle	closed Dunkle	open 4 Way	open 3 Way	closed 3 Way
Los Angeles	1.27	0.688	10.75	12.78	0.805
Chicago	0.723	0.697	0.735	0.868	0.627
Miami	0.572	0.666	0.372	0.443	0.529
$T_{rg}/$ Location					
Los Angeles	38.1	55.7	35.2	35.1	58.8
Chicago	58.5	58.3	52.6	52.0	62.6
Miami	66.7	60.2	70.4	70.1	64.7

*Table 5.6 Simulation Results For the Different Dehumidifiers*

These simulation results are unexpected since the staged dehumidification is primarily designed for high ambient humidity. The simulations show the opposite trend. The open cycles with the Four or Three Way dehumidifiers operate with very high COPs for the Los Angeles Design conditions, whereas the COPs for the Miami design conditions are smaller.

Both dehumidifier configurations have the same problem. Only the heat of adsorption of the first stage can be recovered by the heat exchanger; the adsorption enthalpy of the second stage is always dumped to the ambient (state 9). At higher ambient humidity the second stage works better and therefore the energy which is dumped increases. The very large COPs at low ambient humidity compared to the open Dunkle cycle are difficult to explain since the regeneration and process stream states do not change much during the adsorption/desorption process.

These first results for desiccant cooling cycles with staged dehumidification show the possibility for further improvement of cooling cycles without an increase of the equipment size. The cycles described here are still far away from the optimum COP which can be reached with these configuration for specific ambient conditions. Possible parameters which could be varied are the size of the second stage, the regeneration mass-flow, and the distribution of the regeneration stream between stage one and two.

### 5.5.2 Staged Dehumidification Conclusions

Staged dehumidification is beneficial for the thermal COP of a desiccant cooling cycle even at the same total size of the dehumidifier compared to a Dunkle cycle for conditions with a small enthalpy difference between ambient state and room state.

Higher ambient humidity and a higher related ambient enthalpy lead to a worse performance of the cycles with staged dehumidification. The decrease in the performance is mainly caused by the creation of unrecoverable waste energy streams dumped to the ambient.

The possibilities and limits are still unknown and more future work is necessary to understand the cause for the high dependency of the performance from ambient conditions.

---

## Chapter six

---

### Results and Conclusions

#### Thermodynamic Analysis

The thermodynamic analysis of the isotherm measurements taken by SERI indicates that either the measurements are incorrect since they violate the second Law of Thermodynamics or that the differential heat of adsorption has a large negative value. A negative heat of adsorption requires an endothermic reaction between water vapor and desiccant surface, and does not follow the law of physical adsorption.

#### The Isotherm Formulations

The Dubinin-Polanyi isotherm formulation can be applied only for adsorbents where the temperature dependence of the shape follows the theory of the adsorption potential. This theory does not apply for highly temperature dependent isotherm shapes.

The polynomial Jurinak formulation allows the simulation of almost every isotherm shape. The temperature dependence is a result of the thermodynamic relationship stated by the Clausius-Clapeyron equation between heat of adsorption and isotherm shape. The formulation obeys the Second Law of Thermodynamics since it is derived from a Second Law relationship.

The approximation with this formulation for the basic shape of the SERI measurements for PSSASS is close to the measured values in the range which is important for desiccant cooling application. The approximation provides a good base for the compari-

son between silica gel and PSSASS isotherm. Furthermore with the polynomial Jurinak formulation isotherms can be modeled which fulfill all the requirements of a 'optimum' isotherm with a Type 1 shape for the adsorption step and a Type 2 shape at regeneration temperature.

In the simulations the Dubinin-Polanyi isotherm formulation for regular silica gel and the approximation of this formulation with the Jurinak polynomial expression are so close that the highest difference in the regeneration temperature is in the range of 1°C and the coincident COP is off only 1%. This result shows that the polynomial curve fit is close enough and that both formulations can be exchanged without major effect on the simulation results. Furthermore this gives confidence in the program code.

#### The System Component Models

The dehumidifier model with its assumptions is widely used and the validity of the numerical results is proven by experiments (Van den Bulck 1987).

The MOSHMX program code allows the simulation of an adiabatic rotary dehumidifier. The main features are accuracy, flexibility in terms of convergence criteria /method, and simplicity due to the auto discretization routines. The MOSHMX program code has the disadvantage of a high CPU consumption and is not applicable for long term system simulations.

The rotary regenerative heat exchanger model is based on an effectiveness model. The heat exchanger effectiveness is a curve fit of measured and of simulated data. The exactness of this model is not critical for the solutions in a desiccant cooling cycle since the resulting heat exchanger effectiveness can be used for system comparisons as well as the input parameters NTU and  $\Gamma$ .

The humidifier model is very simple and flexible. It is not based on an effectiveness model or NTU correlations.

### The Cooling Cycles

The classical cooling cycles ventilation and recirculation cycle work always with low COPs. At low ambient humidity the ventilation cycle is better than the regeneration cycle. The low performance is caused by the increase of the necessary regeneration temperature due to the humidity increase of the regeneration stream. This increase in humidity is necessary in order to provide a deeper heat sink for the sensible heat exchanger. The open Dunkle cycle does not increase the humidity of the regeneration stream and operates like an evaporative cooler with a dehumidifier in front which is able to reduce the humidity alone without temperature increase. This fact is a thermodynamic advantage compared to the simple cycles which might predominate the disadvantage of one additional heat exchanger. Furthermore the option to operate the Dunkle cycle open, closed, or in any combination gives enough flexibility to adjust this cycle for a variety of ambient conditions and indoor air quality requirements.

A reduced mass flow of the regeneration stream relative to the process stream is beneficial for the COP of all cycles. For gas fired regeneration equipment any improvement of the COP is beneficial for the cooling machine performance. Another advantage of the reduced mass flow through the regeneration side is the fact that the actual dehumidifier size decreases with decreasing mass flow at constant NTU (equation 4.13). When the regeneration energy is provided by a solar system the advantage of a lower regeneration temperature might predominate the disadvantage of more total energy consumption. In this case the balanced dehumidifier is preferred.

## Temperature Dependent Isotherms

The Clausius Clapeyron equation states that a desiccant isotherm shape changes with temperature only due to a difference between the differential heat of adsorption and the heat of vaporization. There is no way to change an isotherm shape from a Brunauer Type 1 at adsorption temperature to a Brunauer Type 2 at regeneration temperature without an increase in the heat of adsorption. This means that the temperature difference between the dehumidifier inlets and outlets increases with the temperature dependency of the isotherm shapes since the temperature difference is proportional to the amount adsorbed (desorbed) and to the heat of adsorption.

The highly temperature dependent isotherms are not beneficial for adiabatic rotary dehumidifiers since the process stream outlet temperatures are always higher. For all usual applications the COP is lower and the regeneration temperatures are always higher. Only in some special cases, (large NTU, low ambient enthalpy, or low difference between room and room inlet states) where the regeneration temperature is very low, does the temperature dependence result in higher COPs. Even at these special situations the improvement of the COP is not directly a result of the temperature dependence, but a result of the beneficial impact of the Type 1 extreme isotherm shape which is created at lower temperatures by the temperature dependency. Furthermore the limit for the ambient conditions which can be handled by a cooling cycle is lower and the dependence on the ambient state of the COP and of the regeneration temperature increases dramatically.

The measured base shape of PSSASS is beneficial for desiccant cooling applications since the isotherm has a relatively high water uptake at low relative humidity and is therefore closer to a Brunauer Type 1 than regular silica gel which has a more linear isotherm shape. The difference between the base shape for silica gel and the base shape for PSSASS is in the range of one to two percent. This is negligible compared to the major impact of equipment size and inlet state on performance.

## Staged Dehumidification

Staged dehumidification is beneficial for the thermal COP of a desiccant cooling cycle even at the same total size of the dehumidifier compared to a Dunkle cycle for conditions with a small enthalpy difference between ambient state and room state.

Higher ambient humidity and a higher related ambient enthalpy lead to a worse performance of the cycles with staged dehumidification. The decrease in the performance is mainly caused by the creation of unrecoverable waste energy streams dumped to the ambient.

The possibilities and limits are still unknown and more future work is necessary to understand the cause for the high dependency of the performance from ambient conditions.

## Appendix A

### The Nature of Physical Adsorption

This appendix reviews the general principles of physical adsorption. The following description and discussion is based on a literature review done by Eric van den Bulck (1986). His description of the phenomena of adsorption is brief and exact. Thus, the important parts of his discussion are quoted here.

Definitions: The (ad)sorptive is the adsorbable gas, the (ad)sorbent is the adsorbing solid and the adsorbed phase is the (ad)sorbate.

Physical adsorption is a natural phenomena which occurs whenever a gas or liquid is in contact with a solid. Molecules of the gaseous or liquid phase attach to or detach from the surface of the solid in a dynamic transfer-exchange process. The adsorbed molecules accumulate on the surface and form an interfacial layer which has properties similar to those of the liquid or condensed phase of the adsorptive.

Physical adsorption is generally distinguished from chemisorption. In the first process, attraction between the individual molecules of the adsorbate and the adsorbent surface is the result of weak forces and the sorption is reversible. In the latter process, individual molecules react chemically with each other and the formation of the resulting process is irreversible. The main feature of chemisorption is its high heat of sorption which is similar to the heat of chemical reaction. For physical adsorption of gases by solids, the heat of sorption is of the same magnitude as the heat of condensation.

Adsorption is the result of various physical forces between the sorbate and sorbent molecules. These forces always include dispersion forces, which are attractive forces, and short range repulsion forces. These intermolecular forces which, in the case of pure

substances, produce the phase change from gas to liquid. If the molecules are polar (water is a very polar molecule), or/and if the solid has an ionic structure (zeolites, SERI Polymers) , additional strong intermolecular forces arise. The work produces by these combined forces is the heat of adsorption. In the presence of electrostatic forces, the heat of sorption is increased significantly.

The adsorbents discussed by SERI have the same structure as strong acid ion exchange resins. The base structure Polystyrene sulfate sodium salt (PSSA) with the  $\text{SO}_3^-$  group attached to each phenyl group is the best sample for an ionic structure. Thus, theory predicts that these desiccants must have a high heat of adsorption.

## Appendix B

### Program Description

Section B.4 contains additional information for the last versions of MOSHMX, and the simulation program SIMUTYPES

#### B.1 Input Files for Use with CYCLETYPES and SIMUTYPES

##### B.1.1 CYCLE.IN

This file contains the parameters for one cooling cycle run.

1.line: ambient pressure [Pa], specific heat capacity of air [J/kgC]

2.line: (room states); temperature [°C], abs. humidity [kg water/kg dry air], relative humidity, wet bulb temperature [°C]

Comment: It is only one specification for the humidity necessary. Unknown specifications are set to zero.

3.line: (room inlet states); temperature[°C], abs. humidity [kg water/kg dry air], relative humidity, wet bulb temperature [°C], enthalpy difference between room states and room inlet states [J/kg], ratio sensible load/ total load.

Comment: When the enthalpy difference and load ratio is specified, the program calculates temperature and humidity for the room inlet in dependence of the room states.

4.line: (ambient states); same as 2.line

5.line: humidifier specification; temperature of the liquid water added [°C], reached relative humidity of the humidifier at the room outlet.

6.line: simulation specifications; low temperature, high temperature, delta temp., cycletype(integer), print(integer)

Explanation: low temperature; This temperature is the lower limit for the regeneration temperature.

high temperature: This temperature is the upper limit for the regeneration temperature .

delta temp. : search interval length

The program tries to find between these limiting temperatures a regeneration temperature for which the cycle produces demand exceeding room inlet air properties. As soon as a solution is found within the interval, a Newton iteration is started in the middle of the last search interval. For most practical applications it is sufficient to set low and high temperature at the same high value. The program checks then the highest temperature and starts a Newton iteration at high temperature - delta temp./2. Deltatemp. = 0 results in a Newton iteration at low temperature (tguess).

cycletype:        1: ventilation cycle  
                   2: regeneration cycle  
                   3: ventilation + regeneration cycle  
                   4: no dehumidifier (only heat exchanger)  
                   5: closed Dunkle cycle  
                   6: experimental cycle

print:            0: only final result is printed on the screen  
                   1: full information during on simulation run  
                   2: initial states (ambient, room, demanded room inlet states),  
                   print of the solution without dehumidifier, final results  
                   Comment: When the moshmx solution is switched on  
                   messages from the finite difference iteration process are  
                   printed on the screen.

7.line: name of the output file for the results.

## B.1.2 DEHUMIDIFIER.PAR

This file contains the specifications of the dehumidifier in a cycle for use with MOSHMX and ANALOGY.

1:line: specific heat capacity of the dehumidifier wheel [J/kgC], desiccant specification number (integer), heat capacity formulation for desiccant wheel (integer), solution type (integer), precision for polynomial solution (integer).  
 Comment: The desiccant specification number Ides selects different isotherm shapes and formulations.

Ides in the range form            10 to 19 : Dubinin Polany two sided isotherm  
    20 to 29 : Collier - Jurinak formulation  
    30 to 39 : Collier - Jurinak - Polynomial

In the case that Ides is set to 39 the isotherm parameters are read from the file DESICCANT.PAR. The polynomial formulation is similar to the Collier - Jurinak formulation. The polynomial expression is a polynomial 5.th order. The first constant coefficient of a polynomial 5.th order is skipped due to the fact, that isotherms always satisfy the condition that at zero relative humidity the water content of the desiccant is zero.

form: rel. humidity at ref. temp. =  $aW^* + bW^{*2} + cW^{*3} + dW^{*4} + eW^{*5}$

$W^*$  := equilibrium desiccant water content/ maximum water content

(Jurinak formulation :  $G(W^*) = \text{polynomial 5.th order}$ )

Imat: = 0; specific heat capacity is constant; Imat: = 1; heat capacity is a function of temperature formulation prepared in subroutine desset (propsa.for) but not supported.

solu: = 1; dehumidifier solution model : analogy solution

solu: not 1; dehumidifier solution model : finite difference solution (moshmx)

Iprecision: only with polynomial solution effective (Ides: 30 to 39)

Iprecision: = 0; isotherm formulation in single precision

Iprecision: = 1; isotherm formulation in double precision

2.line: number of transfer units for the "cold" stream, NTU for the "hot" stream; index 1: cold inlet; index 2: hot inlet

3.line: Lewis number for cold/hot stream

4.line:  $\Gamma_j$ , dimensionless matrix flow rate/air flow rate(cold/hot)

### B.1.3 MOSHMX.PAR

This file contains the parameter for a moshmx solution of a dehumidifier.

1.line: NM number of space steps, if negative determination by MOSHMX.

It is in most cases not necessary to change the auto initialization of space steps and time steps.

2. line: NF ; number of time steps first wave, second number time steps slow wave, second pair hot stream.

3.line: NFX; this parameter must be in the range of 5 to 10, if the moshmx version for three inlets is switched on.

4.line: IRICH:=1 Richardson extrapolation is performed. The moshmx program code becomes very slow!

5.line: IMTRX:=1 useful for higher gamma (gamma > 0.2)

### B.1.4 ANALOGY.PAR

1.line: reverence stream ;1 or 2; no significant effect on solution.

2.line: Ieff; 0 or 1; no significant effect on analogy solution.

### B.1.5 DESICCANT.PAR

This file is read if Ides in file DEHUMIDIFIER.PAR is equal to 39!

1.line: name of desiccant

2.line: maximum water content

3.line: reference temperature ; The isotherm shape is exactly equal to the polynomial formulation at this temperature. The ratio water vapor saturation pressure at isotherm temperature to water vapor saturation pressure at reference temperature equals one. (compare Collier - Jurinak formulation)

4.line:  $dh^*$ ; scaling parameter for temperature dependence of the isotherm shape. A higher value of this parameter means stronger temperature dependence of the isotherm shapes. (above reference temperature lower water uptake; below reference temperature higher water uptake)

5.line: scaling parameter; always negative: range -2 to -5.

6.line: the polynomial coefficients; a, b, c, d, e .

form: rel. humidity at ref. temp. =  $aW^* + bW^{*2} + cW^{*3} + dW^{*4} + eW^{*5}$

### B.1.3 DESTEST.PAR

This file contains the parameters for an isotherm check and a single dehumidifier test.

1.line: isoshape: = 0; A cooling cycle simulation is calculated by the program CYCLETYPS.

isoshape: = 1; The water content and the partial derivative  $dW_{\text{desiccant}}/dT_{\text{isotherm}})_w$  of a desiccant selected by Ides is calculated with respect to relative humidity. Range for rel. humidity: 0% to 100% rel. humidity. The result is save on the file PLOTISOTHERM.DAT.

isoshape: = 2; A dehumidifier test with the current specifications is performed for increasing gamma. (with moshmx the calculation might be CPU consuming)

2.line: plot temperature of the calculated isotherm shape for the isotherm check, relative humidity step size [%]

3.line: inlet temperature of the cold/ hot stream for the dehumidifier test

4.line: inlet abs. humidity of the cold/ hot stream.

## B.2 Description of the Fortran Program Files

### B.2.1 CYCLETYPS.FOR

This file contains the main program cycletyps, the procedures for the different cooling cycle calculations, the routines for the isotherm check and dehumidifier test and the output procedure.

#### B.2.1.1 Main Program CYCLETYPS

##### Features:

- reads all input files with the exception of the file DESICCANT.PAR which is read by the Isotherm initialization routine DESSET.
- computes the input conversions for the properties of the ambient state, room state and room inlet state.
- calls routine DESSET for the initialization of the desiccant.
- contains start initialization for the different cooling cycle types and runs the search iteration loops for ventilation, regeneration, Dunkle and experimental cycle.
- calls the dehumidifier test routine or isotherm check routine.
- calls the final output routine.

#### B.2.1.2 Subroutine VEN\_CYCLE

##### Features:

- contains a whole ventilation cycle

- calls the routines for the simulation of a sensible heat exchanger, dehumidifier (analogy / finite element solution), humidifier.

Inputs:

- state 1: ambient (temperature, abs. humidity)
- state 6: room state (temperature, abs. humidity)
- state 9: regeneration temperature
- desired rel. humidity of both humidifiers

Outputs:

- all (1) to (10) cycle states (temperature, abs. humidity)
- state 5: The room inlet temperature is the state which is iterated by the main program. The routine meets always the specification for the relative room inlet humidity (exception: rel. humidity at humidifier inlet exceeds already desired rel. humidity at inlet).

States:

1: ambient, dehumidifier inlet; 2=3: dehumidifier outlet, sensible heat exchanger inlet; 4: sensible heat exchanger outlet, humidifier1 inlet; 5: humidifier1 outlet, room inlet; 6: room state, humidifier2 inlet; 7: heat exchanger inlet, humidifier2 outlet; 8: heat exchanger outlet, heater inlet; 9: heater outlet, dehumidifier inlet; 10: dehumidifier outlet, exhaust

### B.2.1.3 Subroutine REC\_CYCLE

Features:

- contains a whole regeneration cycle
- calls the routines for the simulation of a sensible heat exchanger, dehumidifier (analogy / finite element solution), humidifier.

- it is possible to run the regeneration side of the cooling cycle with a reduced mass flow. ( $\gamma(1) < \gamma(2)$ )

Inputs:

- state 1: ambient (temperature, abs. humidity)
- state 6: room state (temperature, abs. humidity)
- state 4: regeneration temperature
- desired rel. humidity of both humidifiers

Outputs:

- all (1) to (10) cycle states (temperature, abs. humidity)
- state 10: The room inlet temperature is the state which is iterated by the main program. The routine meets always the specification for the relative room inlet humidity (exception: rel. humidity at humidifier inlet exceeds already desired rel. humidity at inlet).

States:

- 1: ambient, humidifier2 inlet; 2: humidifier2 outlet, sensible heat exchanger inlet;  
 3: sensible heat exchanger outlet, heater inlet; 4: heater outlet, dehumidifier inlet;  
 5: dehumidifier outlet, exhaust;  
 6: room state, dehumidifier inlet 7=8: dehumidifier outlet, sensible heat exchanger inlet;  
 9: heat exchanger outlet, humidifier1 inlet; 10: humidifier1 outlet, room inlet.

#### B.2.1.4 Subroutine DUNKLE\_CYCLE

Features:

- contains a whole Dunkle cycle
- calls the routines for the simulation of a sensible heat exchanger, dehumidifier (analogy / finite element solution), humidifier.

- it is possible to run the regeneration side of the cooling cycle with a reduced mass flow. ( $\gamma(1) < \gamma(2)$ )

#### Inputs:

- state 1: ambient (temperature, abs. humidity)
- state 5: room state (temperature, abs. humidity)
- state 7: outlet heat exchanger2, inlet dehumidifier
- state 3: regeneration temperature
- desired rel. humidity of both humidifiers

#### Outputs:

- all (1) to (11) cycle states (temperature, abs. humidity)
- state 7; inlet temperature of the cold stream in the dehumidifier must be guessed. Therefore, the routine Dunkel\_cycle is called by the iteration routine iter\_cycle first in order to close the cooling loop with a Newton iteration and to gain T(7).
- state 11: The room inlet temperature is the state which is iterated by the main program. The routine meets always the specification for the relative room inlet humidity (exception: rel. humidity at humidifier inlet exceeds already desired rel. humidity at inlet).

#### States:

1: ambient, sensible heat exchanger1 inlet; 2: sensible heat exchanger2 outlet, heater inlet; 3: heater outlet, dehumidifier inlet; 4: dehumidifier outlet, exhaust; 5: room state, humidifier2 inlet; 6: humidifier2 outlet, sensible heat exchanger2 inlet; 7: heat exchanger outlet, dehumidifier inlet; 8: dehumidifier outlet, sensible heat exchanger1 inlet; 7: heat exchanger1 outlet, heat exchanger2 inlet; 10: heat exchanger2 outlet, humidifier1 inlet; 11: humidifier1 outlet, room inlet.

#### B.2.1.5 Subroutine NO\_DEHUM\_CYCLE

#### Features:

- contains a cycle with a sensible heat exchanger
- calls the routines for the simulation of a sensible heat exchanger, humidifier.

Inputs:

- state 1: ambient (temperature, abs. humidity)
- state 4: room state (temperature, abs. humidity)
- desired rel. humidity of both humidifiers

Outputs:

- all (1) to (6) cycle states (temperature, abs. humidity)

States:

- 1: ambient, sensible heat exchanger inlet; 2: sensible heat exchanger outlet, humidifier2 inlet; 3: humidifier2 outlet, room inlet.
- 4: room state, humidifier1 inlet; 5: humidifier1 outlet, sensible heat exchanger inlet; 6: heat exchanger outlet, exhaust.

#### B.2.1.6 Subroutine EXP\_CYCLE

This cycle is only an experiment. It contains two dehumidifiers, heat exchangers and two or three humidifiers.

Gamma(2) must be in the range of two times gamma(1), since the regeneration stream is split.

#### B.2.1.7 Subroutine ITER\_CYCLE

This routine contains the iteration routine for T(7) in a Dunkle cycle.

#### B.2.1.8 Subroutine ISOPLOT

This routine calculates the desiccant water content for a specified desiccant with respect to relative humidity. The results are save in the file PLOTISOTHERM.DAT.

Output format: first column: rel. humidity; second column: equilibrium desiccant water uptake; third column: partial derivative  $dW_{\text{desiccant}}/dT_w$

#### B.2.1.9 Subroutine DEHUMIDIFIER

This routine performs a dehumidifier test for increasing gamma.

Output: The results are printed on a file with a name specified in the input file CYCLE.IN. Format: 1. column: gamma, 2. column: temp. cold stream out, 3. column: abs. humidity cold out, 4. column: temp. hot steam out, 5. column: abs. humidity out.  
last line: intersection points.

#### B.2.2.10 OUTPUT

This routine creates an reasonable output on screen as well as on an output file with the name specified in CYCLE.in.

#### B.2.2 SENSIBLE.FOR

This file contains the routines for the calculation of a sensible heat exchanger.

#### B.2.3 HUMIDIFIER.FOR

Model of an adiabatic humidifier. The relative humidity of the out let has to be specified. If the inlet humidity is higher than the desired outlet humidity the humidifier is treated as a simple tube.

#### B.2.4 ANALOGY.FOR

Model of a dehumidifier, analogy solution; intersection point effectiveness model.

#### B.2.5 MOSHMX.FOR

Model of a dehumidifier, finite difference solution. This routine calls the analogy solution first in order to gain a first guess for the finite difference solution.

Inputs: SIN(1,1) temp. cold inlet; (1,2) temp. hot inlet; (2,1) abs. humidity cold inlet; (2,2) abs humidity hot inlet.

Pattern: first number; 1: temperature; 2: abs. humidity; 3: enthalpy  
second number; 1: cold stream; 2: hot stream

NTU(1),NTU(2),GAMMA(1),GAMMA(2),LE(1),LE(2)

Outputs: SOUT (same pattern ), EFF(1) temperature effectiveness, (2) humidity effectiveness, (3) enthalpy effectiveness

#### B.2.6 PROPSA.FOR

This file contains the routine for the initialization of a desiccant, the routines for the calculation of the matrix water content and the derivatives of the state property functions and all property calculation routines of a air / water vapor mixture.

##### B.2.6.1 DESSET

This subroutine initializes the isotherm parameters for the chosen desiccant and desiccant formulation. There are three different isotherm formulations available :

Dubini - Polany, Collier - Jurinak and a modified Collier - Jurinak - Polynomial formulation.

#### B.2.6.2 PROPMX

This routine computes the matrix equilibrium states as well as the derivatives of the state property functions in dependence of the air states.

#### B.2.6.3 PMX

This routine computes the derivatives of the state property functions in dependence of the matrix states. (water content of the matrix; temperature of the matrix) It is called by MOSHMX.

#### B.2.6.4 FNCFM

This function calculates the specific heat capacity of the matrix in dependence of temperature.

#### B.2.6.5 FHA

This function calculates the enthalpy of moist air.

inputs: temperature, abs. humidity

output: enthalpy

#### B.2.6.6 FTA

This function calculates the temperature of moist air.

inputs: enthalpy, abs. humidity

output: temperature

**B.2.6.7 FPSAT**

This function calculates the saturation pressure of water vapor.

**B.2.6.8 FDPSAT**

This function calculates:  $(aP_{sat}/dT)/P_{sat}$

**B.2.6.9 HUMREL**

This function calculates: rel. humidity =  $f(\text{abs. humidity, temperature})$

**B.2.6.10 ABSHUM**

This function calculates: absolute humidity =  $f(\text{relative humidity, temperature})$

**B.2.6.11 DRY\_BULB**

This routine calculates the relative and absolute humidity of moist air.

inputs: dry bulb temperature

wet bulb temperature

outputs: relative humidity

absolute humidity

**B.2.6.12 INSTATE\_SUB**

This routine calculates the room inlet states depended on the energy difference between room states and room inlet states ( $dh$ ) and depended on the ratio sensible load to total load.

inputs: room states

energy difference (enthalpy room states - enthalpy inlet states)

enthalpy difference due to temperature difference (sensible load) divided

by total enthalpy difference.

outputs: rel. humidity inlet

abs. humidity inlet

temperature inlet

### B.3 Description of the Output

#### B.3.1 Screen Output

When the parameter 'print' in input file CYCLE.IN is set to one, the output on the screen has the following structure:

- a) The ambient states: temperature, abs. humidity, rel. humidity
  - The room states: temperature, abs. humidity, rel. humidity
  - The room inlet specifications: temperature, abs. humidity, rel. humidity
- b) The maximum cooling with heat exchanger only
  - room inlet states: temperature, abs. humidity, rel. humidity
- c) All cycle states for every chosen regeneration temperature in order to exceed the room inlet specifications.
- d) First guess value for a Newton iteration.
- e) Regeneration temperature after Newton iteration / new guess value.
- f) Full output of the results
  - COP results
  - heat capacity of air, desiccant matrix, heat exchanger matrix
  - total pressure, enthalpy difference room states - room inlet
  - enthalpy difference heater
  - desiccant type and solution method

- for all cycle states temperature, abs humidity, rel. humidity
- the input parameters for the dehumidifier and sensible heat exchanger
- the heat exchanger effectiveness

### B.3.1 Output on File

This file has the name specified in the file CYCLE.IN

In addition to f) five columns are printed above the normal screen output. These five columns have the simple format which is necessary to plot a psychometric chart of a cycle with a normal plot program.

Column 1 and 2 describe a saturation line; column 3 temperature of the cycle states; column 4 abs humidity; column 5 rel. humidity

line1: state (1); line2: state (2) ....

## B.4 Expansion of the Program CYCLETYPS

### B.4.1 The Program SIMUTYPES

This program has some additional features compared to CYCLETYPS. In addition to the closed Dunkle Cycle the program simulates an open Dunkle cycle with the parameter cycletype equal to 7.

Furthermore the experimental cycle (cycletype=5) implemented in the program is the version with the Three Way dehumidifier in the open configuration. The closed version cannot be selected with a simple change of a parameter. The program code has to be edited in the subroutine EXP\_CYCLE. The removal of all \* in front of the lines in this procedure leads to a closed Three Way dehumidifier cycle.

In addition to the normal simulations the program can read upper and lower limits for one or more specific parameters and performs eleven simulations with values between these limits. The simulation procedure is switched on by the parameter

isoshape=3 in the input file DESTEST.PAR. The input parameters which can be varied are listed in the input file SIMULATION.PAR.

#### B.4.2 Input file SIMULATION.PAR

This file is read if isoshape=3. If the upper and lower limit of the input parameters are set to the same value the program does not change them. The simulation parameters are read in other input files such as CYCLE.IN, DEHUMIDIFIER.PAR, HEATEXCHANGER.PAR as well, but the values of the file SIMULATION.PAR delete the other parameters. The output is stored in a file with the name specified in the last line of this input file.

The output consists of eleven rows for the eleven simulation runs.

Columns: 1. COP, 2. regeneration temp., 3. ambient temp., 4. ambient rh., 5. room inlet temp., 6. inlet rh., 7. NTU dehumidifier, 8. NTU heat exchanger, 9.  $\Gamma_2$  gamma (regeneration side), 10. enthalpy difference between room inlet and room state.

#### B.4.3 MOSHMXA.FOR

This is the routine for the evaluation of a dehumidifier with three inlets. The moshmx program code works with the three inlet version if in the input file DEHUMIDIFIER.PAR gamma(3) is set to a value higher than zero.

The most important feature is that NFX must be set to a value of at least 5 in the file MOSHMX.PAR.

The pattern for the input and output properties of the stream through the dehumidifier remains the same; it is merely a third stream added.

SIN(first number, second number), SOUT(first number, second number)

Pattern: first number; 1: temperature; 2: abs. humidity; 3: enthalpy  
 second number; 1: process stream; 2: regeneration stream; 3: second  
 process stream

After every iteration of the procedure the SIN and SOUT is printed on the screen.

## B.5 Components for an Executable Program

### B.5.1 The cooling cycle simulation program CYCLETYPS.

Compile

CYCLETYPS.FOR, SENSIBLE.FOR, HUMIDIFIER.FOR, MOSHMX.FOR,  
 ANALOGY.FOR, PROPSA.FOR

Link all components together.

necessary input files: MOSHMX.PAR, ANALOGY.PAR, CYCLE.IN,  
 DESSICANT.PAR, HEATEXCHANGER.PAR, DEHUMIDIFIER.PAR

### B.5.2 Program EXCHANGER simulates a sensible heat exchanger, dehumidifer, and enthalpie exchanger.

In addition to B.5.1 compile EXCHANGER.FOR, OUTPUT.FOR, UHMX.FOR

Link : EXCHANGER.FOR, SENSIBLE.FOR, UHMX.FOR, ANALOGY.FOR,  
 PROPSA.FOR, OUTPUT.FOR

necessary input files: EXCHANGER.IN, MOSHMX.PAR, ANALOGY.PAR,  
 DESICCANT.PAR

Comment: For a single dehumidifier simulation the program EXCHANGER is sufficient. The inputfile EXCHANGER.IN has almost the same structure as inputfile DEHUMIDIFIER.IN.

### B.5.3 The Simulation Program SIMUTYPES

Compile

SIMUTYPES.FOR, SENSIBLE.FOR, HUMIDIFIER.FOR, MOSHMXA.FOR,  
ANALOGY.FOR, PROPSA.FOR

Link all components together

necessary input files: MOSHMX.PAR, ANALOGY.PAR, CYCLE.IN,  
DESSICANT.PAR, HEATEXCHANGER.PAR, DEHUMIDIFIER.PAR.,  
SIMULATION.PAR

## Appendix C

### C.1 Calculation of the Overall Isotherm Gradient $\frac{dW_D}{dT}$

The following calculation refers to the closed system in Chapter 2. The universal validity is not affected by this assumption.

#### The Isotherm Formulation $W_D = f(r, T)$

The equilibrium water content of the desiccant depends on the relative humidity and the temperature

$$W_D = f(r, T)$$

$$dW_D = \left( \frac{\partial W_D}{\partial r} \right)_T dr + \left( \frac{\partial W_D}{\partial T} \right)_r dT \quad (C.1)$$

The relative humidity depends on the absolute humidity of the air and the temperature.

$$r = f(w, T)$$

$$dr = \left( \frac{\partial r}{\partial w} \right)_T dw + \left( \frac{\partial r}{\partial T} \right)_w dT \quad (C.2)$$

substitute (C.2) into (C.1)

$$dW_D = \left( \frac{\partial W_D}{\partial r} \right)_T \left( \frac{\partial r}{\partial w} \right)_T dw + \left( \frac{\partial W_D}{\partial r} \right)_T \left( \frac{\partial r}{\partial T} \right)_w dT + \left( \frac{\partial W_D}{\partial T} \right)_r dT \quad (C.3)$$

conservation of mass

$$W_D m_D + dw m_a = 0 \quad (C.4)$$

substitute (C.4) into (C.3)

$$dW_D = \left( \frac{\partial W_D}{\partial r} \right)_T \left( \frac{\partial r}{\partial w} \right)_T \frac{-dW_D m_D}{m_{air}} + \left( \frac{\partial W_D}{\partial r} \right)_T \left( \frac{\partial r}{\partial T} \right)_w dT + \left( \frac{\partial W_D}{\partial T} \right)_r dT$$

$$dW_D \left[ 1 + \left( \frac{\partial W_D}{\partial r} \right)_T \left( \frac{\partial r}{\partial w} \right)_T \frac{m_D}{m_{air}} \right] = \left( \frac{\partial W_D}{\partial r} \right)_T \left( \frac{\partial r}{\partial T} \right)_w dT + \left( \frac{\partial W_D}{\partial T} \right)_r dT$$

The derivative  $\frac{dW_D}{dT}$  can be expressed as.

$$\frac{dW_D}{dT} = \frac{\left(\frac{\partial W_D}{\partial r}\right)_t \left(\frac{\partial r}{\partial T}\right)_w + \left(\frac{\partial W_D}{\partial T}\right)_r}{1 + \left(\frac{\partial W_D}{\partial r}\right)_t \left(\frac{\partial r}{\partial w}\right)_t m_{air}} \quad (C.5)$$

For  $m_{air} \gg m_D$  expression (C.5) transforms in

$$\left(\frac{\partial W_D}{\partial T}\right)_w = \left(\frac{\partial W_D}{\partial r}\right)_t \left(\frac{\partial r}{\partial T}\right)_w + \left(\frac{\partial W_D}{\partial T}\right)_r$$

### The Isotherm Formulation: $r_D = f(W_D, T)$

The relative humidity is expressed as a function of the equilibrium water content and the temperature of the desiccant.  $r_D = f(W_D, T)$

At equilibrium:  $r_D = r$

$$dr_D = \left(\frac{\partial r_D}{\partial W_D}\right)_T dW_D + \left(\frac{\partial r_D}{\partial T}\right)_{W_D} dT \quad (C.6)$$

The relative humidity depends on the absolute humidity of the air and the temperature.

$r = f(w, r)$

$$dr = \left(\frac{\partial r}{\partial w}\right)_t dw + \left(\frac{\partial r}{\partial T}\right)_w dT \quad (C.7)$$

substitute (6.2.2) into (6.2.1)

$$\left(\frac{\partial r_D}{\partial W_D}\right)_T dW_D + \left(\frac{\partial r_D}{\partial T}\right)_{W_D} dT = \left(\frac{\partial r}{\partial w}\right)_t dw + \left(\frac{\partial r}{\partial T}\right)_w dT \quad (C.8)$$

conservation of mass

$$dW_D m_D + dw m_{air} = 0 \quad (C.9)$$

substitute (C.9) into (C.8)

$$\left(\frac{\partial r_D}{\partial W_D}\right)_T dW_D + \left(\frac{\partial r_D}{\partial T}\right)_{W_D} dT = \left(\frac{\partial r}{\partial w}\right)_t \frac{-dW_D m_D}{m_{air}} + \left(\frac{\partial r}{\partial T}\right)_w dT$$

$$\left[\left(\frac{\partial r_D}{\partial W_D}\right)_T + \left(\frac{\partial r}{\partial w}\right)_t \frac{m_D}{m_{air}}\right] dW_D = \left[-\left(\frac{\partial r_D}{\partial T}\right)_{W_D} + \left(\frac{\partial r}{\partial T}\right)_w\right] dT$$

The derivative  $\frac{dW_D}{dT}$  can be expressed as.

$$\frac{dW_D}{dT} = \frac{-\left(\frac{\partial r_D}{\partial T}\right)_{W_D} + \left(\frac{\partial r}{\partial T}\right)_w}{\left(\frac{\partial r_D}{\partial W_D}\right)_T + \left(\frac{\partial r}{\partial w}\right)_t \frac{m_D}{m_{air}}} \quad (\text{C.10})$$

For  $m_{air} \gg m_D$  expression (C.11) transforms in:  $\left(\frac{\partial W_D}{\partial T}\right)_w = \frac{-\left(\frac{\partial r_D}{\partial T}\right)_{W_D} + \left(\frac{\partial r}{\partial T}\right)_w}{\left(\frac{\partial r_D}{\partial W_D}\right)_T}$

## C.2 The Evaluation of Expression (C.5) and Expression (C.10)

It was shown in the previous sections, that physical adsorption requires an overall gradient  $\frac{dW_D}{dT} < 0$

### Expression (C.5)

$$\frac{dW_D}{dT} = \frac{\begin{matrix} + & - & ? \\ \left(\frac{\partial W_D}{\partial r}\right)_t & \left(\frac{\partial r}{\partial T}\right)_w & + \left(\frac{\partial W_D}{\partial T}\right)_r \end{matrix}}{1 + \begin{matrix} \left(\frac{\partial W_D}{\partial r}\right)_t & \left(\frac{\partial r}{\partial w}\right)_t & \frac{m_D}{m_{air}} \\ + & + & \end{matrix}} \quad (\text{C.5})$$

Sign determination of each partial derivatives in (C.5)

$\left(\frac{\partial W_D}{\partial r}\right)_t$  : must be positive; all isotherms have increasing adsorbent water content with increasing relative humidity.

$\left(\frac{\partial r}{\partial T}\right)_w$  : always negative. See psychometric relations Figure C.1

$\left(\frac{\partial r}{\partial w}\right)_t$  : always positive. See psychometric relations Figure C.1

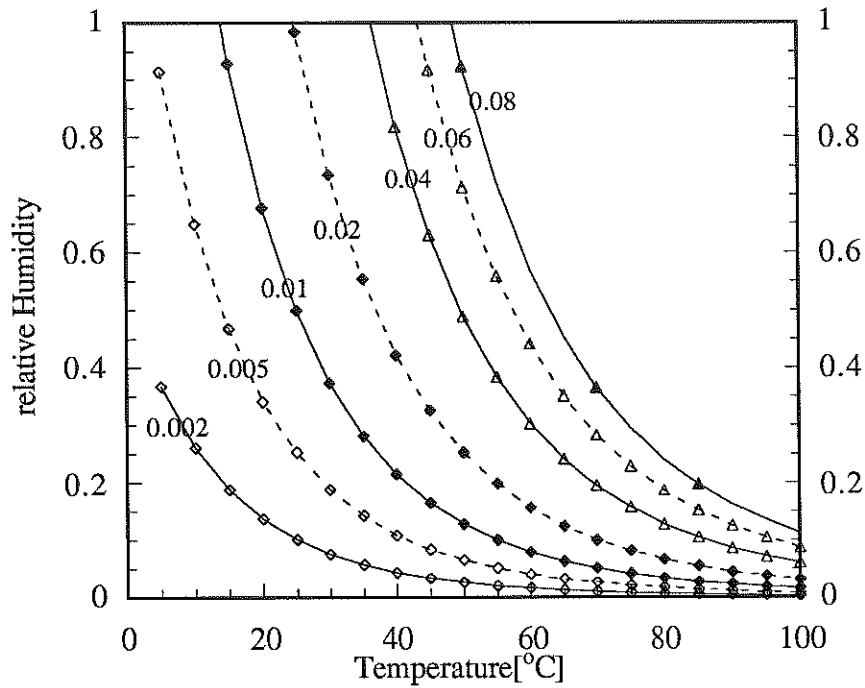


Figure C.1 Relative Humidity at Constant Absolute Humidity

Result: It is necessary for  $\frac{dW_D}{dT} < 0$ , that  $\left(\frac{\partial W_D}{\partial T}\right)_r < abs \left[ \left(\frac{\partial W_D}{\partial r}\right)_t \left(\frac{\partial r}{\partial T}\right)_w \right]$

**Expression (C.11)**

$$\frac{dW_D}{dT} = \frac{\left(\frac{\partial r_D}{\partial T}\right)_{W_D} + \left(\frac{\partial r}{\partial T}\right)_w}{\left(\frac{\partial W_D}{\partial T}\right)_T + \left(\frac{\partial r}{\partial w}\right)_T m_{air}} \quad (C.10)$$

Sign determination of each partial derivatives in (C.10)

$\left(\frac{\partial r_D}{\partial W_D}\right)_T$ : always positive, since  $\left(\frac{\partial W_D}{\partial r}\right)_t$  always positive.

$\left(\frac{\partial r}{\partial T}\right)_w$ : negative, see Figure C.1

$\left(\frac{\partial r}{\partial w}\right)_T$ : positive, see Figure C.1

Result: It is necessary for  $\frac{dW_D}{dT} < 0$ , that  $\left(\frac{\partial r_D}{\partial T}\right)_{W_D} > \left(\frac{\partial r}{\partial T}\right)_w$ .

### C.3 Calculation of the Derivatives for Dubinin-Astakov and Jurinak

#### Isotherm formulation

#### Dubinin-Astakov Two Sited Isotherm Formulation

Adsorption potential:  $A = -RT \ln(r)$

Two sited Dubinin - Polanyi expression:  $W_D = W_1 + W_2$

Where:  $W_1 = W_{01} \exp\left[-\left(\frac{A}{E_{01}}\right)^2\right]$ ;  $W_2 = W_{02} \exp\left[-\left(\frac{A}{E_{02}}\right)^2\right]$

R : universal gas constant; T absolute temperature

$$\left(\frac{\partial W_D}{\partial r}\right)_T = 2ART \frac{1}{r} \left( \frac{W_1}{(E_{01})^2} + \frac{W_2}{(E_{02})^2} \right)$$

$$\left(\frac{\partial W_D}{\partial T}\right)_r = 2AR \ln(r) \left( \frac{W_1}{(E_{01})^2} + \frac{W_2}{(E_{02})^2} \right)$$

#### Jurinak Formulation

$$r_D = G(W_D) \left( \frac{p_S(T)}{p_S(T_0)} \right)^{h^*-1}$$

$h^*$  : is the ratio heat of adsorption to heat of vaporization.

$$h^* = 1 + dh^* \frac{\exp(kW^*) - \exp(k)}{1 - \exp(k)}$$

Partial derivatives based on Jurinak formulation with respect to temperature and matrix water content.

$$\left(\frac{\partial r_D}{\partial T}\right)_{W_D} = G(W_D) \left( \frac{p_S(T)}{p_S(T_0)} \right)^{h^*-2} \frac{(h^* - 1) dp_S}{p_S(T_0) dT}$$

$$\left(\frac{\partial r_D}{\partial W_D}\right)_T = \frac{dG(W_D)}{dW_D} \left( \frac{p_S(T)}{p_S(T_0)} \right)^{h^*-1} + G(W_D) \left( \frac{p_S(T)}{p_S(T_0)} \right)^{h^*-1} \ln\left(\frac{p_S(T)}{p_S(T_0)}\right) \frac{dh^*}{dW_D}$$

#### C.4 Derivatives of Air

$$\left(\frac{\partial r}{\partial w}\right)_T = \frac{0.622}{(0.622 + w)^2} \frac{P}{p_s(T)}$$

$$\left(\frac{\partial r}{\partial T}\right)_w = \frac{-r}{p_s(T)} \frac{dp_s(T)}{dT}$$

#### C.5 Calculation of the Heat of Adsorption

Equation (3.7) gives the relationship between an isotherm shape at temperature  $T_0$  and a unknown temperature  $T$  with respect to the ratio between heat of adsorption and heat of vaporization.

$$\frac{r(T)}{r(T_0)} = \left(\frac{p_s(T)}{p_s(T_0)}\right)^{\frac{h_s}{h_{VL}} - 1} \quad (3.7)$$

rearrangement of (3.7) yields

$$\frac{h_s}{h_{VL}} = \frac{\ln\left(\frac{r(T)}{r(T_0)}\right)}{\ln\left(\frac{p_s(T)}{p_s(T_0)}\right)} + 1 \quad (C.11)$$

Equation (C.11) makes it possible to calculate the differential heat of sorption easily with only two given isotherm shapes at two different temperatures.

Draw a horizontal line through the desiccant water content, where  $h_s$  should be calculated. The intersections with the isotherms determine the relative humidity of isotherm 1 at temperature  $T_0$  and isotherm 2 at temperature  $T$ . Calculate  $p_s(T)$  and  $p_s(T_0)$ . Evaluate C.11.

---

## Bibliography

---

1. Czanderna, A.W. 1990. "Polymers as advanced materials for desiccant applications: Progress Report for 1989." SERI/TP-213-3608. Golden, CO: Solar Energy Research Institute.
2. Collier, K., T. S. Cale, and Z. Laven, 1986. "Advanced desiccant materials assessment." GRI-86/0181, Final Report, February 1985-May 1986. Chicago: Gas Research Institute.
3. Benefield, Larry D. , 1982. " Process Chemistry for water and wastewater treatment." ISBN 0-13-722975-5, Prentice-Hall, Inc. Englewood Cliffs, New Jersey 07632
4. Lambertson, T.J., " Performance Factors of a Periodic Flow Heat Exchanger", ASME Transactions, Vol. 80, 1958
5. Bahnke, G. D. and Howard, C. P., "The Effect of Longitudinal Heat Conduction on Periodic Flow Heat Exchanger Performance", ASME Transactions, Vol. 86, 1964
6. ASHRAE, Handbook of Fundamentals, American Society of Heating, Refrigeration and Air Conditioning Engineers, New York, 1989
7. ASHRAE, Application Handbook, American Society of Heating, Refrigeration and Air Conditioning Engineers, New York, 1991
8. Van den Bulk, E. , "Convective Heat and Mass Transfer in Compact Regenerative Dehumidifiers", Ph.D. Thesis in Mechanical Engineering, University of Wisconsin-Madison, 1987
9. Klein, H., "Heat and Mass Transfer in Regenerative Enthalpy Exchangers", M.S. Thesis in Chemical Engineering, University of Wisconsin Madison, 1988

10. Duffie, J.A. and Beckman, W. A., "Solar Engineering of Thermal Processes", John Wiley and Sons, Second Edition, New York, 1991
11. Jurinak, J. J., "Open Cycle Desiccant Cooling - Component Models and System Simulations", Ph.D. Thesis in Mechanical Engineering, University of Wisconsin-Madison, 1982
12. Maclain-Cross, I. L., "A Theory of Combined Heat and Mass Transfer in Regenerators", Ph.D. Thesis in Mechanical Engineering, Monash University, Australia, 1974
13. Dunkle, R. V., "A Method of Solar Air Conditioning", Mechanical and Chemical Engineering Transactions, Institution of Engineers, Australia, MC 1, 73, 1965
14. D. Bharathan, J. M. Parsons, I. L. Maclain-cross, "Experimental Study of an Advanced Silica Gel Dehumidifier", Solar Energy Research Institute 1617 Cole Boulevard Golden, Colorado 80401, 1987
15. Daniel R. Crum, "Open Cycle Desiccant Air Conditioning Systems ", M.S. Thesis in Mechanical Engineering, University of Wisconsin-Madison, 1986